Historical Development of Heavy Metal Input into Near-Coastal Areas

– Reconstruction, Assessment & Ecological Response –

Dissertation

zur Erlangung des

Doktorgrades der Naturwissenschaften

(Dr. rer. nat.)

am Fachbereich Geowissenschaften

der Universität Bremen

Vorgelegt von

Sandy Boehnert

Bremen, Mai 2019

Gutachter

1. Gutachter Prof. Dr. Dierk Hebbeln
2. Gutachter Prof. Dr. Martin Frank

Datum des Promotionskolloquiums

18. Juli 2019

Universität Bremen INTERCOAST marum

Abstract

Global change induced by human activity has been an ongoing process for millennia, intensifying since the onset of industrialisation. One of the major concerns is the man-made release of pollutants into the environment through for example mining operations, burning of fossil fuels or manufacturing industries. In particular, the release of heavy metals poses a potential threat to the health of individual organisms, whole ecosystems and consequently humans because of their toxicity and persistence. In this context, coastal areas are of particular interest as they are prone to heavy metal accumulation due to their proximity to the source of the released pollutants, while also providing crucial ecosystem services.

Monitoring programs record levels of heavy metals in coastal areas in order to assess the current degree of pollution and state of ecosystem health. To quantify the anthropogenic impact, sediment heavy metal contents need to be compared to their naturally occurring background values, varying for different regions depending on the surrounding lithologies, weathering and erosion processes, transport paths or volcanic activity. Determination of these baseline values for a specific region is key to evaluate the anthropogenic impact in a distinct area.

Benthic foraminifera are likewise widely used as a monitoring tool for pollution because of their sensitivity to environmental changes and the preservation of their tests in sedimentary records. Overall, increased levels of heavy metals can result in severe ecotoxicological consequences for marine biota. With respect to benthic foraminifera, a rising proportion of deformed tests is a characteristic often interpreted as increasing environmental stress caused by elevated levels of heavy metals. However, little is known about the relation between heavy metal contents in sediments, incorporation into foraminifera tests and the abundance of test deformities.

Near-coastal sediment cores have the potential to provide high-resolution archives to determine pristine background values, reconstruct the pollution history in sediments and evaluate its ecotoxicological effects. Therefore, this dissertation aims to unravel the pollution history and define natural background values in three study areas, the Firth of Thames (New Zealand), the Helgoland Mud Area (SE North Sea) and the Skagerrak (NE North Sea). The contrasting history of human settlement in the North Sea area and New Zealand makes these sites promising areas to obtain crucial insights into the temporal development of anthropogenic heavy metal release.

New Zealand offers the unique opportunity to investigate true natural background values of heavy metals because of its well-defined three-stage development: the pre-human era (until ~1300 CE), Polynesian era (~1300-1800 CE) and European era (since ~1845 CE). Within this developmental context, anthropogenic impacts can be quantified, and the most likely source of heavy metals can be deduced from the onset of elevated levels. Eight marine sediment cores collected from the Firth of Thames were analysed for their elemental composition by X-ray fluorescence (XRF) and temporally resolved by a pollen and radiocarbon-based stratigraphic framework. Sharp increases in Pb and Zn contents occurred

during the early European Era simultaneously with the onset of gold mining activities (1867 CE) in the nearby catchment area. The contents of Pb and Zn increase concurrently from very stable values in the older sediments (Pb = 13 ppm, Zn = 60 ppm), interpreted as natural background, to an average maximum of 60 ppm (Pb) and 160 ppm (Zn) near the core top, interpreted as an anthropogenic signal.

In the Helgoland Mud Area, such a baseline study was already conducted earlier and built the base for a study on ecotoxicological effects on the local biota, specifically the benthic foraminifera *Ammonia beccarii* and *Elphidium excavatum*. Two nearby sediment cores from the southeastern North Sea, covering the pollution history of the past 400 years, were used to implement a combined approach of test deformation and test chemistry in relation to bulk sediment Pb contents. Test chemistry (Pb/Ca and Cd/Ca) of the investigated species mirrors the heavy metal increase in the bulk sediment at the beginning of the 20th century. A slight temporal offset is interpreted as a biological defence mechanism, inhibiting incorporation until a yet to define threshold is overcome. However, the total abundance of aberrant foraminiferal tests does not seem to be correlated with historical heavy metal pollution, suggesting that environmental stressors other than heavy metals cause foraminiferal test deformation.

To complement these two near-coastal research areas, the third study focusses on the questions, if and to what extent human impact, exemplified by Zn contents, is recorded in the deep marine sediments of the Skagerrak in the NE North Sea. Quantitative XRF, grain size and carbon-nitrogen-elemental analyses were conducted on an SW-NE transect of three short sediment cores (~40 cm). The southwesternmost core indicates an increase in Zn contents at c.1920 CE, while the other two cores show no increase but contain generally higher values; leading to the conclusion that sediments containing the pre-industrial background values were not recovered. For better comparability (between cores as well as with other regions), Zn contents were normalised to 5% Al according to the OSPAR guidelines. The resulting values vary from 54 to 95 ppm normalised Zn in the bulk sediment. According to the OSPAR background contents (BCs), heavy metal enrichment in the Skagerrak takes place on a rather low level. However, there are reasons to argue that the suggested BC by OSPAR overestimates the true natural background contents by about 50%, leading to a possibly much higher pollution degree than formerly assumed.

Overall, the present study substantiates the relevance of near-coastal sediments as an archive for the reconstruction of the anthropogenic heavy metal input. All three study sites recorded an increase in heavy metal accumulation during industrial times. In the Firth of Thames, truly pristine natural background values were obtained, while the previously suggested OSPAR BC for Zn was questioned in the Skagerrak study. The ecotoxicological response of foraminifera proved to be multi-faceted, with foraminiferal test chemistry being a better indicator for heavy metal pollution than the abundance of deformed test morphologies. Hence, the outcomes of this thesis significantly improve our understanding of the historical release of heavy metals into coastal areas, offer valuable information on the ecological response and contribute to future decision making in environmental management.

Kurzfassung

Der durch menschliche Aktivitäten ausgelöste globale Wandel ist ein seit Jahrtausenden fortlaufender Prozess, der sich seit Beginn der Industrialisierung verschärft. Eines der Hauptprobleme ist die anthropogen verursachte Freisetzung von Schadstoffen in die Umwelt, beispielsweise durch Bergbau, Verbrennung fossiler Brennstoffe oder verarbeitende Industrie. Insbesondere die Freisetzung von Schwermetallen stellt aufgrund ihrer Toxizität und Persistenz eine potenzielle Gefahr für die Gesundheit einzelner Organismen, ganzer Ökosysteme und folglich des Menschen dar. In diesem Zusammenhang sind Küstengebiete von besonderem Interesse, da sie aufgrund ihrer Nähe zu Schadstoffquellen zur Anreicherung von Schwermetallen neigen und gleichzeitig entscheidende Ökosystemleistungen erbringen.

In Überwachungsprogrammen werden Schwermetallbelastungen in Küstengebieten erfasst, um den aktuellen Verschmutzungsgrad und den Gesundheitszustand der Ökosysteme zu beurteilen. Zur Quantifizierung der anthropogenen Auswirkungen müssen die Schwermetallgehalte der Sedimente mit ihren natürlich vorkommenden Hintergrundwerten verglichen werden, die regional je nach umgebender Lithologie, Verwitterungs- und Erosionsvorgängen, Transportpfaden oder vulkanischer Aktivität variieren. Die Bestimmung dieser Basiswerte für eine bestimmte Region ist der Schlüssel zur Bewertung der anthropogenen Auswirkungen in diesem Gebiet.

Des Weiteren werden benthische Foraminiferen aufgrund ihrer Empfindlichkeit gegenüber Umweltveränderungen und der Erhaltung ihrer Gehäuse in der Sedimentabfolge häufig als Überwachungsinstrument für Verschmutzung eingesetzt. Insgesamt können erhöhte Mengen an Schwermetallen schwerwiegende ökotoxikologische Folgen für die Meeresbiota haben. In Bezug auf benthische Foraminiferen ist ein steigender Anteil verformter Gehäuse ein Merkmal, das häufig als zunehmende Umweltbelastung durch erhöhte Schwermetallwerte interpretiert wird. Über den Zusammenhang zwischen Schwermetallgehalten in Sedimenten, dem Einbau in Foraminiferengehäuse und der Häufigkeit von Gehäusedeformationen ist jedoch wenig bekannt.

Sedimentkerne aus Küstengebieten haben das Potenzial, als hochauflösende Archive zu dienen, um natürliche Hintergrundwerte zu bestimmen, die Verschmutzungsgeschichte in Sedimenten zu rekonstruieren und ihre ökotoxikologischen Wirkungen zu bewerten. Daher zielt diese Dissertation darauf ab, in drei Untersuchungsgebieten, dem Firth of Thames (Neuseeland), dem Helgoländer Schlickgebiet (südöstliche Nordsee) und dem Skagerrak (nordöstliche Nordsee), die jeweilige Verschmutzungsgeschichte nachzuvollziehen und natürliche Hintergrundwerte zu definieren. Die unterschiedliche Geschichte der menschlichen Besiedlung in der Nordseeregion und in Neuseeland prädestiniert diese Gebiete um wertvolle Einblicke in die zeitliche Entwicklung der anthropogenen Freisetzung von Schwermetallen zu erhalten.

Neuseeland bietet aufgrund seiner klar definierten dreistufigen Entwicklung (vormenschliche Ära bis ~1300 n.Chr., polynesische Ära ~1300-1800 n.Chr. und europäische Ära seit ~1845 n.Chr.) die einzigartige Gelegenheit, die wahren natürlichen Hintergrundwerte von Schwermetallen zu untersuchen. Daraus ergibt sich die Möglichkeit, die anthropogenen Auswirkungen zu quantifizieren. Indem der zeitliche Beginn erhöhter Konzentrationen begrenzt wird. kann zudem die wahrscheinlichste Schwermetallquelle ermittelt werden. Acht marine Sedimentkerne aus dem Firth of Thames wurden mittels Röntgenfluoreszenzanalyse (RFA) hinsichtlich ihrer Elementzusammensetzung untersucht und zeitlich in ein Pollen- und Radiokarbon-basiertes stratigraphisches Gerüst eingehängt. Mit dem Beginn des Goldabbaus (1867 n. Chr.) im angrenzenden Einzugsgebiet durch die frühen europäischen Siedler trat ein starker Anstieg der Gehalte an Pb und Zn auf. Die sehr stabilen Pb und Zn Werten in den älteren Sedimenten (Pb = 13 ppm, Zn = 60 ppm), interpretiert als natürlicher Hintergrund, steigen zeitgleich auf ein durchschnittliches Maximum von 60 ppm (Pb) und 160 ppm (Zn) nahe der Sedimentoberfläche, interpretiert als anthropogenes Signal, an.

Im Helgoländer Schlickgebiet wurde eine solche Basisstudie bereits früher durchgeführt und bildete die Grundlage für die Untersuchung über ökotoxikologische Auswirkungen auf die lokale Biota, insbesondere die benthischen Foraminiferen *Ammonia beccarii* und *Elphidium excavatum*. An zwei dicht beieinanderliegenden Sedimentkernen aus der südöstlichen Nordsee, die die Verschmutzungsgeschichte der letzten 400 Jahre erfassen, wurde in einem kombinierten Ansatz das Auftreten von Gehäuseverformung mit der Gehäusechemie sowie dem Pb-Gehalt im Sediment verglichen. Die Gehäusechemie (Pb/Ca und Cd/Ca) der untersuchten Spezies spiegelt den Anstieg der Schwermetalle im Sediment zu Beginn des 20. Jahrhunderts wider. Ein geringfügiger zeitlicher Versatz wird als biologischer Abwehrmechanismus interpretiert, der den Einbau von Schwermetallen ins Gehäuse hemmt, bis ein noch zu definierender Schwellwert überschritten ist. Die Häufigkeit abnormaler Foraminiferengehäuse scheint jedoch nicht mit der historischen Schwermetallbelastung korreliert zu sein, was darauf hindeutet, dass andere Umweltbelastungen die Gehäusedeformationen verursachen.

Zur Ergänzung dieser beiden küstennahen Forschungsgebiete, konzentriert sich die dritte Studie auf die Frage, ob und inwieweit menschliche Einflüsse, am Beispiel von Zn-Gehalten, in den tiefmarinen Sedimenten des Skagerrak in der nordöstlichen Nordsee nachweisbar sind. Quantitative RFA, Korngrößen- und Kohlenstoff-Stickstoff-Elementanalysen wurden an einem SW-NE-Transekt aus drei kurzen Sedimentkernen (~40 cm) durchgeführt. Die Untersuchungsergebnisse des südwestlichsten Kerns deuten auf einen Anstieg des Zn-Gehalts um 1920 n. Chr. hin. Die beiden anderen Kerne zeigen keinen Anstieg, enthalten jedoch im Allgemeinen höhere Zn-Werte, was die Schlussfolgerung nahelegt, dass Sedimente mit vorindustriellen Hintergrundwerten dort nicht gewonnen wurden. Zur besseren Vergleichbarkeit (sowohl zwischen Kernen als auch mit anderen Regionen) wurden die Zn-Gehalte gemäß den OSPAR-Richtlinien auf 5% Al normiert. Die resultierenden Werte schwanken zwischen 54 und 95 ppm normalisiertem Zn im Sediment. Entsprechend der OSPAR-Hintergrundgehalte findet

die Anreicherung von Schwermetallen im Skagerrak auf einem eher niedrigen Niveau statt. Es gibt jedoch Gründe anzunehmen, dass die von OSPAR empfohlenen Hintergrundgehalte die tatsächlichen natürlichen Hintergrundgehalte von Zn um etwa 50% überschätzt, was einen potentiell viel höheren Verschmutzungsgrad als zuvor angenommen bedeuten würde.

Insgesamt belegt die vorliegende Studie die Relevanz von küstennahen Sedimenten als Archiv für die Rekonstruktion des anthropogenen Schwermetalleintrags. Alle drei Untersuchungsstandorte wiesen einen Anstieg der Schwermetallablagerung während der Zeit der Industrialisierung auf. Im Firth of Thames wurden natürliche Hintergrundwerte (sensu stricto) ermittelt, während die Skagerrak-Studie die empfohlenen OSPAR Hintergrundgehalte für Zn in Frage stellt. Die ökotoxikologische Reaktion von Foraminiferen erwies sich als vielschichtig, wobei die chemische Zusammensetzung der Foraminiferengehäuse ein besserer Indikator für die Schwermetallbelastung ist, als die Häufigkeit an deformierten Gehäusen. Somit verbessern die Ergebnisse dieser Arbeit unser Verständnis des historischen Schwermetalleintrags in Küstengebiete erheblich, liefern wertvolle Informationen zu ökologischen Reaktionen und tragen zur zukünftigen Entscheidungsfindung im Umweltmanagement bei.

Danksagung

Ich danke Prof. Dr. Dierk Hebbeln für die Vergabe der Stelle, für die Betreuung meiner Arbeit und die Nachsichtigkeit bei den kleineren und größeren Fehlern, aus denen ich auf meinem Weg lernen konnte. Den Mitgliedern meines Thesis Committees, Dr. Willem de Lange, Dr. Beth Fox, Dr. Jürgen Titschack und Dr. Jeroen Groneveld möchte ich für die vielen wertvollen Diskussionen danken. Außerdem bedanke ich mich bei Beth und Willem für die Möglichkeit ein anderes Forschungsumfeld an der Universität von Waikato kennen gelernt zu haben. Bei Prof. Dr. Martin Frank möchte ich mich für die Bereitschaft zur Bewertung meiner Dissertation als Zweitgutachter bedanken.

Dankbar bin ich auch dem Graduiertenprogram INTERCOAST für die Möglichkeit zur Teilnahme an Kursen und eines mehrmonatigen Forschungsaufenthaltes in Neuseeland um mich fachlich und persönlich weiterentwickeln zu können. Außerdem hatte ich so die Möglichkeit in einem Netzwerk mit 11 weiteren Doktoranden sofort gut eingebunden zu sein. Der Deutschen Forschungsgemeinschaft danke ich für die Förderung dieses Projektes.

Meinen Co-Autoren Salvador Ruiz Soto, Beth Fox, Yusuke Yokoyama, Anniken Rotstigen Birkelund, Gerhard Schmiedl, Henning Kuhnert, Gerhard Kuhn, Christian Hass und Dierk Hebbeln danke ich für die gute und konstruktive Zusammenarbeit.

In den Laboren an der Universität Bremen bin ich Christina Gnade, Silvana Pape und Vera Lukies für ihre Hilfsbereitschaft dankbar. Für die technische Unterstützung bei der Feldkampagne in Neuseeland bedanke ich mich recht herzlich bei Dean Sandwell und Chris Morcom, sowie bei Anette Rodgers und Kirsty Vincent für ihre organisatorische Unterstützung im Labor, alle von der Universität in Waikato. Für einen überaus lehrreichen Besuch an der *Thames School of Mines* möchte ich mich bei John Isdale bedanken, der mir nicht nur historische und geologische Aspekte des Goldabbaus erklärt hat, sondern auch durch seine Begeisterung und Herzlichkeit einen bleibenden Eindruck hinterlassen hat.

Ein Dankeschön an die Verwaltung richtet sich insbesondere an Carmen Murken, Nicole Bammann, Anja Rademacher und Jasmin Fahrenholz. Nicht auszudenken welche Formulare ich sonst noch hätte ausfüllen müssen. Mein Leben in IT-Fragen mehrfach gerettet haben Jutta Bülten und Lina Büschler, vielen Dank dafür!

Ein großer Dank geht an meine Arbeitsgruppe *Marine Sedimentologie* für eure offene, freundliche Art und die vielen lustigen Kaffeerunden. Ihr seid großartig! Danke sage ich Jürgen Titschack, dem *Robin Hood* der Doktoranden, der immer ein offenes Ohr für seine Kollegen hat, und Claudia Wienberg, die mich mit ihrer offenen und direkten Art wahlweise unterhalten oder meinen Fokus zurechtgerückt hat.

Was wäre ein PhD am MARUM ohne eine Ausfahrt? Daher danke ich allen die auf der *RV Sonne* dabei waren, aber insbesondere Mahyar Mohtadi, der mir den Begriff ‘Schanghaien’ am praktischen Beispiel erklärt hat. *SO 256* war eine unvergessliche und lehrreiche Ausfahrt.

Meinen Bürokollegen Conny Kwiatkowski, Florian ‚Boxi' Boxberg und Jens Weiser danke ich für die lustigen Stunden (kumulativ versteht sich, wir haben ja tatsächlich die meiste Zeit gearbeitet) und die entspannte und ehrliche Atmosphäre im Büro. Für ihre Ehrlichkeit möchte ich auch Jens, Chelsea, Hadar und Claudia danken, die jeweils Teile meiner (fast) fertigen Dissertation gelesen und konstruktiv kritisiert haben. Ein ganz großes Dankeschön geht auch an Sinah, ohne deinen PC hätte ich dieses Exemplar nie formatiert bekommen.

Meinen Freunden (und Leidensgenossen) Hadar, Susi, Dharma, Marine, Tina und Nine danke ich für die zahlreichen Gelegenheiten einer Auszeit, die Krisengespräche, das entgegengebrachte Verständnis, den zugesprochenen Mut und vieles mehr.

Meiner Familie möchte ich sagen: Danke das Ihr immer an mich geglaubt habt! Mir ist bewusst, dass ihr oft keine genaue Vorstellung davon hattet, was ich hier so treibe. Aber trotzdem hat euer Rückhalt einen ganz entscheidenden Teil dazu beigetragen. Meinem Freund danke ich für die ausgestrahlte Ruhe, das entgegengebrachte Verständnis und die vielen schönen Momente in den vergangenen Monaten.

Table of Contents

Chapter 1 Introduction

1.1 Motivation

Humans have been influencing the Earth in many ways to adapt it to the needs of society for millennia. These changes include resource exploitation such as agricultural land use, deforestation, and mining. However, modifications of the 'pristine' environment have a potentially negative effect on ecosystems, for example through the increasing release of pollutants. Amongst one of the most concerning pollutants are heavy metals.

The term 'heavy metals' is not clearly defined and inconsistently used to refer to a group of metals (and sometimes metalloids) with relatively high densities or atomic numbers (see Duffus, 2002). Commonly, they are characterised as toxic and persistent, meaning that they do not degrade. Heavy metals occur naturally in magmatic, sedimentary and metamorphic rocks and are therefore part of the geochemical cycle. Natural processes involving the release and redistribution of heavy metals include weathering and erosion (Elberling and Langdahl, 1998), soil formation (Bradl, 2005) but also volcanic eruptions (Varrica et al., 2000), forest fires (Pereira and Úbeda, 2010) and biogenic processes (Pongratz and Heumann, 1998). In addition to the natural processes, heavy metals are released by anthropogenic activities, such as mining operations, smelting, burning of fossil fuels, agricultural and industrial applications etc.

The origin of heavy metal release can be categorised into point sources (e.g., power and industrial plants, mines, volcanoes) and diffuse sources (e.g., exhaustion by cars, surface runoff, man-made and natural erosion) (see also Vink et al., 1999). Most of these sources are located on land. From there, they are distributed through either atmospheric (Injuk and van Grieken, 1995) or aquatic transport (Kersten et al., 1988).

Atmospheric transport occurs via fine airborne particles, for example generated by volcanoes, forest fires, fuel combustion or industrial processes, that can carry considerable quantities of toxic trace metals (e.g., Pb, Cd, Hg, As) (Patterson and Settle, 1987). Regarding the spatial extent of distribution, the detection of Pb and Cu in Greenland ice core records (Murozumi et al., 1969; Hong et al., 1996) demonstrate the potential for long-distance transport.

Aquatic transport of heavy metals takes place in ground and surface water (e.g., rivers, streams, springs), where the water composition is greatly influenced by the host rock and soil the water is flowing through (Bradl, 2005). However, additional heavy metals are introduced through human activity. Rivers, for example, also acquire heavy metals (and other pollutants) from agricultural and urban runoff or industrial effluents and sewage that are discharged directly into streams. Transport either occurs in dissolved form or adsorbed on suspended matter (e.g., Salomons, 1985). Eventually, heavy metals reach the coasts via this aquatic pathway and end up in the oceans as their 'ultimate' sink. Nevertheless, deposited sediments themselves, especially in shallow marine settings, represent a potential source of

contaminants to the overlying water, for instance through natural resuspension (e.g., by waves, tides and currents), bioturbation or human activity (e.g., dredging).

Coastal areas are the transitional zones between land and sea, and experience strong physicochemical gradients concerning salinity, pH, load of suspended matter, oxygenation and biological activity especially in the vicinity to rivers (e.g., Martin and Brun-Cottan, 1988). As coastal areas receive the highest input of riverine suspended matter (Eisma and Kalf, 1987), they are prone to heavy metal accumulation (Puls et al., 1997). This process has potentially a negative impact on the sensitive coastal ecosystems because many organisms take up heavy metals through either respiration or dietary intake.

While some heavy metals are essential, meaning they play an important role in biological processes in low concentrations and only become harmful above a specific threshold (e.g., Zn, Fe, Cu, Mn) (Rengel, 1999), others are non-essential and can cause damage already at very low doses (e.g., Pb, Hg, As) (Brathwaite and Rabone, 1985). As heavy metals are not degradable, they concentrate in the tissue of organisms when the absorption exceeds the excretion (bioaccumulation) and biomagnify throughout the food web, resulting in progressively negative health consequences for the ecosystem (Jakimska et al., 2011). Eventually, heavy metals can end up in the human body, where they can cause severe health problems such as dysfunctions of organs, cancer and eventually death (e.g., Duruibe et al., 2007). Since coastal zones serve as habitat and recreation sites for people and also as highly productive economic zones for fishery and mariculture, heavy metal consumption by organisms becomes also a socio-economic consideration (e.g., tourism, food security).

Numerous monitoring programs aim to observe the temporal and spatial concentrations of hazardous substances, such as heavy metals, in the marine environment. An example is the Coordinated Environmental Monitoring Programme (CEMP) under the Convention for the Protection of the Marine Environment of the North-East Atlantic (OSPAR) Joint Assessment and Monitoring Programme. One crucial purpose of such initiatives is to evaluate the current environmental status of water and sediment quality and their ecotoxicological consequences. Furthermore, they aim to assess the performance (i.e. success or failure) of implemented measures, such as governmental regulations, restrictions or prohibitions, that intent to reduce or eliminate coastal pollution.

To evaluate the degree of pollution, current levels of heavy metals need to be compared to a natural pre-human baseline. Because heavy metals also occur as part of the natural geochemical cycle, their pure presence is no direct evidence of anthropogenic pollution, whereas that is the case for artificial compounds such as synthetic insecticides, herbicides or wood protection agents. Therefore, the quantitative determination of the natural baseline is needed to evaluate which observed levels of heavy metals are above a normal, naturally occurring background. However, the determination of natural background values is challenging because heavy metal pollution is not a recent phenomenon. Emission of heavy metals started thousands of years ago (e.g., Hong et al., 1996; Monna et al., 2000; Leblanc et

al., 2000). As monitoring programs were only established during the past decades and do not cover the onset of anthropogenic heavy metal release, natural baselines have to be assessed by other means. Baseline data are obtained commonly from areas considered as relatively pristine (i.e. areas subjected to minimal human impacts) or from deeper segments of sediment cores pre-dating 1850 CE (e.g., OSPAR, 2009; BSH, 2016). Sediments from diverse localities with different properties (e.g., grain size, mineralogy, content of total organic carbon) pose the problem of low comparability. In order to enhance this comparability, a number of strategies are applied to adjust measured values to a common variable. This so-called normalisation can be performed with regards to a specific grain size (BSH, 2016), element content (OSPAR, 2009) or total organic carbon content (Kuijpers et al., 1993), among others.

Another problem monitoring programs face is the evaluation of ecotoxicological effects resulting from heavy metals. Ecotoxicological effects are modifications in the condition or dynamics of individual organisms, populations, communities and ecosystems caused through the exposure to a chemical (Traas and Leeuwen, 2007). The cause-effect relationship between bulk sediment heavy metal contents and indigenous biota is interfered by factors such as bioavailability, species-specific tolerance levels and biological regulatory mechanisms as well as temperature, pH or life cycle and physiological behaviour (e.g., Bryan, 1971). These manifold influences make the assessment, especially of past biological impacts of pollutants in ecosystems, a complex issue.

Marine sediment cores provide excellent records for reconstructing changes in the palaeoenvironment. Near-coastal settings are especially suitable to unravel the history of heavy metal release in the adjacent hinterland due to their close proximity to the sources and the high loads of suspended matter received from rivers. The reconstruction of the historical input is the basis to determine the natural baseline content of heavy metals in the sediment prior to human influences and to verify suggested background levels currently applied in monitoring programs. Furthermore, they offer the possibility to estimate the historical ecological response to heavy metal pollution on preserved microfossil communities, such as foraminifera.

The goal of this thesis is to provide new insights into the historical heavy metal release to near-coastal areas and its potential ecological effects. The generated knowledge aims to contribute to a better evaluation of the present degree of pollution and can stimulate future decision making regarding environmental protection and conservation of the coastal marine region.

1.2 Why compare New Zealand and the North Sea?

By studying the Firth of Thames in New Zealand and the North Sea in Europe, this project has the unique opportunity to compare the effects of anthropogenic activities on two regions with very different human settlement histories. While Europe has a long, millennial-scale history of human settlements, New Zealand was the last major landmass to be occupied by humans only ~800 years ago.

The timing of the first settlements of modern humans in Europe is still under debate (see Carbonell et al., 1996). However, Nigst et al. (2014) date the arrival of humans north of the Alps to 43,500 years ago. The size of the initial population was potentially small and therefore the environmental impact minimal (Behre, 1988). The first major landscape transformation occurred with the onset of agriculture in the mid-Holocene (Price, 2010) and the accompanying increase in deforestation (e.g., Kaplan, 2009). The history of mining in Europe can be traced back up to 4,500 years in Spain (Leblanc et al., 2000) and 3,500 years in the Harz Mountains (Monna et al., 2000), the latter one being located in the catchment area of the Weser and Elbe Rivers draining directly into the North Sea. The gradually increasing population and technological advances over the millennia led to a rather slow but steady increase in anthropogenic pressure. This changed eventually with the onset of the Industrial Revolution around 200 years ago. Many studies in the coastal regions of the North Sea detected a significant elevation in heavy metals in marine sediments after 1800 CE (e.g., Pederstad et al., 1993; Croudace and Cundy, 1995; Spencer et al., 2003; Lepland et al., 2010; Polovodova Asteman et al., 2015). However, the steady increase in human impact prior to industrialisation, as well as the long-time interval this pre-industrial change spans, make it difficult to define the truly natural background of heavy metals in the environment. This natural background is a necessity to put current observations into perspective.

In contrast, New Zealand was the last major landmass colonised by humans (e.g., McGlone et al., 1994) and experienced a clear development of human settlement described by three stages: the pre-human era, the Polynesian era and the European era. The pre-human stage lasted until ~1300 CE and was characterised by a pristine flora and fauna influenced only by natural climate variations, wildfires and volcanic eruptions (McGlone and Wilmshurst, 1999). This untouched environmental state allows the determination of purely natural background variations in heavy metal release. With the onset of the Polynesian era, the first severe changes to flora and fauna (i.e. extinction of species) occurred (e.g., McGlone, 1989). The increased occurrence of charcoal indicates significant deforestation through the slash-and-burn method, which thereby increased soil erosion and shifted the vegetation markedly from tall trees (i.e. *Podocarpus* spp.) to bracken fern (*Pteridium* spp.) (Byrami et al., 2002). Furthermore, exotic species such as sweet potato and taro were introduced for agricultural purposes (Atkinson and Cameron, 1993). Polynesian era sediments therefore allow the study of the relationship between deforestation, and potentially resulting changes in erosion, and heavy metal release to the coastal zones.

Finally, with the discovery of New Zealand by James Cook in 1769 CE and the establishment of the European settlements around ~1845 CE (Augustinius et al., 2006), anthropogenic pressure on the environment increased significantly, and human impact in New Zealand caught up to that of Europe in only a few decades. The developments in agriculture, mining, construction and the simultaneous industrial revolution led to rapid alteration of the landscape. In the studied region on the more densely populated North Island, such a rapid development was potentially more pronounced. Here, the most

significant changes with regards to the near-coastal marine environment were probably caused by the extensive Kauri logging between 1830 to 1900 CE (Steward and Beveridge, 2010) as well as the beginning of the mining industry on the Coromandel Peninsula in the year 1867. In the Firth of Thames, sediment influx peaks correspond with large-scale deforestation associated with timber production, gold mining and land transformation to pastoral farming by European settlers (Healy, 2002; Swales et al., 2015).

Despite the dissimilar patterns in anthropogenic development and even though the two study areas are located on opposite sides of the globe, they share some important similarities. The North Sea and the Firth of Thames are both semi-enclosed marginal seas and are suspected to receive high inputs of heavy metals due to their proximity to highly-industrialised areas. Furthermore, the hydrodynamic conditions in the respective study sites result in trapping of suspended matter and consequently relatively high sedimentation rates (e.g., Reineck et al., 1967; Rodhe, 1987; Healy, 2002).

In summary, the North Sea region has been influenced by anthropogenic activity significantly longer and at a more gradual rate than the Firth of Thames. However, especially when investigated in combination, both regions offer the potential to untangle the differences of historical human impact on coastal areas in high-resolution sediment records.

1.3 Scientific Objectives and Approach

The goal of this thesis is to decode the history of heavy metal pollution in near-coastal marine sediments and their influence on the local benthic biota in two key study areas – the Firth of Thames in New Zealand and the wider North Sea area, with particular emphasis on the German Bight and the Skagerrak.

The Firth of Thames was selected to conduct the first baseline study to reconstruct the region's pollution history (Chapter 4). The main objective was the determination of the natural background values with regards to the heavy metal content of Zn and Pb in the marine bulk sediments. Secondly, this study aims to resolve the temporal onset and identify the most likely source of enhanced heavy metal release in the Firth of Thames, and thereby evaluate the environmental status with regards to marine sediment pollution. To answer the question of the temporal and spatial distribution in a quantitative manner, X-ray fluorescence analysis (XRF) was performed on eight gravity cores retrieved from the study area in the southeastern Firth of Thames. A stratigraphic framework based on radiocarbon ages and pollen data resolves the temporal aspect of the previously posed questions.

In the German Bight, several studies on the historical heavy metal accumulation have been conducted (Förstner and Reineck, 1974; Irion et al., 1987; Boxberg, 2017). While baseline studies on heavy metal accumulation in marine sediments certainly build the foundation to understand human impacts, they provide few clues about the cause-effect relationship with the local biota. Foraminifera are widely accepted as sensitive indicators for changing environmental conditions. The biological response to increased heavy metal inputs depends on several factors, such as adaptation to environmental conditions,

compensatory mechanisms or the occurrence of additional stressors like eutrophication (e.g., Alve, 1995). Therefore, this research focuses on the question if foraminifera tests can serve as an ecotoxicological monitoring tool to unravel the biological effects of heavy metal pollution during the past (Chapter 5). Their suitability is assessed using an approach that combines the occurrence of foraminiferal test deformities and the chemical signal of heavy metals in the tests with bulk sediment Pb contents on two gravity cores from the Helgoland Mud Area.

As the main sediment depocentre of the North Sea (van Weering et al., 1993), the Skagerrak has the potential to record a combined regional signal of the anthropogenic heavy metal release of the entire North Sea region. To complement the nearshore studies of heavy metal pollution in the Firth of Thames and the German Bight, this study investigates if and to what extent heavy metal deposition occurs in deeper marine settings. To do so, a transect of three short cores were analysed for their bulk sediment Zn contents using energy-dispersive XRF (Chapter 6). The subsequent goal is the assessment of the environmental state according to the OSPAR background contents and to determine whether the Zn signal is of rather regional or local origin.

Together, these three projects provide new insights regarding the questions if, when, and to what extent anthropogenically released heavy metals enter coastal marine environments. Furthermore, it will be shown how their presence in nearshore environments affected local biological (foraminiferal) assemblages throughout the past.

1.4 Thesis outline and declaration of authors contributions

This dissertation was conducted within the framework of the International Research Training Group INTERCOAST – "Integrated Coastal Zone and Shelf-Sea Research", an interdisciplinary project based at the University of Bremen (Germany) in collaboration with the University of Waikato (New Zealand). In the course of this programme, twelve PhD-students collaborated to enhance the understanding of social, legal, and environmental aspects in coastal research. Training early stage researchers in an interdisciplinary work environment was a primary objective of INTERCOAST. Additionally, an obligatory research stay of several months at the University of Waikato allowed the participants to gain international research experience and extend the study area to the southern hemisphere. Therefore, this resulting dissertation is a comparative study on the history of anthropogenic heavy metal input into the coastal zone in New Zealand (Firth of Thames) and Northern Europe (North Sea).

The thesis is composed in a cumulative form. In Chapter 2 the regional setting of the three different study areas is introduced. Chapter 3 provides a comprehensive description of the materials and methods used for this dissertation. The results of the performed research are presented and discussed in three individual manuscripts (Chapter 4 to 6). They address the scientific objectives stated above and build the main body of the thesis. Chapter 7 synthesises the findings and offers an outlook for potential future research.

The three stand-alone manuscripts are or will be submitted to peer-reviewed international scientific journals and were prepared in collaboration with other researchers. In the following, a brief outline provides an overview of the content and authors contributions:

Manuscript 1 (Chapter 4)

Historical Development of Heavy Metal Contamination in the Firth of Thames, New Zealand

Sandy Boehnert, Salvador Ruiz Soto, Bethany Fox, Yusuke Yokoyama and Dierk Hebbeln

Submitted to Geo-Marine Letters

The manuscript reconstructs the history of heavy metal release into the Firth of Thames using X-ray fluorescence on eight gravity cores. The determination of the temporal onset of elevated levels of Pb and Zn allows the identification of local 'pristine' natural background contents of these elements in the marine sediment. These baseline values are of key importance to evaluate the human impact on the study area in a quantitative manner. Additionally, the results provide the possibility to constrain the potential source of increased heavy metal release in the Firth of Thames.

Authors contributions:

S. Boehnert – design of the study, planning and conducting of field campaign, macroscopic core description, sampling, picking of foraminifera for radiometric dating, performing grain size analysis and heavy metal analysis (by portable XRF and XRF core scanner), sample preparation for WD-XRF analysis, data processing and evaluation, generation of figures and writing of the manuscript;

S. Ruiz Soto – execution of pollen analysis including sample preparation, provided a paragraph on the method description for the manuscript;

B. Fox – support for planning of coring campaign and discussion of results;

Y. Yokoyama – radiocarbon dating on bulk organic matter;

D. Hebbeln – supervision of the project, design of the study, discussions on design of coring campaign and interpretation of data.

All co-authors further contributed by commenting and improving earlier versions of the manuscript.

Manuscript 2 (Chapter 5)

Test Deformation and Chemistry of Foraminifera as Response to Anthropogenic Heavy Metal Input

Sandy Boehnert, Anniken R. Birkelund, Gerhard Schmiedl, Henning Kuhnert, Gerhard Kuhn, Christian Hass and Dierk Hebbeln

To be submitted to Marine Pollution Bulletin

This manuscript addresses the question to what extend fossil benthic foraminiferal test are suitable indicators for historical heavy metal pollution. Two sediment cores from the Helgoland Mud Area are compared with respect to bulk sediment Pb content, foraminiferal test chemistry and the occurrence of

abnormal test morphologies. This combined approach provides insights about ecotoxicological effects of exposure to increased sediment heavy metal contents.

Authors contributions:

S. Boehnert – conception of study, sampling, picking of foraminifera, sample preparation for and conduction of ICP-MS analysis, processing and interpretation of results, data visualisation, preparation of the manuscript;

A. Birkelund – provided majority of data on deformed foraminiferal tests and foraminifera diversity;

G. Schmiedl – provided further data on foraminifera deformation and discussion on results;

H. Kuhnert – supervision of and help with sample preparation for and measurements on ICP-MS;

G. Kuhn – provided XRF core scanner data for HE 215/4-2;

C. Hass – provided XRF core scanner data for HE 215/4-2;

D. Hebbeln – supervision of the project, conception of study, discussions on data interpretation.

All co-authors further contributed by commenting and improving earlier versions of the manuscript.

Manuscript 3 (Chapter 6)

Evaluation of Human Impact in the Skagerrak applying the OSPAR Assessment Criteria

Sandy Boehnert and Dierk Hebbeln

In preparation

The third manuscript intends to unravel if and to what extend heavy metal pollution is affecting deep marine settings. Heavy metal contents of bulk sediment are determined by X-ray fluorescence analysis on a transect of three short cores. In order to assess the status of anthropogenic impact exemplified by Zn, normalisation of the Zn contents to 5% Al was performed according to the OSPAR guidelines. The study presents the evaluation of heavy metal pollution in the Skagerrak and provides a critical view on the applied OSPAR assessment criteria.

Authors contributions:

S. Boehnert – performing all sample preparations and analyses, data processing and evaluation, generation of figures and drafting of the manuscript;

D. Hebbeln – supervision of the project, contribution by discussing and interpreting analytical data, helped to improve an earlier version of the manuscript.

Chapter 2 Regional Setting

2.1 Firth of Thames

The Firth of Thames is a shallow, semi-enclosed marine embayment (Naish et al., 1993) situated at the northeastern tip of the North Island of New Zealand (Figure 2.1). With an east-west extension of 20 km and a north-south length of 30 km, the Firth of Thames covers an area of about 600 km². The water depth reaches 35 m in the north and decreases towards the coastline in the south, where a ~70 km² intertidal zone is located (Swales et al., 2016).

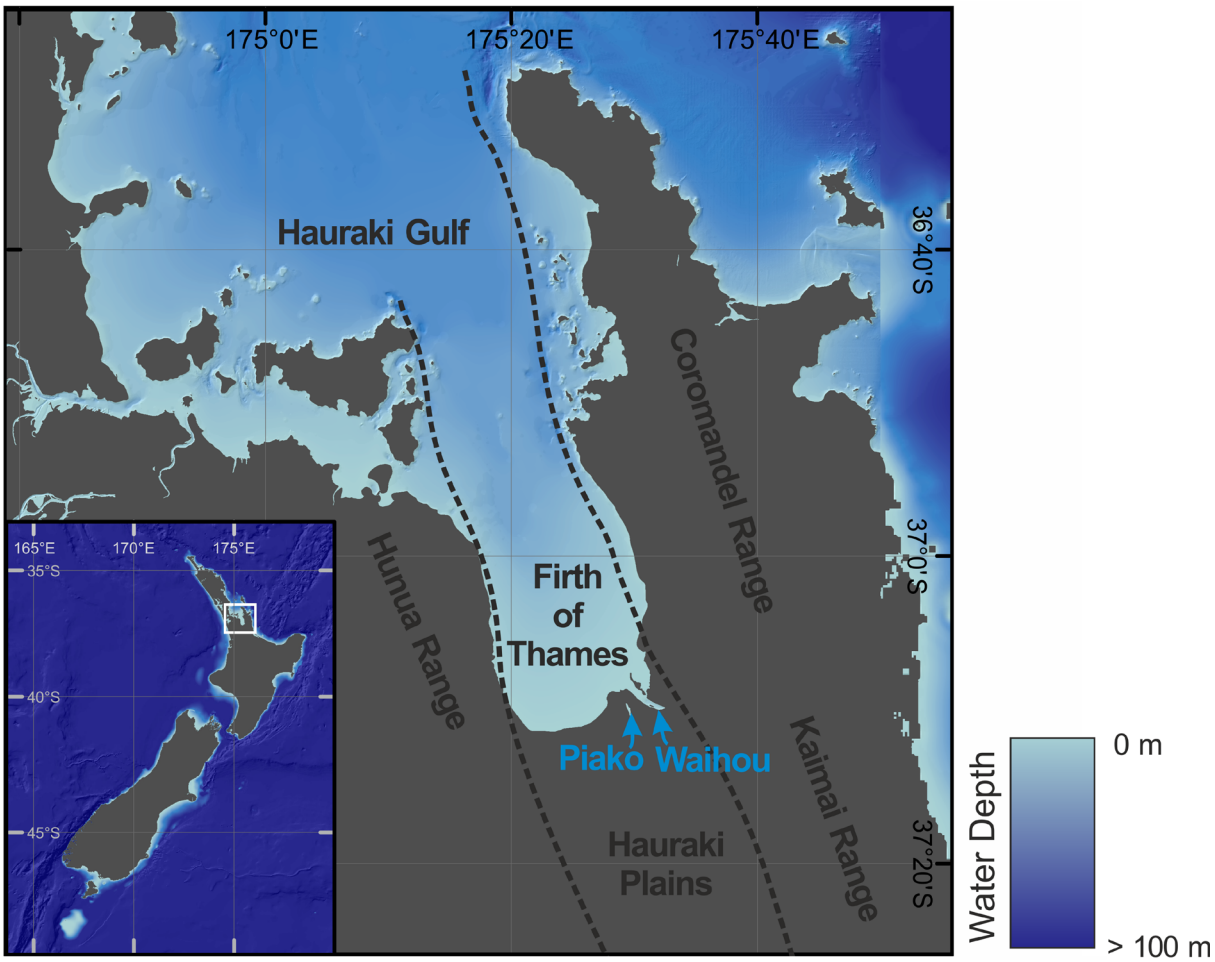

Figure 2.1 Bathymetric map of the Firth of Thames. Dashed line indicates the Hauraki Rift (after Livingston, 1987). Inserted map shows the location of the Firth of Thames in New Zealand (white square). The map was created with data derived from the National Institute of Water and Atmospheric Research Ltd (Mackay et al., 2012; Mitchell et al., 2012).

The Firth of Thames is part of the tectonically active north-south striking Hauraki Rift, forming the Hauraki Depression, which consists of the Hauraki Plains in the south, the Firth of Thames in the centre and continues into the Hauraki Gulf in the north (Persaud et al., 2016). The rift is bounded by the Coromandel-Kaimai Range in the east and the Hunua Range in the west (Hochstein and Nixon, 1979). It has been active since the late Neogene, and the resulting Hauraki Depression is estimated to be filled with up to 3 km of Tertiary and Quaternary terrestrial sediments (Hochstein and Nixon, 1979). The

surrounding bedrock consists of Mesozoic meta-greywackes and Cenozoic volcanics (Persaud et al., 2016). Particularly interesting for the scientific objectives of this thesis is the Coromandel Range. Its Jurassic meta-greywackes, overlain by Miocene andesitic rocks and capped by Pliocene rhyolitic rocks, are locally altered by hydrothermal solutions, resulting in either disseminated-porphyry or epithermal-vein mineralisation; both types are gold-bearing (Livingston, 1987). Moreover is the Coromandel Range characterised by a steep topography (more than 600 m) and high rainfall rates, and therefore potentially high rates of erosion (Livingston, 1987).

Hydrodynamically, the Firth of Thames is a partially- to well-mixed, tidally-dominated estuary with low-wave energy (Naish et al., 1993). Tides are semi-diurnal with spring- and neap-tidal ranges averaging around 2.9 and 2.2 m, respectively (Swales et al., 2016). Typical tidal currents are ≤ 0.3 m s^{-1} (Black et al., 2000). Major sediment supply into the Firth of Thames is derived from the Waihou River (160 kt/yr sediment) and Piako River (30kt/yr sediment) (Hicks et al., 2011), which enter the Firth from the south.

With a catchment area of 1,984 km^2 (Hicks et al., 2011), the Waihou River is the largest river in the Coromandel Region with several tributaries draining gold mining districts in the Coromandel Range (e.g., Golden Cross, Tui mine) (Webster, 1995). The highest loads of suspended sediment occur off the mouth of the Waihou River on the eastern side of the Firth (van Leeuwe, 1991). The prevailing hydrodynamic conditions cause the transport of suspended sediment northward along the east coast before swinging to the west. Simultaneously, the residual tidal current on the west coast is southward directed, resulting in a counter-clockwise circulation pattern that causes suspended silts and clays to remain trapped within the southern Firth (Healy, 2002).

However, the river discharged suspended matter accounts for only ~40% of the 430 kt/yr of sediment presently accumulated in the southern Firth of Thames (Green and Zeldis, 2015). Green and Zeldis (2015) attribute the remaining ~60% to the wave- and current-induced reworking of old sediments accumulated during large-scale mining operations and deforestation in the late 1800s and early 1900s.

Late Holocene sediments in the Firth of Thames can be distinguished in three lithofacies: (i) laterally extensive greenish muds with occasional interbedded shell layers, (ii) near-shore siliciclastic sands at the Waihou River mouth, and (iii) near-shore delta fan gravels related to streams draining the Coromandel Range. The mud facies is dominated by the clay and silt fraction and consists of volcanic glass, smectite and halloysite, with minor amounts of illite and allophane (Naish, 1990).

2.2 North Sea - The bigger picture

The North Sea is a shallow marginal sea in the east of the North Atlantic, located on the northwestern European shelf (Figure 2.2). It covers an area of about 750,000 km^2 (including the English Channel, fjords and estuaries), extending from 51°N to 61°N and 5°W to 11°E (OSPAR, 2000). Bounded by Great Britain to the west and continental Europe to the south and east, the North Sea is characterized as semi-

enclosed. The main connection with the North Atlantic occurs between Scotland and Norway in the north and through the English Channel in the southwest. In the east, it is connected to the Baltic Sea via the Kattegat. Additionally, freshwater is discharged along the coastline from rivers, the major ones being the Humber (Estuary), Thames, Meuse, Rhine, Weser, Elbe and Glomma. In total, rivers drain a densely-populated and highly-industrialised catchment area of 841,500 km² and transport 296-354 km³ of run-off per year into the North Sea (OSPAR, 2000). Based on water depth, the North Sea can be subdivided into three regions:

1) The shallow southern part with mean water depths of less than 50 m, including the study site in the Helgoland Mud Area;
2) The central part characterised by water depths between 50 and 200 m;
3) The deeper northern North Sea with water depths of up to 700 m, comprising the Norwegian Trench and the Skagerrak.

The circulation pattern in the North Sea is primarily driven by the North Atlantic Current entering between Scotland and Norway, fuelling a counter-clockwise circulation (Figure 2.2). While parts of the Atlantic water masses follow the bathymetry via the Tampen Bank Current (TBC) and Southern Trench Current (STC) directly into the Skagerrak (Rodhe, 1998), other parts follow the coastline around the entire North Sea. This leads to modifications in water mass composition (e.g., chemistry, sediment load) by mixing with Atlantic water entering through the English Channel and freshwater discharges by rivers, with its riverine suspended matter and pollution loads. The altered North Sea water is transported northward along the Danish coast by the South and North Jutland Current (SJC, NJC) and eventually reaches the Skagerrak. Further water mass modifications occur in the eastern Skagerrak, where the water deriving directly from the North Atlantic and the one transported by the North Jutland Current meet the less saline water mass conveyed by the Baltic Current (BC) from the south. The resulting water mass deviates counter-clockwise towards the northwest and west, following the Norwegian coast as the Norwegian Coastal Current (NCC) (Longva and Thorsnes, 1997; Rodhe, 1998) (Figure 2.2). The circulation pattern is interconnected with the atmospheric circulation, such as the variation in the strength of westerly winds controlled by the North Atlantic Oscillation (NAO) (Hurrell, 1995). For example, Winther and Johannessen (2006) investigated the annual variability of the Atlantic inflow resulting from changes in the strength of westerlies, while Brückner and Mackensen (2006) studied a 1200 years sediment record in the Skagerrak and linked the deep-water renewal to the NAO.

This complex circulation transports about 40 million tons of suspended matter every year throughout the North Sea. The suspended matter is largely sourced by the North Atlantic via the NAC between Scotland and Norway as well as the English Channel with each contributing ~30% of the annual supply. Rivers account for only ~15%, with the remaining suspended matter deriving from the Baltic Sea, the atmosphere, primary production and processes like seafloor or coastal erosion (Eisma and Kalf, 1987).

Because of high-energy tidal currents and wave actions especially in the shallower regions of the North Sea, redistribution of suspended matter is the predominant process influencing sedimentation patterns. Permanent accumulation occurs only in a few sediment depocentres; the most important being the Skagerrak, followed by the Helgoland Mud Area and nearshore areas such as tidal flats, river mouths and lagoons (Eisma and Kalf, 1987; Lohse et al., 1995).

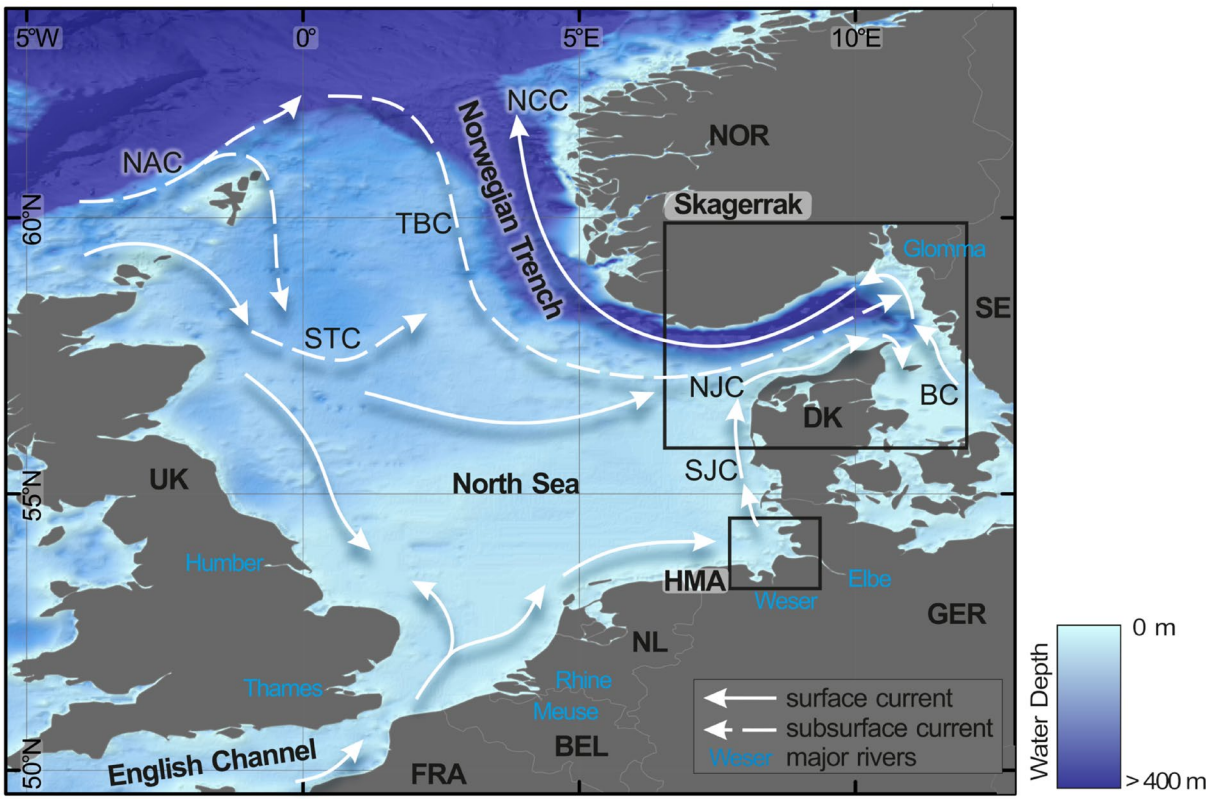

Figure 2.2 Bathymetric map of the North Sea with indicated counter-clockwise surface currents (solid arrows), subsurface currents (dashed arrows) and locations of the study areas (black squares). Countries: BEL – Belgium, DK – Denmark, FRA – France, GER – Germany, NL – Netherlands, NOR – Norway, SE – Sweden, UK – United Kingdom; Study sites: Helgoland Mud Area (HMA), Skagerrak; Currents: BC – Baltic Current, NAC – North Atlantic Current, NCC – Norwegian Continental Current, NJC – North Jutland Current, SJC – South Jutland Current, STC – Southern Trench Current, TBC – Tampen Bank Current. Modified from Nordberg (1991). The map was created with data derived from the EMODnet Bathymetry portal - http://www.emodnet-bathymetry.eu.

2.2.1 Helgoland Mud Area

The Helgoland Mud Area (HMA) is a prominent depocentre for fine sediments in the German Bight, located southeast of the island Helgoland (Figure 2.3). Covering an area of ~500 km², with a mean water depth of 20 m, the HMA accumulated up to 30 m of Holocene sediments (Figge, 1981; von Haugwitz et al., 1988). The sea floor rises from about 30 m water depth in the western part with dominating clayey silts, to ~15 m water depth in the eastern part with an increasing sand content (Hertweck, 1983).

The evolution of the Helgoland Mud Area is still not fully understood. Following the theory of Hertweck (1983) and von Haugwitz et al. (1988), the Elbe-Weser estuary was located in the region of the HMA during the early Holocene. This palaeo-estuary was blocked to the north by a morainic ridge (today the so-called Steingrund), stretching from Helgoland to the Eiderstedt Peninsula. After the sea level rise

during the Flandrian Transgression (6,000 years ago) to -15 m relative to modern sea level, the former estuary was transformed into a small bight, accumulating reworked marine sediments from the Pleistocene and fluvial sediments from the Elbe and Weser. Between 2,000-3,000 years ago (Irion et al., 1987) and 1,500 years (von Haugwitz et al., 1988), the previously existing barrier in the north was breached by erosion (von Haugwitz et al., 1988). As a result, the present-day circulation pattern in the German Bight was established with a longshore residual current flowing from the west to the east, subsequently deviating north along the coastline. It was suggested that this hydrographic change was the main cause for the beginning accumulation of suspended particulate matter (SPM) in the HMA (Reineck et al., 1967).

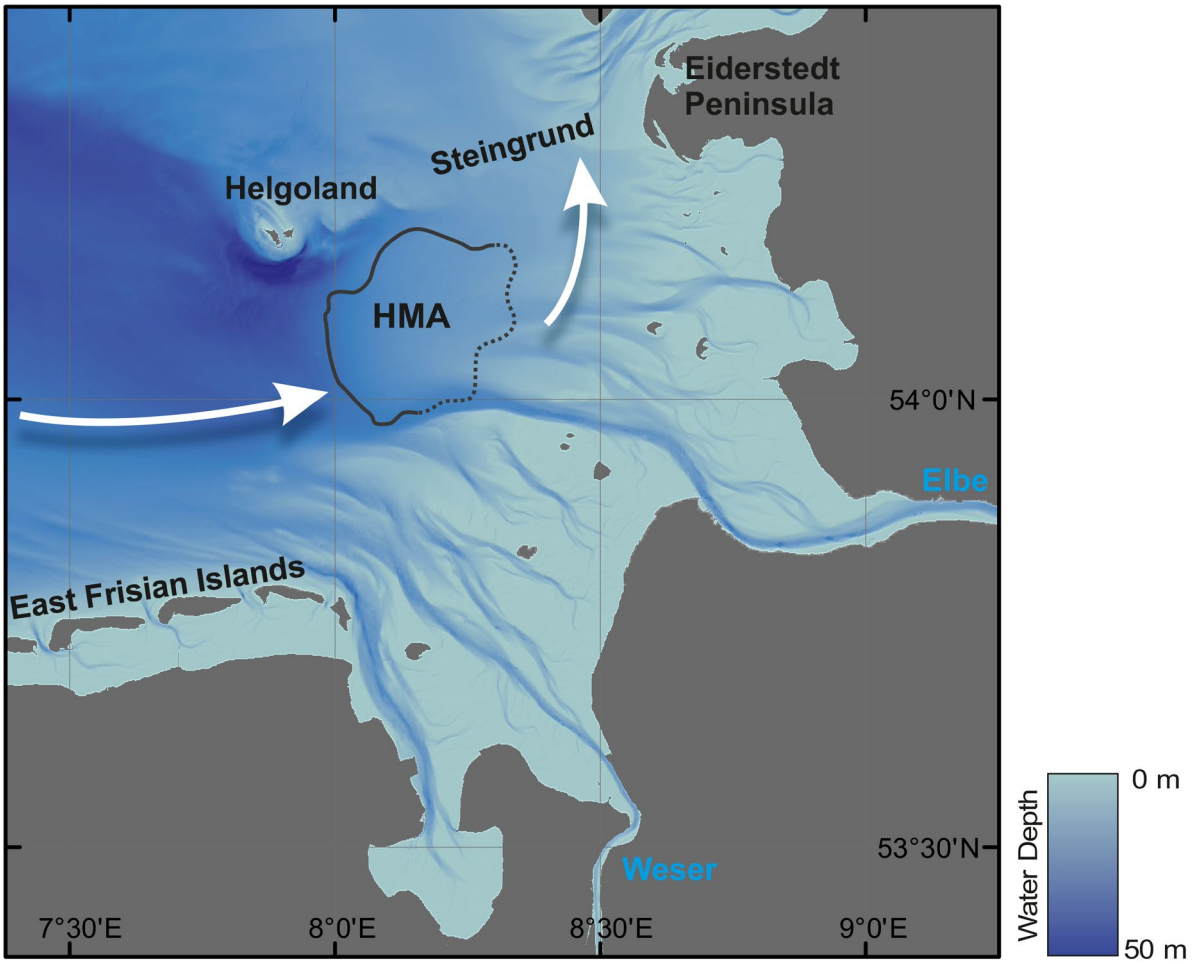

Figure 2.3 Bathymetric map of the southeastern German Bight with indicated residual currents (arrows) and the location of the Helgoland Mud Area (HMA; outlined by the solid (confirmed limit) and dotted (estimated limit) black line). Modified from von Haugwitz et al. (1988). The map was created with data derived from the EMODnet Bathymetry portal - http://www.emodnet-bathymetry.eu.

Reported sedimentation rates vary between 2 mm/year (Reineck, 1963) and 7.7 mm/year (Dominik et al., 1978). Hebbeln et al. (2003) observed a marked drop in the sedimentation rate from > 13 to 1.6 mm/year at around 1250 CE and related this to the cessation of strong land loss of the island of Helgoland at the same time. However, the origin of the deposited fine sediments is still debated. Some authors argue that the suspended matter does not derive from rivers because the fluvial sediments are

trapped directly in the estuaries (Irion et al., 1987) or by-passed towards the Skagerrak (Wirth and Wiesner, 1988). In contrast, Dellwig et al. (2000) postulate that the SPM originates from the back-barrier systems of the East Frisian Islands. More recent studies attribute the deposited fine material at least partially to riverine input based on provenance analysis (Pache et al., 2008) or linking heavy metal signals in the HMA to mining activity in the river catchment (Hebbeln et al., 2003; Boxberg, 2017).

2.2.2 Skagerrak

The Skagerrak is the northeastern extension of the North Sea and inner part of the Norwegian Trench, bordered by the coasts of Denmark, Sweden and Norway (Figures 2.2 and 2.4). With a mean water depth of 210 m and a maximum water depth of about 700 m in the central part, the Skagerrak is the only area in the North Sea with deep marine conditions. It is also the main depocentre for fine suspended particulate matter in the region (e.g., Eisma and Kalf, 1987). The bathymetry of the Skagerrak is characterised by an asymmetric shape, with a relatively gentle convex southern slope and a steep northern slope with irregular topography, indicating significant sediment supply from the south (e.g., Svansson, 1975; van Weering et al., 1993; Kuijpers et al., 1993). The combination of the slope and shelf morphology makes the Skagerrak a unique feature of the North Sea (van Weering et al., 1993).

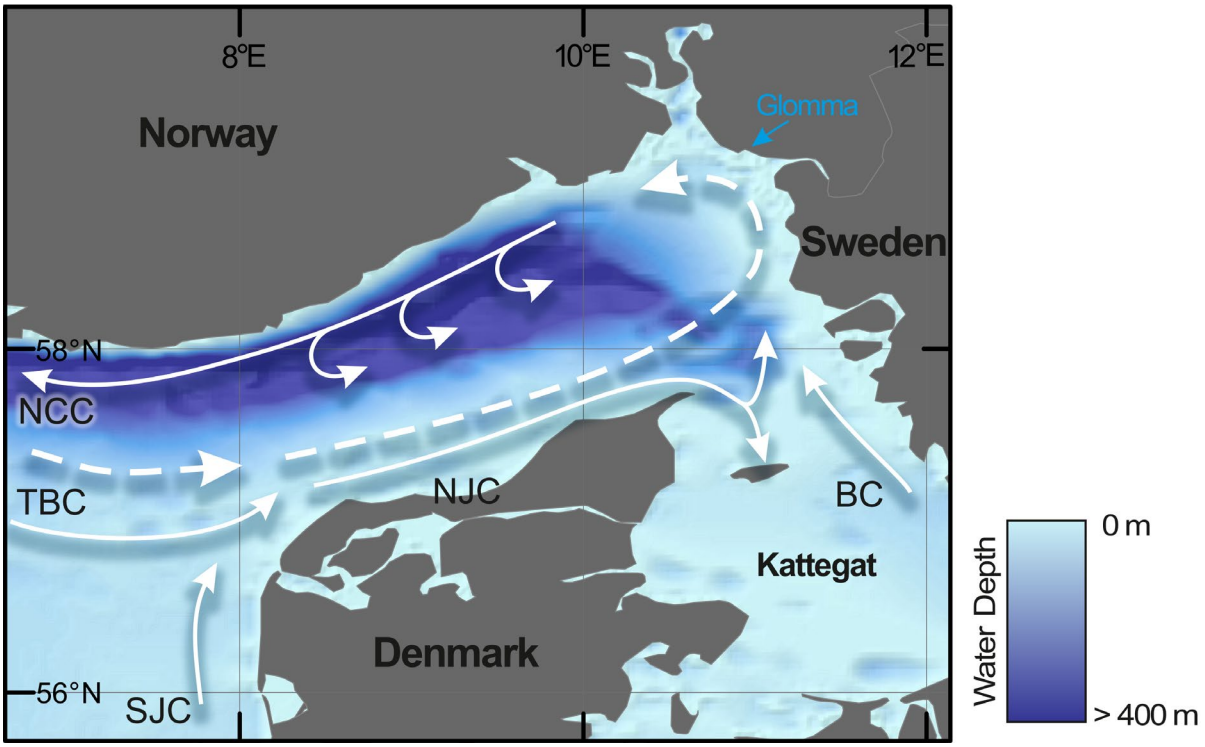

Figure 2.4 Bathymetric map of the Skagerrak with indicated surface (solid arrows) and subsurface (dashed arrows) circulation pattern. Currents: BC – Baltic Current, NCC – Norwegian Continental Current, NJC – North Jutland Current, SJC – South Jutland Current, TBC – Tampen Bank Current. Modified from Nordberg (1991). The map was created with data derived from the EMODnet Bathymetry portal - http://www.emodnet-bathymetry.eu.

Hydrodynamic conditions in the Skagerrak are characterised by the inflow of water masses from the North Atlantic (Tampen Bank Current, Southern Trench Current), the southern North Sea (South and

North Jutland Current) and the outflow of Baltic waters (Baltic Current). The water masses can be distinguished according to their salinity – with only 20 to 30 psu for the less saline Baltic waters, 31 to 35 psu for the North Jutland Current and >35 psu for the waters deriving from the North Atlantic (Rodhe, 1987). Even though the waters from the southern North Sea display the highest suspended matter load, the majority of sediment is derived from the large volume of low concentrated Atlantic inflow (Eisma and Kalf, 1987, Gyllencreutz et al., 2006). Additional inputs are received from the Baltic Sea and the Scandinavian mainland. However, suspended particulate matter discharged from Swedish and Norwegian rivers remains largely trapped in the fjords (Pederstad et al., 1993).

The mixing of the water masses results in a counter-clockwise circulation pattern forming a vortex with significantly reduced current speeds, allowing the fine suspended matter to deposit in the Skagerrak (Eisma and Kalf, 1987; Rodhe and Holt, 1996). Thus, the Skagerrak serves as a natural sediment trap (Rodhe, 1987).

Sedimentation rates in the Skagerrak vary considerably between 1 and 10 mm/yr (van Weering et al., 1993) but were locally reported to be up to 30 mm/yr (Fält, 1982). Fine-grained muddy and silty sediments are only deposited in water depths exceeding 70 m (Kuijpers et al., 1993). In the shallower areas, especially north of Jutland (Denmark), sediments consist predominantly of sand (Pederstad et al., 1993). Mineralogy of the fine fraction is mainly composed of illite and smectite, with minor proportions of chlorite, kaolinite, quartz and feldspar (Pederstad et al., 1993).

The circulation pattern is furthermore influenced by large-scale atmospheric forcing, i.e. the North Atlantic Oscillation (NAO). During times of positive NAO with stronger westerly winds, the circulation in the Skagerrak (and the entire North Sea) is enhanced, while periods of negative NAO are characterised by weaker winds from the west and an inhibited water circulation (Hurrell, 1995; Brückner and Mackensen, 2006). Tidal influences in the Skagerrak, with a range of about 20 cm, have a minimal effect on the hydrodynamic regime (Svansson, 1975).

Chapter 3 Material and Methods

3.1 Material

The research conducted for this thesis relies mainly on geochemical analysis of bulk sediment and benthic foraminifera tests from a total of ten marine gravity cores (GCs) and three multicores (MUCs): eight gravity cores from the southeastern Firth of Thames, two gravity cores from the Helgoland Mud Area as well as three multicores from the central Skagerrak. Details on core locations, water depths and lengths are given in Table 3.1.

The eight sediment cores in the Firth of Thames were collected during a field campaign from 20 to 22 March 2017 with a QR300 Vibracore, aboard the crane barge *Quest* leased from *Bay Marine Works Limited*. The selection of the coring sites was based on the assumption that the highest input of heavy metals would occur through the Waihou River in the southeast and a potentially significant contribution from the small streams of the Coromandel Range in the east of the Firth of Thames. Accordingly, the coring sites were located in the southeast of the embayment to obtain a proximal to distal gradient from the Waihou River mouth as well as from the adjacent gold mining area on the Coromandel Peninsula.

The vibracore was used in a gravity mode to not disturb the very soft sediment with the vibrations, as the sediments in the Firth of Thames were soft enough to let the liner sink in with the weight of the 150 kg vibrating head. The QR300 Vibracore generally is capable of recovering cores with a diameter of 76 mm and a length of up to 6.0 m in unconsolidated sediments in water depths of up to 300 m. However, the setup used for our sampling campaign allowed a maximum achievable core length of 3 m, which, based on previously published sedimentation rates at the study site (Naish, 1990), were sufficient for our scientific objectives and also easier to operate.

The recovered sediments cores were sealed with fitting PVC end caps and electrical tape after the removal of the core catchers and then carefully labelled. The cores with lengths between 1.94 and 2.58 m were retrieved in water depths from 0.4 to 8.5 m. In general, the sediments consist of homogeneous olive-green silt and clay with a minor proportion of fine sand. Near the Waihou River mouth, the sand fraction is dominant, and several layers contain significant shell debris and in situ shells.

In the Helgoland Mud Area (HMA) two sediment cores were investigated. Gravity core (GC) GeoB 4801-1 was collected in 25 m water depth from aboard RV METEOR in 1997, with a total core length of 11.41 m. The sediment consists of brownish olive-green mud with a minor sand fraction content. GC HE 215/4-2 was collected from aboard RV Heincke in 2004, and 4.86 m of sediment core were recovered from 23 m water depth. The sediment consists of homogeneous olive-brown mud with some darker brown layers.

The multicores (MUCs) GeoB 6001-2, GeoB 6002-2, and GeoB 6003-1 from the Skagerrak were retrieved during RV Meteor cruise M45/5 in 1999. Multicores are used to obtain undisturbed surface

sediment samples. From 308 to 460 m water depth, between 36- and 43-cm long sediment cores were recovered. The sediments were directly subsampled into 1 cm slices aboard and stored at 4°C in the MARUM core repository prior to analysis. All three MUCs showed a very similar lithology of olive-grey silty clay.

Table 3.1 Information on the ten sediment cores used in this study, including study area, specific GPS locations, mean water depth and recovered core length. GC – gravity core, MUC – multicore.

	Core identification	Latitude	Longitude	Water depth (m)	Core length (m)	Type
Firth of Thames	NZ-M-1	037° 02.7' S	175° 30.5' E	2.6	2.47	GC
	NZ-M-2	037° 07.1' S	175° 30.7' E	1.0	2.41	GC
	NZ-M-3	037° 09.0' S	175° 30.8' E	0.4	1.94	GC
	NZ-M-4	037° 08.3' S	175° 26.7' E	2.2	2.50	GC
	NZ-M-5	037° 04.7' S	175° 28.0' E	5.6	2.44	GC
	NZ-M-6	037° 06.3' S	175° 25.7' E	4.0	2.58	GC
	NZ-M-7	037° 01.4' S	175° 27.1' E	8.5	2.46	GC
	NZ-M-8	036° 59.6' S	175° 27.8' E	7.8	2.51	GC
Helgoland Mud Area	HE 215/4-2	054° 04.3' N	008° 04.4' E	23	4.86	GC
	GeoB 4801-1	054° 06.7' N	008° 02.2' E	25	11.41	GC
Skagerrak	GeoB 6001-2	058° 09.4' N	009° 48.2' E	460	0.42	MUC
	GeoB 6002-2	058° 04.8' N	009° 37.2' E	428	0.43	MUC
	GeoB 6003-1	057° 58.3' N	009° 23.2' E	308	0.36	MUC

3.2 Methods

3.2.1 Age Determination

For the reconstruction of past developments on a historical or even geological time scale, precise age estimates are an essential requirement to link specific events to a specific time. In the course of this thesis, a stratigraphic framework based on radiocarbon dating and pollen analysis was constructed for the study in the Firth of Thames (Chapter 4). ^{210}Pb dating, a common tool for determining ages up to 150 years, is rather difficult to apply on the southern hemisphere as the depositional flux is markedly lower in comparison to the northern hemisphere due to the lower land to sea ratio (e.g., Baskaran, 2011). Age models based on AMS ^{14}C and ^{210}Pb dating were already available for the two cores analysed in the Helgoland Mud Area (Chapter 5) (HE 215/4-2: Serna et al., 2010; GeoB 4801-1: Hebbeln et al., 2003). In addition, the age model for core GeoB 4801-1 has been further improved by linking the record to instrumental (Scheurle and Hebbeln, 2003) and historical (Scheurle et al., 2005) data. For the Skagerrak, the age-depth relationship was derived from the previously published sedimentation rate of 1.8 mm/year obtained by ^{210}Pb dating on gravity core GeoB 6003-2 (Hebbeln et al., 2006), and used correspondingly for the analysed multicore GeoB 6003-1 (Chapter 6).

Radiocarbon Dating

Radiocarbon dating is a standard technique used to determine the age of materials containing organic carbon by measuring ^{14}C concentrations and covers the time span between approximately 50,000 years

BCE and 1950 CE. Carbon naturally exists as two stable isotopes ^{12}C (98.89%) and ^{13}C (1.11%) as well as one radiogenic isotope ^{14}C ($1.176x10^{-12}$%). Radiocarbon (^{14}C) is continuously generated in the lower stratosphere through the collision of cosmic ray neutrons with atmospheric nitrogen isotopes (^{14}N). Thereby, ^{14}N emits one proton and is transformed into ^{14}C. The newly formed radiocarbon isotope is oxidised and becomes a part of the atmosphere as $^{14}CO_2$.

All organisms in direct contact with the atmosphere assimilate carbon of the same isotopic composition as the atmosphere through photosynthesis and the food chain. This balance is retained as long as they are alive. After death, the ^{14}C content incorporated in their organic matter (e.g., shells, bones, wood) decreases constantly because of its radioactive decay. Knowing that the half-life time of radiocarbon is 5,730 ± 40 years (Godwin, 1962), an age can be calculated from a measured ^{14}C concentration (usually relative to ^{12}C) and its comparison to a modern standard.

In 1949, Willard Libby introduced the radiocarbon dating method under the conventional assumption that the radiocarbon concentration in the atmosphere stayed constant in the past. However, atmospheric radiocarbon concentrations are subject to prevailing natural fluctuations, for example due to changes in sunspot activity and intensity of the earth's magnetic field. Such fluctuations cause variations in the flux of cosmic rays and hence the formation of ^{14}C (e.g., Bard, 1998). Other, non-naturally-occurring variations are for example caused by the combustion of fossil fuels (Suess, 1955) or atomic bomb tests (Rafter and Fergusson, 1957).

Therefore, a calibration is needed to convert radiocarbon ages into calendar ages (e.g., Damon and Peristykh, 2000). For this purpose, calibration curves are built based on ^{14}C dates on materials with known ages independently derived, such as tree rings (e.g., Reimer et al., 2013). The nuclear tests in the 1950s generated excess ^{14}C (e.g., Nydal, 1963). Due to the artificial change in isotopic composition, the calendar year 1950 was set as the reference year 'zero before present'. Hence, all ages after calibration are reported in calibrated ^{14}C years before present (0 cal BP = 1950 CE).

Another issue that has to be addressed for marine samples is the correction of the so-called reservoir age (Reimer et al., 2013). Samples that obtain their carbon from another source (e.g., a deep-water mass) than directly from the atmosphere appear older than they actually are. This is caused by a delayed exchange between different carbon reservoirs, and the resulting disequilibrium with the atmosphere. The contained radiocarbon already decays without being constantly replaced by newly formed ^{14}C. The time-dependent global average reservoir age of the ocean is about 400 years (e.g., Stuiver et al., 1998a) and is incorporated in marine calibration curves (e.g., MARINE13, Reimer et al., 2013). However, on a regional scale, the reservoir age might deviate significantly as a result of the mixing of water masses (e.g., upwelling, ocean currents). This should be taken into account if the local reservoir age correction (ΔR) is known.

For the Firth of Thames, New Zealand, radiocarbon dating of mixed benthic foraminifera (n=12), bulk sediment organic matter (n=18) and unidentified marine shells (n=3) was performed. Bulk organic matter usually constitutes a mixture of organic carbon from several sources (e.g., Eglinton et al., 1996), resulting in relatively large age uncertainties. Furthermore, sedimentary organic matter is rather buoyant (Bienfang, 1980) and therefore susceptible to resuspension. As the content of total organic carbon (TOC) in the Firth of Thames was unknown, sample size was about 30 g of wet sediment to ensure enough organic carbon for the measurement. Samples were kept in a drying cabinet for 72 hours at 40°C. Weights of the dry samples were about 10 g. This large volume led to the 'discovery' of embedded shells during sample preparation in the laboratory at the University of Tokyo. Therefore, these shells were additionally radiocarbon dated but remain unidentified. More radiocarbon dates were obtained on mixed benthic foraminifera, a very common material for dating marine sediment cores (e.g., Hebbeln et al., 2003). However, fossil foraminifera can be subject to transport and redeposition (e.g., Murray, 2006). In order to minimise the effects of reworked foraminifera on the radiocarbon ages, great care was taken only to select specimens not showing signs of transport (e.g., breakage, abrasion).

Samples were measured using accelerator mass spectrometry (AMS) at the Atmosphere and Ocean Research Institute at the University of Tokyo and at the MICADAS Laboratory at the Alfred-Wegener-Institute in Bremerhaven (see Chapter 4). Radiocarbon ages were converted to calibrated calendar ages using CALIB 7.1 (Stuiver et al., 2018) based on the Marine13 dataset (Reimer et al., 2013). No local reservoir correction ($\Delta R = 0$) was available.

Pollen Analysis for Age Determination

Pollen grains are highly resistant with respect to diagenesis, uniform in distribution and occur in large numbers, making them an ideal tool to reconstruct past vegetation from a geological record from marine, lacustrine or terrestrial sedimentary deposits (Faegri and Iversen, 1989). In addition, pollen records reflect secondary influences, such as climate history (e.g., Guiot et al., 1989; Elenga et al., 1994; Wilmshurst et al., 2007) and land use changes (e.g., Elliot et al., 1998, Yasuda et al., 2000; Li et al., 2008, and references therein).

New Zealand's isolated location in the southwestern Pacific Ocean led to the development of a uniquely pristine flora during the pre-human era. With the arrival of the Polynesian (c.1300 CE) and later the European settlers (c.1845 CE), the vegetation cover changed (Byrami et al., 2002). The Polynesian era is marked by a decline in hardwood pollen (e.g., *Podocarpus*) through widespread forest clearance. While the European settlers continued with deforestation of the hardwood forests, they additionally introduced exotic species like *Pinus* and *Olea europaea* (Heenan et al., 1999; Abrahim et al., 2013). Therefore, the first occurrence of these exotic pollen provides a stratigraphic marker in sediment cores, while changes in abundance deliver additional age information, such as land-use changes.

In the Firth of Thames, palynological analyses were conducted on 19 samples from core NZ-M-4 as a dating method (see Chapter 4). Sample preparation followed the standard laboratory procedures for the absolute frequency count approach by Faegri and Iversen (1989). Sediment (2 cm^3) was weighed, dried overnight in a stove at 62°C and weighed again prior to decalcification with diluted HCl (10%). Samples were then treated with HF (40%) for silicate dissolution for at least 24 hours. Consecutive stages of decanting and adding water were executed after the HCL and HF treatments, respectively, to remove the resulting dissolved phases. Once the chemical treatment was completed, samples were wet sieved over a 10 µm nylon screen using an ultrasonic bath to disaggregate organic matter. An aliquot (50 µL) was mounted on a permanent glass slide using glycerine jelly and the slide was sealed with paraffin wax.

For counting the absolute pollen frequencies, the exotic marker technique (Benninghof, 1962) was used by adding one calcium carbonate tablet of exotic *Lycopodium* spores (Batch N° 483216 Sept.2004) prior to the decalcification treatment. Adding a known number of marker grains (18.583 ± 1.708 *Lycopodium* spores per tablet) to a known sample volume (2cm^3) gives a constant numerical ratio of pollen to marker grains throughout the sample:

$$Total\ pollen = \frac{Pollen\ counted\ x\ Total\ Lycopodium\ spores\ added}{Lycopodium\ spores\ counted}$$ (after Stockmarr, 1971)

During the light microscopy analysis of the samples, only *Podocarpus*, *Pinus* and *Olea europaea* pollen and the number of marker grains were counted. Documenting only three taxa is acceptable in this case as the purpose of pollen analysis in the study was to determine the introduction of exotic species into New Zealand's flora as a stratigraphic marker. The concentration of pollen per gram was then calculated by dividing the total pollen by the sample dry weight.

Stratigraphic framework for the Firth of Thames

The aim of defining the stratigraphy of the three principal cores in the Firth of Thames (NZ-M-2, NZ-M-4 and NZ-M-7) was to differentiate between the European, the Polynesian, and the pre-human eras. The stratigraphy was mainly based on linear interpolation of 12 radiocarbon dates on mixed benthic foraminifera and the first occurrence of exotic pollen as distinct markers for the onset of the European era (hard constraints). As explained, foraminifera are considered to provide the most reliable ages of the radiocarbon dated materials due to their lower risk of resuspension. ^{14}C dates measured on bulk sediment organic matter were only used as a soft constraint as they consist of mixed organic carbon from different sources (Eglinton et al., 1996) and are prone to resuspension (Bienfang, 1980). Considering that the Firth of Thames is a semi-enclosed embayment and cores were retrieved in a coastal setting, it is likely that a significant proportion of the organic matter originates from land. Terrestrial bulk organic matter was reported to be generally older than the time of actual deposition because it has long residence times, depending on the size, morphology and climate of the catchment area (Blaauw et al., 2011). Therefore, radiocarbon dates based on organic matter serve only to constrain maximum ages. The dates of the

unidentified shells were only considered if they fit into the overall pattern because nothing was known about their ecology (epifaunal, infaunal). The reason why the shells are unidentified is, that they derive from the rather large samples for bulk sediment organic matter analysis and were only 'found' in the laboratory at the Atmosphere and Ocean Research Institute, University of Tokyo. There, the shells were used as additional dating material, but not identified. For more details on the age-depth relationship in the Firth of Thames, see Chapter 4.

3.2.2 X-Ray Fluorescence Spectrometry

X-ray fluorescence (XRF) analysis is a well-established, cost-effective and relatively fast method to determine elemental compositions of a sample, applicable in a wide range of disciplines (e.g., material science, earth and environmental science, archaeology, medicine, forensics) for both research and industry purposes.

The method is based on the underlying physical principle of excitation of electrons in a sample by an incident X-ray causing characteristic emission of secondary X-rays (Barkla, 1911). Irradiation of atoms with high-energy X-ray photons (e.g., from an X-ray tube) leads to ionisation, meaning that electrons are expelled from their orbitals (Figure 3.1). Generally, the most loose, outer valence electrons are most prone to ejection, but incident X-rays are energetic enough to expel more tightly-bound electrons from inner orbitals. The resulting voids are filled with electrons falling back from the outer orbitals, emitting the surplus of energy as secondary X-rays (fluorescence). The emitted X-rays are element-specific as radiation energy and wavelength depend on atomic number (Moseley, 1913). While energy-dispersive (ED-) XRF spectrometers detect the energy of a photon over a given energy spectrum, wavelength dispersive (WD-) XRF spectrometers distinguish between elements according to wavelength. The intensities of the recorded peaks by the XRF detector reflect the relative abundance of the elements contained in the sample.

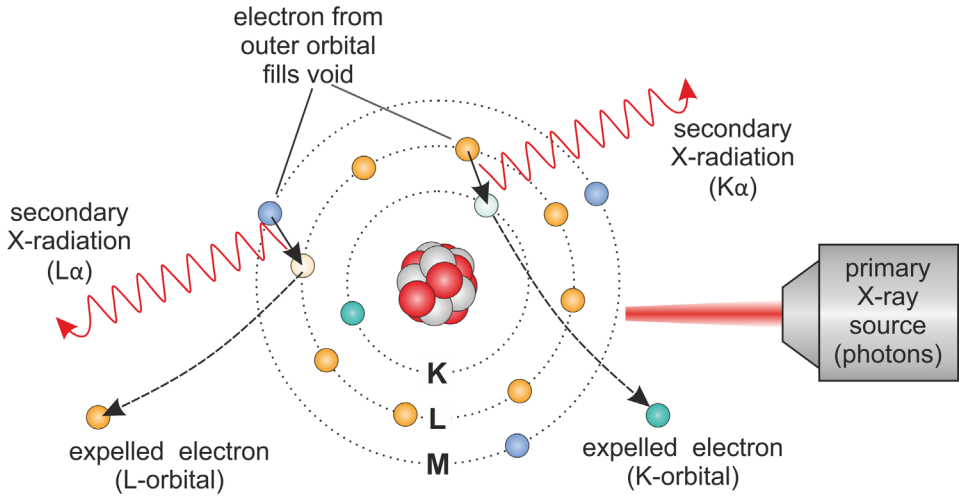

Figure 3.1 Physical principle of XRF analysis. Irradiation of an atom by photons results in the ejection of electrons from the inner orbitals. Electrons from the outer orbitals fill the subsequent vacancies, emitting the surplus energy as element-specific secondary X-radiation.

In this research project, four different types of XRF analyses were applied to determine heavy metal contents in marine sediments. The gravity cores from the Firth of Thames were analysed with an XRF Core Scanner, a portable XRF (pXRF) and a WD-XRF (see Chapter 4), GC HE 215/4-2 in the Helgoland Mud Area with an XRF Core Scanner only (Chapter 5), while the MUC samples from the Skagerrak were analysed using a bench-top ED-XRF (see Chapter 6).

X-Ray Fluorescence Core Scanner Analyses (energy dispersive)

XRF spectrometry became a standard yet time-consuming method in the 1970s, requiring the preparation of discrete samples. The development of CORTEX, the first XRF core scanner prototype developed in 1988, opened the opportunity to analyse the elemental composition of sediment cores on-line in high spatial resolution quickly (Jansen et al., 1998). Because it is a non-destructive method, it can be performed directly at the split surface of the cores. The XRF core scanner became an essential tool for reconstructing climate variability (e.g., Arz et al., 1999; Blanchet et al., 2009), sediment provenance (e.g., Monien et al., 2012), marine productivity (e.g., Cheshire et al., 2005), or anthropogenic environmental changes (Guyard et al., 2007; McGregor et al., 2009) from paleo-environmental records.

However, XRF core scanners only provide semi-quantitative data on elemental composition. Data quality depends on beam energy, the size of the excitation volume used, secondary X-ray air path, and sediment porosity, water content, texture, and mineralogy (Rothwell and Croudace, 2015). Therefore, XRF interpretation should be based on normalised and/or calibrated data.

In Chapter 4, normalisation of the individual element intensity to the total intensity (sum of intensities for all detected elements) was applied to reconstruct the heavy metal input into the Firth of Thames in historic times. The resulting net intensities for Pb and Zn were then calibrated with quantitative Pb and Zn contents, measured by WD-XRF on 28 discrete samples. A simple linear regression equation derived from cross plots of element contents and net intensities was then used to convert the semi-quantitative data into parts per million (ppm).

Measurements were performed on the archive halves of cores NZ-M-2, -4 and -7 with the XRF Core Scanner III (AVAATECH Serial No. 12) at the MARUM - University of Bremen. Sample preparation included smoothing of the split core surface and covering with a 4-micron thin SPEXCerti Prep Ultralene1 foil to avoid contamination of the XRF measurement unit and prevent shrinking or crack formation through drying of the sediment. XRF data were logged with a generator setting of 30 kV and a current of 0.5 mA in 1 cm intervals over a 1.2 cm^2 area with down-core slit size of 10 mm, permitting the detection of the elements Ni, Cu, Zn, Ga, Br, Rb, Sr, Zr, Nb, Mo, Ru, Rh, Pb and Bi. The sampling time was 10 seconds directly at the split core surface. An SGX Sensortech Silicon Drift Detector (Model SiriusSD® D65133Be-INF with 133eV X-ray resolution), the Topaz-X High-Resolution Digital MCA, and an Oxford Instruments 100W Neptune X-Ray tube with rhodium (Rh) target material acquired the data. Processing of raw data spectra was conducted by the analysis of X-ray spectra via Iterative Least

square WIN AXIL software package by Canberra Eurisys. Resulting data prior to normalisation and calibration are reported in counts per second (cps).

For sediment core HE 215/4-2 (Chapter 5) XRF data were collected every 1 cm down-core over a 1.2 cm^2 area with down-core slit size of 12 mm using generator settings of 10 (and 30) kV, a current of 300 (700) mA. The live time was 30 seconds directly at the split core surface of the archive half with XRF Core Scanner I (AVAATECH Model Nr.: 41240, Serial No.005) at the Alfred-Wegener-Institut Helmholtz-Zentrum für Polar- und Meeresforschung, Bremerhaven. The split core surface was covered with a 4-micron thin SPEXCerti Prep Ultralene1 foil. The here reported data have been acquired by a Silicon-PIN Amptek XR-100CR Detector with 139eV X-ray resolution (at 5.9keV, Fe), a MCA8000A multi-channel analyser and an Oxford Instruments 50W X-Ray tube with Rh target material. Raw data spectra were processed by the analysis of X-ray spectra by Iterative Least square software (WIN AXIL) package by Canberra Eurisys.

Portable X-Ray Fluorescence Analyses (energy dispersive)

The great benefit of the portable X-ray fluorescence (pXRF) analysis is the possibility of taking the XRF device to the sample and not vice versa. Furthermore, pXRF is a non-destructive method similar to the XRF Core Scanner, but even quicker and less expensive. Many examples of in-situ application are reported in exploration and mining (e.g., Hall et al., 2014), soil contamination (e.g., Weindorf et al., 2013), paint (e.g., Turner et al., 2015), plants (e.g., Reidinger et al., 2012) and the analysis of museum and archaeological artefacts (e.g., Hunt and Speakman, 2015; Shackley, 2018). The handheld pXRF is battery operated with comparably little power that secures a low health risk during measurements. However, the lower beam energy causes a weaker signal, and thus the emitted secondary X-rays of lower energies increase detection limits, especially for lighter elements (Young et al., 2016). Additionally, data quality is affected by the same factors stated earlier for the XRF Core Scanner such as sediment porosity, water content, etc.

All cores collected from the Firth of Thames (Chapter 4) were measured with a handheld energy-dispersive XRF analyser gun (Olympus Innov-X 50 KV DP4050CX) directly after splitting the cores. Prior to measuring, the surface of the core was smoothed and measuring spots were covered with a thin polypropylene film LS-240-2510 (from Premier Lab Supply Ltd) to avoid contamination of the pXRF device or desiccation of the sediment. Expecting potential human impact only in the uppermost sediments, XRF data were collected in 5-cm intervals in the upper 21 cm of the cores (starting at 1 cm) and 10 cm intervals further downcore. The pXRF analyzer gun was operated in “Soil mode” and mounted directly on the sampling spots. Each scan took 90 seconds with 15-second calibration checks every 30 samples for automatic evaluation of accuracy and precision on a reference material (Stainless Steel Calibration Check Reference Coin provided by Olympus).

Contents of the following major and trace elements were recorded by Innov-X Delta Advanced PC software: Nd, Pr, Ce, La, Ba, Y, P, S, Cl, K, Ca, Ti, V, Cr, Mn, Fe, Co, Ni, Cu, Zn, As, Se, Rb, Sr, Zr, Nb, Mo, Ag, Cd, Sn, Sb, Ta, W, Au, Hg, Pb, Bi, Th, U. Only Pb and Zn are used in this study and limits of detection for elements analysed by pXRF are in the ppm range.

Because of the higher detection limit with lower precision and accuracy explained earlier, the results obtained by pXRF are considered as rather qualitative, even though the output data is given in ppm. Therefore, the recorded values were, similarly to the XRF scanner data, calibrated with quantitative Pb and Zn contents measured with WD-XRF on discrete samples.

Wavelength-dispersive X-Ray Fluorescence Analyses

As the two previously described energy-dispersive XRF techniques only provide semi-quantitative data, a calibration is needed to obtain quantitative heavy metal contents. WD-XRF devices apply the same physical principle as ED-XRF spectrometer, i.e. the excitation of atoms. The difference between both methods is the detection technique. While ED-XRF detects the energy of resulting secondary X-radiation directly, in WD-XRF spectrometers the secondary X-rays are diffracted on a single crystal before reaching the detector. The diffraction is based on Bragg's law, allowing the crystal to scatter the fluorescence spectrum into individual wavelengths. Wavelength-selective detection is performed through rotation of the crystal and detecting unit, while the sample remains stationary (Rothwell and Croudace, 2015).

The main advantages of WD-XRF over ED-XRF are high-resolution spectra with lower background, resulting in a lower detection limit and better accuracy (Kawahara and Shoji, 2006). The obtained spectra are used for the accurate determination of element contents in a sample. The disadvantage of this method is that measuring times are longer and sample preparation results in the destruction of the material.

WD-XRF works for a wide range of elements (i.e., Si, Ti, Al, Fe, Mn, Mg, Ca, Na, K, P, S, Cl, As, Ba, Ce, Co, Cr, Cu, Ga, Mo, Nb, Ni, Pb, Rb, Sr, Th, U, V, Y, Zn, Zr). However, in the study in the Firth of Thames, only the elements Pb and Zn were of interest (Chapter 4). From the marine sediment cores, 28 discrete samples of 20 g wet sediment were taken for quantification of the Pb and Zn contents. The sample positions were carefully chosen to cover the full range of Zn and Pb intensities obtained by the semi-quantitative XRF core scanner measurements. Samples were dried for 48 hours in the drying cabinet at 40°C and ground to a fine powder using a ring mill. Prior to the analysis, 700 ± 0.6 mg per sample were weighed in a ceramic crucible and mixed with 4,200 ± 1 mg of a di-lithium tetraborate fusion flux (SpectromeltR A10, Merck) and about 1,000 mg of ammonium nitrate. The samples were fused into glass beads with a diameter of 30 mm after the pre-annealing overnight at 500°C. Analyses were carried out at the ICBM, Institut für Chemie und Biologie des Meeres, at the University of Oldenburg using the wavelength dispersive XRF-spectrometer AXIOS^{mAX} by Panalytical. Data

acquisition for the elements Pb (Lβ-line) and Zn (Kα-line) was performed using a high energy Rh-anode (tube setting: 60kV and 50mA), the curved analysing crystal PX10 and the HI-PER scintillation counter. Additionally, a 0.75mm Al beam filter was applied. Measurement time for one sample was circa 80 minutes. The measurements of the black shale in-house standard PS-S over a period of 6 months was used to determine precision (for Zn (Pb) = 1 (7) rel-%) and accuracy (root means square error for Zn (Pb) 9ppm (5ppm)) of the method. While for Zn the Kα peak is detected, Pb is using the weaker Lβ peak to avoid peak overlaps of the Pb Kα peak with other elements.

Bench-top energy-dispersive X-Ray Fluorescence Analyses

This technique was solely used for the analysis of the sediment samples from the Skagerrak (Chapter 6) and follows the same principles as the XRF Core Scanner and the portable XRF. However, it offers some advantages and disadvantages in comparison. The use of a bench-top device does not allow in-situ measurements and requires a sample preparation, including drying, grinding and compressing of the material. Therefore, this method cannot be regarded as non-destructive with respect to mechanical damage, but sample material could theoretically still be used for follow-up analysis not requiring the original texture. The advantage of homogenisation is the reduction of interfering differences in physical properties between samples, such as sediment porosity, texture and water content, improving the accuracy and precision of the measurements (Boyle et al, 2015).

Prior to analysis, samples were kept in a drying cabinet at 40 °C for 48 hours and homogenized to a fine powder using an agate mortar and pestle. About 4 g of the sample was transferred in a sampling cuvette with a prolene thin-film base and compressed with a stamp to obtain a smooth surface. The analysis was performed on an EPSILON 3 by PANalytical with Rh-anode and high-resolution Si drift detector. The major and trace elements detected were Al, Br, Ca, Cl, Fe, K, Mg, Mn, Si, Sr, Ti, Zr, Rb and Zn. For the case study in the Skagerrak, only Zn and Al contents are discussed. Instrumental set-up for Zn detection (50kV, 200µA, silver filter, in air) differs from the settings for the lighter element Al (5kV, 1004µA, no filter, in helium atmosphere). Calibration was performed with the certified marine sediment standard MAG-1. Precision of Al is 0.19% and 0.94% for Zn. Measuring time for all the above-listed elements in one sample is approximately 6 minutes.

3.2.3 Inductively Coupled Plasma Mass Spectrometry (ICP-MS)

Inductively coupled plasma mass spectrometry (ICP-MS) is a widely used technique for the analytical determination of elemental concentrations down to the lower parts per trillion (ppt) range. Samples are measured as liquid solutions, or if a laser ablation unit is used, as solids. The method has a broad application for industrial and scientific questions relating to toxicology (e.g., Goullé et al., 2005), pharmaceuticals (e.g., Wang et al., 2000), material science (e.g., Ge et al., 2008) and geoscience (e.g., Kuhnert and Mulitza, 2011). In this thesis, the heavy metal incorporation in foraminiferal calcite in the Helgoland mud area was studied by solution ICP-MS (see Chapter 5).

The functional principle of an ICP-MS is based on the high-temperature sample ionisation in argon plasma and the subsequent detection by a mass spectrometer. The instrument used in this study is a high-resolution sector-field ICP-MS, offering different mass resolutions. Low resolution (about 0.8 atomic mass units) yields maximum signal intensity, but the measurement is susceptible to interferences (see below). Medium resolution (about 0.06 atomic mass units) removes many interferences by exploiting tiny mass differences between the analyte and interfering ion, but at the cost of losing about 92% signal intensity. High resolution (about 0.02 atomic mass units) further reduces interferences, at a signal loss of 97%.

The sample is self-aspirated from the pre-cleaned test tube by the nebuliser (flow rate 100 µl*min^{-1}), where it is mixed with argon gas to form an aerosol. Larger droplets are removed as it passes through the spray chamber, allowing only fine spray to reach the plasma torch. At over 6000°C, the aerosol is decomposed, atomised and finally ionised to form a plasma of positively charged ions and free electrons. The ions are extracted from the plasma and transferred to the high vacuum within the mass spectrometer proper. Here, a quadrupole focusses the ion beam to pass through the entrance slit. Then, a magnetic sector field disperses the analyte ions based on their mass to charge ratio. This unit scans sequentially across the mass range. Finally, electrostatic lenses focus the ion beam, discriminating according to the ion energies. Only the target ions (and some undesired interfering ions) reach the detector.

Ions striking the detector generate a flow of secondary electrons that is multiplied and eventually produces a measurable voltage. The latter is then processed into a mass spectrum. In the absence of interferences, the intensity recorded at a given mass is proportional to the concentration of the isotope of that mass in the sample solution. The relative abundances of the different isotopes of a specific element are the same in the sample and calibration solutions. Therefore, concentrations of an element can be determined by measuring just a single isotope. Interferences can occur through polyatomic or doubly charged ions with mass to charge ratios identical to that of the target ion (Table 3.2). Therefore, the selection of the isotope and instrument resolution for the target element should consider potential interferences and the abundance of the isotope.

Table 3.2 Common polyatomic interferences in ICP-MS (May and Wiedmeyer, 1998)

Isotope	Abundance	Examples of interferences
^{27}Al	100.0	$^{12}C^{15}N^+$, $^{13}C^{14}N^+$, $^{1}H^{12}C^{14}N^+$
^{43}Ca	0.145	$^{27}Al^{16}O^+$
^{55}Mn	100.0	$^{40}Ar^{14}N^{1}H^+$, $^{39}K^{16}O^+$, $^{37}Cl^{18}O^+$, $^{40}Ar^{15}N^+$, $^{38}Ar^{17}O^+$, $^{36}Ar^{18}O^{1}H^+$, $^{37}Cl^{17}O^{1}H^+$, $^{23}Na^{32}S^+$
^{89}Y	100.0	$^{49}Ti^{40}Ar$, $^{73}Ge^{10}O$
^{111}Cd	12.8	$^{95}Mo^{16}O^+$, $^{94}Zr^{16}O^{1}H^+$, $^{39}K_2{}^{16}O_2{}^{1}H^+$
^{208}Pb	52.4	$^{192}Pt^{16}O^+$

Sample preparation

Prior to measurement, the 46 sediment samples were wet sieved over a 63 µm, 150 µm and 500 µm sieve and stored in a drying cabinet for 48 hours. The benthic foraminifera *Ammonia beccarii* and

Elphidium excavatum, selected because of their abundance and tolerance, were picked separately from the > 150 µm fraction under the light microscope (about 30 tests per species and sample). Broken or partly dissolved specimens were avoided. The cleaning protocol for elemental analysis of foraminiferal calcite by Barker et al., (2003) was used. Work was carried out under a clean bench to prevent dust contamination. (1) Foraminifera were gently crushed between two glass slides in order to open all chambers. This is a necessary step before starting the cleaning procedure to avoid remains of foreign matter (grains, overgrowth) inside a closed chamber. Samples were then transferred into twice acid washed vials (0.5 ml) for cleaning. (2) Removal of clays through multiple rinsing and ultrasonication,five times with MilliQ water and subsequently twice with methanol; (3) two successive cycles of ultrasonication after an addition of alkali buffered H_2O_2 for oxidation of organic matter followed by two rinses with MilliQ water; (4) transfer of samples to new pre-cleaned vials to remove settled coarse-grained silicates and three more MilliQ water rinses, subsequent control under a light microscope; (5) removal of adsorbed contaminants by a weak nitric acid leach (0.001 M HNO_3) and rinses with MilliQ water; (6) dissolution of test fragments using 0.075 M HNO_3 and a final transfer to test tubes (10 ml). Nitric acid and deionised water of ultra-high purity grade were used for all dilutions (sample preparation and calibration standards). All samples were measured on a Thermo Finnigan Element 2 high-resolution sector field ICP-MS at the Department of Geosciences, University of Bremen.

Calibration

A pre-test with laser ablation (LA-) ICP-MS was conducted on five undissolved foraminifera of each species to estimate the range of metal concentrations to be measured. Results were used to prepare calibration standards from certified element standard solutions (Merck, 1000 ppm for each element, except Ca: 10000 ppm) for a 4-point calibration, covering the full range of Ca, Al, Mn, Pb, Cd and Zn concentrations (Table 3.3). Additionally, two blanks were analysed for blank correction. Yttrium (Y) was added as an internal standard in a final concentration of 4 parts per billion (ppb) to all calibration standards and sample solutions to correct for sensitivity changes of the ICP-MS. Pb, Cd and Ca were measured to determine the incorporation of the heavy metals into the calcite structure of foraminiferal tests. Al and Mn were used to monitor contaminations from clay minerals and iron-manganese crusts. Al/Ca was usually below 0.2 mmol/mol, and samples with >0.5 mmol/mol were discarded. Mn/Ca was below 0.2 mmol/mol, with 2 exceptions, and no correlations of Pb/Ca and Cd/Ca with either Al/Ca or Mn/Ca were observed, suggesting that heavy metal values were not adversely affected by mineral coatings. As Zn was measured in the XRF based studies, we also attempted to obtain Zn/Ca ratios for the foraminifera test. Unfortunately, the high background level and low signal-to-noise ratio prevented analysis of Zn in the extremely low target concentration range.

Repetitive analyses of an in-house standard as well as calibration standard S3 after every three samples allowed the offline correction of the instrument drift and ensured consistency between measurements carried out on different days. Average analytical precision (1 standard deviation based on 50 replicates

per measurement of a standard solution) was 1.4E-05 % for Pb/Ca, 4.6E-06 % for Cd/Ca, 3.5E-03 % for Al/Ca and 2.8E-03 % for Mn/Ca. Because of a lack of material, no replicate samples were analysed.

Table 3.3 Overview of the standard concentrations (converted in content per foraminiferal sample mass) for the 4-point calibration curve.

Element	Standard S1	Standard S2	Standard S3	Standard S4	unit
Ca	2	4	6	8	ppm
Zn	30	60	90	120	ppt
Cd	250	500	750	1000	ppq
Pb	3	6	9	12	ppt
Al	0.1	0.2	0.3	0.4	ppb
Mn	0.5	1.0	1.5	2	ppb
Y	4	4	4	4	ppb

Measurement settings

To obtain optimum intensity, peak shape and stability of the signal, instrument tuning was performed daily. The measurement method was set to 5 minutes wash time between samples and 2.5 minutes sample take-up time (time the samples runs through the system without being measured) to exclude contaminations from sample carry-over. Data acquisition time was circa 5 minutes in five passes with 10 runs each (total of 50 measurement replicates), in low-resolution mode (^{27}Al, ^{55}Mn, ^{89}Y) and medium resolution mode (^{43}Ca, ^{89}Y, ^{111}Cd, ^{208}Pb).

3.2.4 Laser Diffraction Particle Size Analysis

Grain size analyses were performed to ensure the comparability of X-ray fluorescence results both throughout a core and among cores, as it plays an important role regarding porosity and water content and consequently signal strength. Furthermore, it is well known that heavy metal contents are reversely correlated to grain size because of the greater adsorption capacity of finer material (Horowitz, 1991). This is mainly caused by a higher specific surface area, negative surface charge and cation exchange capacity of clay minerals versus coarser size fractions. Therefore, determination of the lithogenic grain-size distribution is a valuable supporting measure for heavy metal loads.

Grain-size analyses were conducted on the marine gravity cores from the Firth of Thames (Chapter 4) as well as for the MUCs from the Skagerrak (Chapter 6). Sampling resolution was every centimetre for the latter location (n=115), while the three principal cores from New Zealand were sampled in 5 cm intervals for the upper 146 cm and 10 cm further down-core (n=116). Sample preparation and measurements were carried out with deionized, degassed and filtered water (filter mesh size: 0.2 µm) to reduce the potential influence of gas bubbles or particles within the water (subsequently called deionised water). In order to avoid bias of biogenic particles, such as organic matter, shells and other microorganisms, the terrigenous fraction needed to be isolated following the method of Stuut (2001).

Therefore, about 1 ml of wet sample was transferred into a glass beaker with about 25 ml deionised water. The first step comprises the oxidation of the organic matter by adding 10 ml H_2O_2 (35%) boiling

on a heat plate until the reaction (foam formation) stopped. Afterwards, the sample was filled with deionised water to a volume of 100 ml, and10 ml HCl (10%) were added before boiling exactly 1 minute for removal of calcium carbonate (e.g., shells, foraminifera). Thereafter, the glass beaker was filled with deionised water to 1000 ml and left for settling of the particles. After 8 hours the clear overlying acid fluid was decanted to ~100 ml and refilled with deionised water. After decanting the next morning, the adding of NaOH pellets (6 g) and boiling for 10 minutes removed biogenic silica, such as diatoms. The glass beaker was again filled with deionised water to a volume of 1000 ml, left for particle settling and decanted after 8 hours. This washing procedure was repeated once more (overnight) before 300 mg of tetra-sodium diphosphate decahydrate ($Na_4P_2O_7*10H_2O$) were added and shortly boiled for securing disaggregation of all particles (see also McGregor et al., 2009).

All measurements were performed in the Particle-Size Laboratory at MARUM, University of Bremen, with a Beckman Coulter Laser Diffraction Particle Size Analyzer LS 13320. A sample is added to the pumping unit from where it passes two different measuring cells and is kept in suspension by adjustment of the pumping speed. For detection of the coarser particles (0.4 to 2,000 µm), a parallelised laser beam with a wavelength of 780 nm is passed through the suspended sample (sample cell 1) and diffracted by the particles. Subsequently, the diffraction pattern is detected in a detector array consisting of 92 channels, equivalent to the grain-size classes spanning 0.4 to 2,000 µm. Sizes are calculated based on the Fraunhofer diffraction theory, describing the bending of waves around the edges of an obstacle, resulting in a geometrical pattern of dark and bright areas through the interference of the waves. Smaller particles lead to wider diffraction angles than larger particles. For measuring the fine fraction (0.04 to 0.4 µm; 26 size classes), samples pass the second measuring cell, where polarised light is emitted through the suspension and finer particles are detected by the Polarisation Intensity Differential Scattering (PIDS) array.

In total, the obtained results provide the particle-size distribution of a sample from 0.04 to 2,000 µm divided into 116 size classes. The reproducibility was checked regularly by replicate analyses of three internal glass-bead standards and is found to be better than ± 0.7 µm for the mean and ± 0.6 µm for the median particle size (1σ). The average standard deviation integrated overall size classes is better than ± 4 Vol-% (note that the standard deviation of the individual size classes is not distributed uniformly). All provided statistic values are based on a geometric statistic.

3.2.5 Carbon and Nitrogen Elemental Analysis

CN elemental analysis (sometimes also referred to as CHN elemental analysis) is a widespread combustion method aiming to determine the elemental composition of materials with respect to total nitrogen (TN), total carbon (TC), total organic carbon (TOC) and inorganic carbon (IC) by subtraction. In marine sediments, these contents play for example an important role in the global carbon cycle (e.g., Burdige, 2005), reconstruction of productivity (e.g., Müller and Suess, 1979) or the differentiation of

terrestrial and marine organic carbon sources (Müller, 1977). In the Skagerrak (Chapter 6), TOC was measured as an indicator of organic matter with its capacity to bind heavy metals (e.g., Horowitz, 1991).

First, the sample material was kept in a drying cabinet at 40°C for 48 hours and subsequently ground to a homogeneous fine powder using an agate mortar and pestle. For total nitrogen and total carbon analysis, about 35 mg dry sample was weighed into silver cups and carefully pressed into tight pellets. For organic carbon analysis, the same procedure was applied using silver cups, acidified with HCl to remove carbonates and dried at 50-60°C before pressed into pellets. Samples were then placed in the autosampler of the *vario EL III Element Analyzer* by *elementar,* and sample weights were entered into the PC. The used CN operation mode was set to a combustion temperature of 950 °C. Duration of measuring time for one sample is self-optimising (dependent on element contents) but ranges between 6 to 12 minutes.

After sample loading, the sample drops into a ball valve, where air (atmospheric nitrogen and carbon) is flushed out with Helium. From there, the sample is transferred into the oxygen-filled combustion tube, digesting explosively into the elements C, H, N, S as well as the oxidation products (O_2, H_2O, NO_x, SO_2, SO_3). After passing several filters (absorbing and reducing materials), foreign gases are removed and only CO_2 and N_2 remain in the gas stream. As the thermal conductivity detector cannot discriminate between the different elements, carbon is separated by an adsorption column. Nitrogen being unaffected by this procedure is measured first. After N analysis is concluded, C is thermically desorbed and detected next.

For calibration check the two standards wst4 (internal standard) and acetanilide (NIST141D) as well as empty cups (tin and silver respectively) as blanks were analysed every morning and after a batch of samples in the evening. Further calibration checks were conducted after every 10 samples, using the wst4 and empty cup only. Precision of the analysis is < 0.1% absolute.

3.2.6 Additional analysis

For the comparison of foraminiferal test deformation rates and incorporation into the calcite structure in the Helgoland Mud Area (Chapter 5), data from the Master Thesis of Rotstigen (2009) were used in parts. For that thesis, the temporal changes of foraminiferal assemblage on the >125µm fraction in gravity core HE 215/4-2 were determined, including the calculation of absolute abundance, the Shannon-Wiener diversity index and principal component analysis. Furthermore, Rotstigen (2009) described morphological abnormality modes and calculated the percentages of abnormal tests on the same size fraction. These changes in test deformation over the past 1000 years are an essential part of Manuscript 2. For further methodological details on the foraminiferal analysis, please see Rotstigen (2009).

Chapter 4 Manuscript 1

Historical Development of Heavy Metal Contamination in the Firth of Thames, New Zealand

S. Boehnert[1], S. Ruiz Soto[1], B.R.S. Fox[2,3], Y. Yokoyama[4] and D. Hebbeln[1]

[1] MARUM — Centre for Marine Environmental Sciences, University of Bremen, Leobener Straße 8, 28359 Bremen, Germany

[2] Department of Biological and Geographical Sciences, University of Huddersfield, Queensgate, Huddersfield, HD1 3DH, United Kingdom

[3] School of Science, University of Waikato, Private Bag 3105, Hamilton 3240, New Zealand

[4] Atmosphere and Ocean Research Institute, The University of Tokyo, 5-1-5 Kashiwanoha, Kashiwa, Chiba 277-8564, Japan

Abstract

Near-coastal marine sediments often provide high-resolution records of various anthropogenic influences such as the release of heavy metals, which pose a potentially negative influence on aquatic ecosystems because of their toxicity and persistence. In places, the gradual onset of man-made heavy metal emission dates back to ~ 4,500 years BP and is difficult to distinguish from potential natural sources. New Zealand offers a perfect setting for studies on anthropogenic impact due to its well-defined three-step development: pre-human era (until ~1300 CE), Polynesian era (~1300-1800 CE) and European era (since ~1845 CE). However, hardly any information exists about the degree of heavy metal input to New Zealand's coastal areas and the 'pristine' natural background values. This study determines the natural background contents of Pb and Zn in marine sediments of the Firth of Thames, a shallow marine embayment on New Zealand's North Island, and investigates anthropogenic inputs in historic times. Eight sediment cores were analysed by X-ray fluorescence (XRF) for their element composition and temporally resolved by a pollen and radiocarbon-based stratigraphic framework. Sharp increases in Pb and Zn contents occurred simultaneously with the onset of gold mining activities (1867 CE) in the nearby catchment area. The contents of Zn (Pb) increase from very stable values around 60 (13) ppm in the older sediments, interpreted to reflect the natural background values, to an average maximum of 160 (60) ppm near the core top, interpreted to reflect a significant anthropogenic input. These findings unravel the history of contamination in the Firth of Thames and provide an urgently needed database for the assessment of its current ecological state.

4.1 Introduction

Anthropogenic influences on coastal marine ecosystems can date back several centuries or even millennia, however, with severely increasing impacts during the last two centuries. Often this is accompanied by the rising release of various pollutants into the environment. A prominent example is

the increasing release of heavy metals by mining and metallurgy, with the beginning traced back to the Copper and Early Bronze Age ~4,500 yrs BP (e.g., Leblanc et al., 2000). To understand the sources, the causes and the temporal development of enhanced inputs of contaminants, such as heavy metals, to the marine environment, near-coastal sediment depocentres can provide high-resolution sedimentary archives. These have great potential for the reconstruction of heavy metal inputs through time and to differentiate between anthropogenic or natural causes.

Pollution history recorded in marine sediments (e.g., Irion et al., 1987; Fukue et al., 1999; Hebbeln et al., 2003; Badr et al., 2009; Seshan et al., 2010) has been decoded from many places in the world. However, only a few studies exist about anthropogenic heavy metal enrichment in sediments from New Zealand. These are mainly concerned with streams (Webster, 1995; Craw and Chappell, 2000; Sheppard et al., 2009; Clement et al., 2017) and more recent releases by urban runoff near major cities (Dickinson et al., 1996; Abrahim and Parker, 2002; 2008).

New Zealand offers an exceptional setting to study the historical development of human impact, as it was the last main landmass that was colonised by people (e.g., McGlone et al., 1994). Three different stages can be distinguished: (i) the pre-human era until ~1300 CE, with pristine flora and fauna influenced by volcanic activity and natural wildfires, (ii) the Polynesian era with first human settlements and slash-and-burn deforestation starting ~1300 CE (e.g., McFadgen, 1994; Ogden et al., 1998; McGlone and Wilmshurst, 1999; Horrocks et al., 2001), followed by (iii) the onset of the European era due to the "discovery" of New Zealand by James Cook in 1769 with the successive land use changes linked to European settlement and the onset of gold mining at about the same time as the industrial revolution. This very short history of human influences is a suitable precondition to define the regional natural background conditions. In the course of such a short anthropogenic history, the obtained pristine background values are less prone to reflect major environmental changes as for example triggered by climatic variations or tectonic activities.

Abrahim and Parker (2008) evaluated the heavy metal pollution in the Tamaki Estuary (Auckland area, New Zealand) and found elevated levels of Cu, Pb, Zn and Cd in the uppermost 10 cm compared to 'pristine' values in the older sediments. They linked this contamination to the development of the urbanization and industrialization in the catchment area, especially over the past 50 years. Another study in the Wellington Harbour by Dickinson et al. (1996) showed post-1900 anthropogenic increases in the elements Cu, Pb and Zn. However, neither of these studies covers the pre-human era and, thus, it is not clear, if the baseline presented shows the actual pristine (pre-human) values, or if the presented values already reflect an impact triggered by the Maori's widespread slash-and-burn deforestation (pre-European baseline). Secondly, both studies concentrate on highly urbanised areas with multiple sources for heavy metal input (e.g., industrial areas, port development, dredging, boatyards and yacht anchorages). Thus, the degree of pollution of New Zealand's coastal areas and 'pristine' heavy metal background contents are still only poorly known.

In this study, XRF data obtained on subtidal sediment cores from the Firth of Thames are used to (i) reconstruct past heavy metal inputs, here Pb and Zn, into the shallow marine environment, (ii) identify the source for human-induced inputs and (iii) quantify the impact of anthropogenic change. This is especially important to validate a truly pristine baseline for Pb and Zn in order to put past, current and future heavy metal contaminations in relation to the natural background.

4.2 Regional setting

Geography and hydrodynamics

The Firth of Thames is a mesotidal, shallow estuarine embayment (Naish et al., 1993), located at the northeastern North Island of New Zealand (Figure 4.1). It is part of the north-south striking Hauraki Rift, bounded by the Coromandel-Kaimai Range in the east and Hunua Range in the west (Hochstein and Nixon, 1979). The rift continues to the south into the Hauraki Plains. To the north, the Firth is bordered by the Hauraki Gulf. Hydrodynamically it is a partially to well mixed, tidally dominated

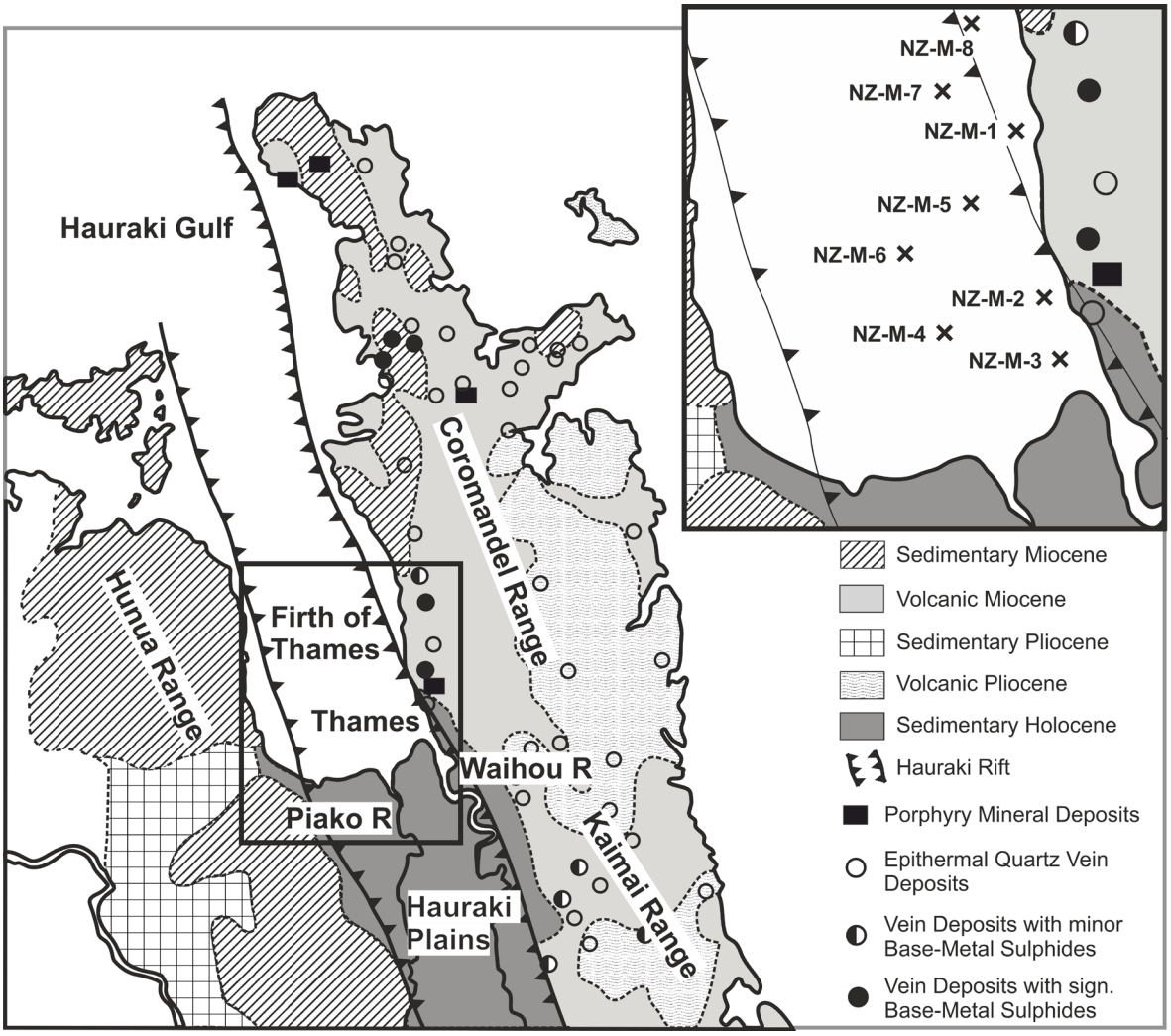

Figure 4.1 Geological map of the Coromandel region (after Livingston, 1987 and Dredge, 2014), black square indicates the study area. Crosses in insert map mark the core locations, circled crosses indicate the 3 high-resolution principal cores NZ-M-2, NZ-M-4 and NZ-M-7.

estuary with low-wave energy (Naish et al., 1993). On average, tidal currents are ≤0.3 m s^{-1} (Black et al., 2000).

Major sediment supply into the Firth of Thames derives from the Waihou River (160 kt/yr sediment) and Piako River (30kt/yr sediment) (Hicks et al., 2011), which enter the Firth from the South. With a catchment area of 1,984 km^2 (Hicks et al., 2011) the Waihou River is the largest river in the Coromandel Region, with several tributaries draining gold mining districts (e.g., Golden Cross, Tui mine) (Webster, 1995).

Human impacts on vegetation

The first major human impact on New Zealand resulted from the widespread forest clearance by the Polynesian settlers. Even though this vegetation change is well recorded in pollen-based paleoenvironmental reconstructions, the exact timing is still under debate and location dependent (McGlone, 1983; Newnham et al., 1998; Ogden et al., 1998; McGlone and Wilmshurst, 1999; Byrami et al., 2002, Newnham et al., 2018). South of the Coromandel Peninsula, the onset of deforestation is dated to c. 1200-1300 CE (Newnham et al., 1995a, b); in the following 1300 CE is used to refer to this onset. Byrami et al. (2002) give a detailed reconstruction of the vegetation composition from pollen records in the Kauaeranga Valley, Coromandel Peninsula: (i) in pre-human times, the native forest was dominated by tall trees (e.g., *Podocarpus spp.*) and no major changes in floral makeup could be detected over a period of 1000 years, (ii) the onset of deforestation during the Polynesian era is indicated by a significant increase in *Pteridium* and charcoal as well as a decrease in forest taxa (tall trees), and (iii) the European era is marked by the occurrence of the exotic *Pinus spp.* pollen and losses in *Agathis australis*, the New Zealand Kauri tree.

Human impact during European era

With the establishment of European settlements at c.1845 CE (Augustinus et al., 2006), there was a marked change in land use including further deforestation for agriculture, construction works, Kauri logging and gum digging. Kauri logging posed a special threat for the environment, as it not only meant clearance of native forest but also damming rivers and regularly flushing them in order to transport the logs to the coast in the rough terrain.

Another major human impact were gold mining operations in the Coromandel Range (1867 CE in Thames township). The Coromandel Peninsula consists of Mesozoic greywacke capped and intruded by Neogene andesites and rhyolites (Williams, 1974; Brathwaite, 1989; Adams et al., 1994). Hydrothermal quartz veins cut through these host rocks and scatter small discrete alteration zones with variable gold and base metal content throughout the Coromandel Range (Figure 4.1) (Williams, 1974; Livingston, 1987; Brathwaite et al., 2001).

4.3 Material & Methods

Coring

The sampling campaign was conducted from March 20th-22th, 2017 on the crane barge *Quest* belonging to *Bay Marine Works Limited*. A set of 8 sediment cores was collected in the southeastern part of the Firth of Thames (Figure 4.1 and Table 4.1) using a QR 300 Vibracore with a total weight of ~250 kg and a tube diameter of 76 mm. The QR 300 Vibracore was configured to take up to 3 m long cores of unconsolidated or semi-consolidated sediment in a wide range of geological settings. Due to its weight and the very soft sediments in the Firth of Thames, the QR 300 Vibracore was deployed in a gravity corer mode in order to recover undisturbed sediments from the very top layers.

After cutting the 194-258 cm long sediment cores into 1 m long core segments, these were split along the c-axis into working and archive halves. After opening all cores were described sedimentologically and logged immediately with a handheld X-ray fluorescence (XRF) device (see below). Further analyses focused on three cores ('principal cores': NZ-M-2, -4, and -7) from which samples from the working and archive halves were taken at discrete depths for radiocarbon dating, wavelength-dispersive XRF (WD-XRF), particle size and pollen analysis (195 samples in total). Archive halves of the principal cores also have been rescanned (prior sampling) with an XRF core scanner.

Table 4.1 Meta-data of the eight sediment core locations in the Firth of Thames.

Core no.	Latitude	Longitude	Water Depth (m)	Core length (m)
NZ-M-1	37°02.6894'S	175°30.5168'E	2.6	2.47
NZ-M-2	37°07.1123'S	175°30.6993'E	1.0	2.41
NZ-M-3	37°08.9551'S	175°30.8024'E	0.4	1.94
NZ-M-4	37°08.3227'S	175°26.6615'E	2.2	2.50
NZ-M-5	37°04.6947'S	175°27.9617'E	5.6	2.44
NZ-M-6	37°06.2822'S	175°25.7361'E	4.0	2.58
NZ-M-7	37°01.4124'S	175°27.1250'E	8.5	2.46
NZ-M-8	36°59.6255'S	175°27.7667'E	7.8	2.51

Age determination

Radiocarbon dating

Accelerator mass spectrometry (AMS) radiocarbon (^{14}C) dating was performed on bulk sediment organic matter (n=18), unclassified marine shells (n=3), and mixed benthic foraminifera (n=12) at the Atmosphere and Ocean Research Institute, University of Tokyo, and at the MICADAS Laboratory, Alfred-Wegener-Institute in Bremerhaven (Table 4.2). Single stage accelerator mass spectrometry was used to obtain radiocarbon ages on bulk organic matter (Hirabayashi et al., 2017), with graphitisation completed using the protocol described by Yokoyama et al. (2007, 2010). Sediment samples were pre-treated in 1 M HCl for 1 h to remove the calcium carbonate and subsequently heated in a muffle furnace to 850 °C for 2 h. Carbon incorporated in the sample was recovered as CO_2 (Ishizawa et al., 2017). Pre-

treatment of marine shell samples followed the protocol of Yokoyama et al. (2007). Radiocarbon ages were converted to calibrated calendar ages using CALIB 7.1 (Stuiver et al., 2018) based on the Marine13 dataset (Reimer et al., 2013) and no local reservoir correction ($\Delta R = 0$).

Palynological analysis for dating

Nineteen samples from core NZ-M-4 were prepared for palynological analysis using the standard laboratory procedures (Faegri and Iversen, 1989). Sediment (2 cm^3) was weighed and dried overnight in a stove at 62°C. The dried sediment was weighed again, decalcified with diluted HCl (10%), and treated with HF (40%) to remove silicates. One tablet of exotic *Lycopodium* spores (18,583 ± 1,708 spores per tablet) was added to the samples previous to decalcification to allow the calculation of pollen grain abundance. After chemical treatment, samples were wet sieved over a 10 µm nylon mesh using an ultrasonic bath to disaggregate organic matter. One aliquot (50 µL) was mounted on a permanent glass slide using glycerine jelly and the slide sealed with paraffin wax. Samples were checked for *Pinus spp., Olea europaea* and *Podocarpus spp.* pollen only.

Grain size analysis

Grain-size measurements on 115 samples taken from the three principal cores were performed in the Particle-Size Laboratory at MARUM, University of Bremen, with a Beckman Coulter Laser Diffraction Particle Size Analyzer LS 13320. Prior to the measurements, the terrigenous sediment fractions were isolated by removing organic carbon, calcium carbonate, and biogenic opal by boiling the samples (in about 200 ml water) with 10 ml of H_2O_2 (35%; until the reaction stopped), 10 ml of HCl (10%; 1 min) and 6 g NaOH pellets (10 min), respectively. After every preparation step the samples were diluted (dilution factor: >25). Finally, remaining aggregates were disaggregated prior to the measurements by boiling the samples with ~0.3 g tetra-sodium diphosphate decahydrate ($Na_4P_2O_7$ * $10H_2O$, 3 min) (see McGregor et al., 2009). Sample preparation and measurements were carried out with deionized, degassed and filtered water (filter mesh size: 0.2 µm) to reduce the potential influence of gas bubbles or particles within the water. The obtained results provide the particle-size distribution of a sample from 0.04 to 2000 µm divided into 116 size classes. The calculation of the particle sizes relies on the Fraunhofer diffraction theory and the Polarization Intensity Differential Scattering (PIDS) for particles from 0.4 to 2000 µm and from 0.04 to 0.4 µm, respectively. The reproducibility was checked regularly by replicate analyses of three internal glass-bead standards and is found to be better than ± 0.7 µm for the mean and ± 0.6 µm for the median particle size (1σ). The average standard deviation integrated over all size classes is better than ± 4 Vol-% (note that the standard deviation of the individual size classes is not distributed uniformly). All provided statistic values are based on a geometric statistic.

Heavy metal analysis

Portable XRF analyzer (pXRF, energy-dispersive)

A handheld XRF analyzer gun (Olympus Innov-X 50 KV DP4050CX) was used in "Soil mode" and mounted directly on the smoothed core surface of all collected sediment cores. Sample spots were covered with a thin polypropylene film LS-240-2510 (from Premier Lab Supply Ltd). Contents of major and trace elements were recorded by Innov-X Delta Advanced PC software. Limits of detection for elements analysed by pXRF are in the ppm range. From a range of elements analysed, only Pb and Zn are used. Each scan took 90 seconds with calibration checks made every 30 samples on a reference material (Stainless Steel Calibration Check Reference Coin provided by Olympus) for evaluation of accuracy and precision. Expecting anthropogenic impact only in the youngest sediments, sample spacing was 5 cm for the upper 21 cm of the cores and 10 cm further downcore.

XRF core scanner (energy-dispersive)

XRF Core Scanner data were collected with the XRF Core Scanner III (AVAATECH Serial No. 12) at the MARUM - University of Bremen on the three principal cores every 1 cm down-core over a 1.2 cm^2 area with down-core slit size of 10 mm using generator settings of 30 kV and a current of 0.5 mA. The sampling time was 10 seconds directly at the split core surface of the archive half, which was covered with a 4 µm thick SPEXCerti Prep Ultralene1 foil to avoid contamination of the XRF measurement unit and desiccation of the sediment. The data were acquired by an SGX Sensortech Silicon Drift Detector (Model SiriusSD® D65133Be-INF with 133eV X-ray resolution), the Topaz-X High-Resolution Digital MCA, and an Oxford Instruments 100W Neptune X-Ray tube with rhodium (Rh) target material. Raw data spectra were processed by the analysis of X-ray spectra by the Iterative Least square software (WIN AXIL) package by Canberra Eurisys and interpreted for Pb and Zn.

XRF spectrometer (wavelength-dispersive)

For quantification, 28 discrete samples of 20 g wet sediment were taken from the three principal cores at positions that cover the full range of Zn and Pb values according to the semi-quantitative XRF core scanner measurements. Samples were kept in the drying cabinet at 40°C for 48 hours and ground using a ring mill. Prior to the analysis, 700 ± 0.6 mg per sample were weighted into a ceramic crucible and mixed with 4,200 ± 1 mg of a di-lithium tetraborate fusion flux (SpectromeltR A10, Merck) and about 1,000 mg of ammonium nitrate. Following the pre-annealing at 500°C overnight, the samples were fused into glass beads and analysed using the wavelength dispersive XRF-spectrometer $AXIOS^{mAX}$ by Panalytical at the ICBM, Institut für Chemie und Biologie des Meeres, at the University of Oldenburg. For the determination of precision and accuracy of the method, the in-house standard PS-S was used (root means square error for Zn (Pb) 9ppm (5ppm); precision in rel-% for Zn (Pb) = 1 (7)).

Calibration of X-Ray fluorescence data

The net intensities for Pb and Zn in counts per second (cps) measured with the XRF Core Scanner were divided by the total cps from the according 30kV run to normalise the data (i.e. for deviations resulting from varying water content, grain size variations and others). These normalised net intensities from the XRF Core Scanner data were converted to element contents using linear regressions between XRF scanner-derived intensities and element contents measured on the corresponding 28 discrete samples measured quantitatively (e.g., Jansen et al., 1998; Kido et al., 2006; Tjallingii et al., 2007). The obtained data of the pXRF were calibrated using the same method, but normalisation was not conducted as values given by the instrument were already in ppm.

4.4 Results

Core description

A strong H_2S smell was obvious after splitting of the cores NZ-M-1, NZ-M-4, NZ-M-5, NZ-M-6, NZ-M-7 and NZ-M-8. These cores consist of a dark greenish mud (Munsell colour chart 5Y) with only minor internal textures, which include thin layers of fine sand or shell debris. No lamination, burrowing or change in colour was observed. In general, the cores revealed no obvious changes in grain size with the exception of cores NZ-M-2 and NZ-M-3. Core NZ-M-2 is composed of fine-sandy material in the core section below 96 cm that gradually changed to the same dark greenish, homogeneous mud as described before with a minor sand content (<5%) that makes up the uppermost 90 cm of the core. Core NZ-M-3 (near Waihou river mouth) is dominated by black middle to coarse sand with fine shell debris and had a smell of rotten fish. In the sediments below 120 cm depth, the sand alternates with black muddy layers similar to those described from the other cores, but very compact.

Radiocarbon dating

For all three principal cores (NZ-M-2, -4, and -7), the 33 obtained ^{14}C dates show generally consistent trends to become younger towards the top with the exception of only a few samples (Table 4.2). Such 'outliers' are restricted to either bulk organic matter or not classified shell dates. The upper 150 cm of cores NZ-M-2 and NZ-M-4 comprise ~1,500 yrs and ~1,660 yrs, respectively. Core NZ-M-7 displays slightly older ages and shows an age of 2,380 yrs at 141 cm sediment depth. Therefore, the pre-human era is covered in all three cores. NZ-M-2 is the core with the most radiocarbon dates on foraminifera (n = 8) with the four ages above 56 cm showing ages of <~250 years. Taking the 1σ range into account, the resulting ages overlap without any age reversals and all dates potentially reach the time past 1845 CE. Below 56 cm the samples become successively older and date back to ~405 CE (maximum 1σ age) at 141 cm depth. The cores NZ-M-4 and NZ-M-7 contain only two radiocarbon dates on foraminifera

Table 4.2 Radiocarbon dates for the 3 principal cores NZ-M-2, NZ-M-4 and NZ-M-7 from the Firth of Thames, New Zealand (bulk OM - bulk organic matter; benth. forams – mixed benthic foraminifera; shell – unclassified marine shell). The 1 σ calendar age range given here encloses 68.3% of the probability distribution [Stuiver et al., 1998b]. Values in parentheses are the relative areas under the probability distribution. - too young for calibration, therefore CE 1950±60 was assumed.*

Laboratory Code	Core	Sample Depth (cm)	Sample Material	^{14}C age (yrs BP)	Calendar Age CE	1σ Calendar Age range CE/BCE
YAUT-034228	NZ-M-2	20	bulk OM	2100±28	273	cal CE 232-331 (1.000)
AWI-1529.1.1	NZ-M-2	26	benth. forams	563±112	1756	cal CE 1659-1890 (0.987), 1946-1950* (0.013)
AWI-1529.1.2	NZ-M-2	26	benth. forams	557±103	1764	cal CE 1667-1885 (0.996); 1949-1950* (0.004)
YAUT-034229	NZ-M-2	40	bulk OM	962±30	1393	cal CE 1353-1374 (0.248); 1381-1430 (0.752)
AWI-1729.1.1	NZ-M-2	41	benth. forams	modern	1950*	CE 1890-2010*
AWI-1730.1.1	NZ-M-2	56	benth. forams	459±104	1828	cal CE 1760-1787 (0.123); 1803-1950* (0.877)
YAUT-034231	NZ-M-2	60	bulk OM	1041±27	1334	cal CE 1300-1356 (0.889); 1372-1383 (0.111)
YAUT-034702	NZ-M-2	90	bulk OM	5020±30	-3423	cal BCE 3467-3369 (1.000)
AWI-1530.1.1	NZ-M-2	91	benth. forams	1110±105	1274	cal CE 1194-1386 (1.000)
AWI-1530.1.2	NZ-M-2	91	benth. forams	967±105	1385	cal CE 1307-1458 (1.000)
YAUT-034232	NZ-M-2	120	bulk OM	1366±27	1035	cal CE 1002-1063 (1.000)
YAUT-034723	NZ-M-2	120	shell	935±37	1414	cal CE 1387-1454 (1.000)
YAUT-032409	NZ-M-2	139.5	bulk OM	2536±29	-265	cal BCE 322-214 (1.000)
YAUT-032403	NZ-M-2	139.5	shell	28854±95	-30465	cal BCE 30755-30222 (1.000)
AWI-1531.1.1	NZ-M-2	141	benth. forams	1893±103	501	cal CE 405-623 (1.000)
AWI-1531.1.2	NZ-M-2	141	benth. forams	1850±112	541	cal CE 436-660 (1.000)
YAUT-034703	NZ-M-4	20	bulk OM	930±28	1420	cal CE 1401-1450 (1.000)
YAUT-034724	NZ-M-4	20	shell	193±38	1950*	CE 1890-2010*
AWI-1731.1.1	NZ-M-4	31	benth. forams	550±48	1771	cal CE 1692-1822 (1.000)
YAUT-034704	NZ-M-4	40	bulk OM	1143±31	1259	cal CE 1234-1291 (1.000)
AWI-1732.1.1	NZ-M-4	56	benth. forams	848±48	1474	cal CE 1438-1508 (1.000)
YAUT-034705	NZ-M-4	60	bulk OM	1041±31	1336	cal CE 1300-1358 (0.867); 1371-1384 (0.133)
YAUT-034706	NZ-M-4	90	bulk OM	2351±31	-21	cal BCE 69-cal CE 31 (1.000)
YAUT-034709	NZ-M-4	120	bulk OM	1733±35	664	cal CE 632-697 (1.000)
YAUT-031531	NZ-M-4	148.5	bulk OM	2085±53	289	cal CE 224-368 (1.000)
YAUT-034713	NZ-M-7	15	bulk OM	1574±29	813	cal CE 773-866 (1.000)
AWI-1733.1.1	NZ-M-7	16	benth. forams	426±48	1950*	CE 1890-2010*
AWI-1734.1.1	NZ-M-7	26	benth. forams	629±48	1674	cal CE 1591-1609 (0.063); 1611-1722 (0.926); 1793-1797 (0.011)
YAUT-034715	NZ-M-7	30	bulk OM	1023±36	1352	cal CE 1316-1389 (1.000)
YAUT-034716	NZ-M-7	55	bulk OM	1521±41	873	cal CE 806-926 (1.000)
YAUT-034717	NZ-M-7	80	bulk OM	1508±36	889	cal CE 833-948 (1.000)
YAUT-034718	NZ-M-7	110	bulk OM	1607±32	773	cal CE 722-813 (1.000)
YAUT-031536	NZ-M-7	141.5	bulk OM	2674±65	-433	cal BCE 521-345 (1.000)

with no age reversals. In both cases, the deeper sample represents the Polynesian era (NZ-M-4 at 56 cm = 1438-1508 CE; NZ-M-7 at 26 cm = 1611-1722 CE), whereas the upper sample falls into the European era (NZ-M-4 at 31 cm = 1692-1822 CE; NZ-M-7 at 16 cm = modern CE). The ^{14}C data from mixed benthic foraminifera are generally younger than those obtained on bulk organic matter. Radiocarbon ages too young for calibration with CALIB 7.1 were assumed to be 1950 ± 60 CE and are marked in Table 4.2 with an asterisk.

Palynology

Core NZ-M-4 has been analysed for the occurrence of pollen from *Podocarpus spp., Pinus spp.* and *Olea europaea* with 19 samples taken from 17 cm down to 230 cm core depth (Figure 4.2). For the amount of *Podocarpus spp*. pollen a general decrease in the number of pollen per gram from the core base towards the core top is obvious, with a slower decline from 230 cm to 72 cm and a sharp drop above 72 cm. The first specimen of *Pinus spp.* pollen occur in a depth of 53 cm with a constant increase to a depth of 22 cm. In the very top sample at 17 cm depth an extensive increase in *Pinus spp.* is recorded. Additionally, this is the only sample were a specimen of *Olea europaea* was found, another exotic plant to New Zealand with the earliest records of naturalisation in the 1970s (Heenan et al., 1999).

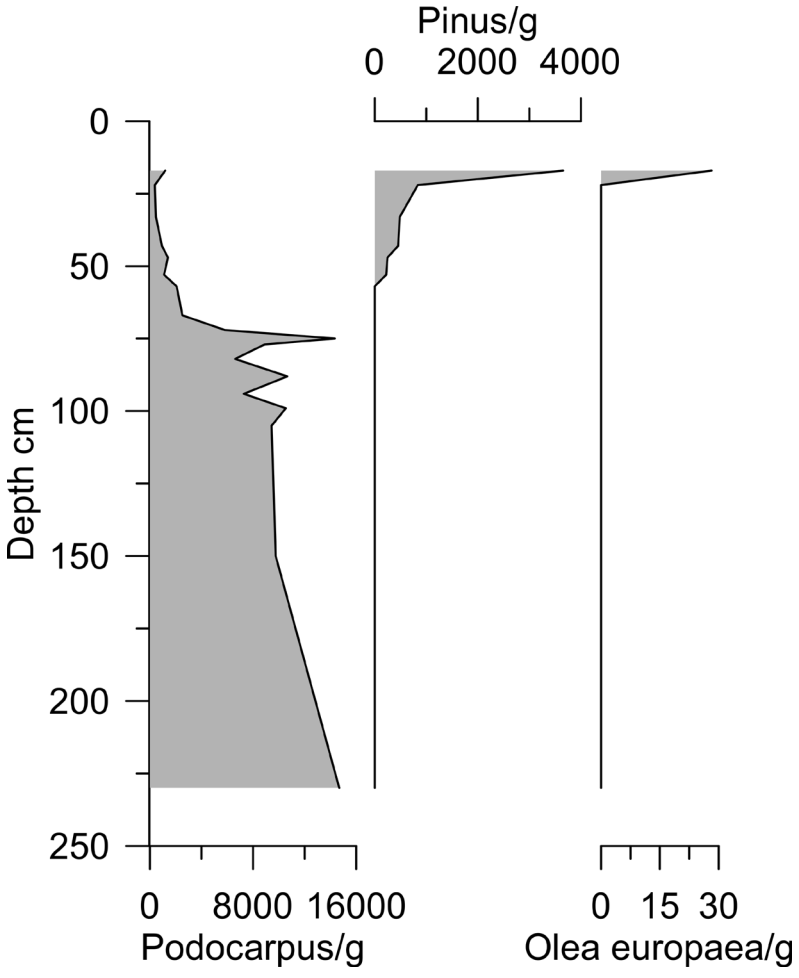

Figure 4.2 Pollen data of core NZ-M-4 showing the absolute abundances (number per grams) of the counted pollen types (Podocarpus, Pinus, Olea europaea).

Grain size analysis

Core NZ-M-2 displays the already macroscopically observed change in grain size. From 226 to 91 cm the sediment is rather coarse in the fine sand range (mean ~70 µm, mode ~195 µm), whereas from 91 cm to the core top, the grain size is significantly finer (mean ~13 µm, mode ~19 µm) (Figure 4.3). The cores NZ-M-4 and NZ-M-7 dominantly consist of silt and clay and show no major changes in grain size. In comparison, core NZ-M-4 (mean ~14 µm, mode ~30 µm) is slightly coarser than core NZ-M-7 (mean ~9 µm, mode ~15 µm) that has been retrieved somewhat further offshore.

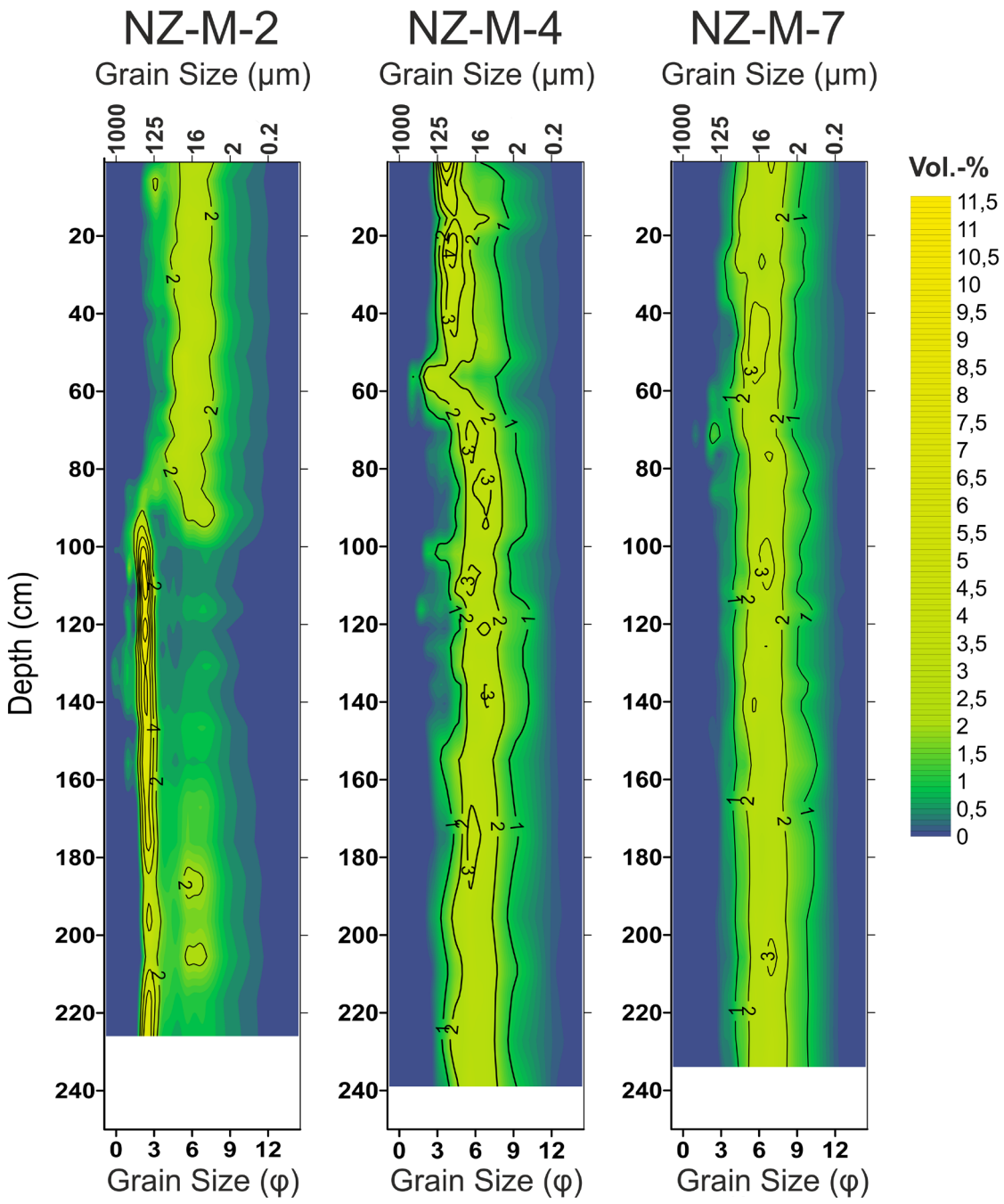

Figure 4.3 Grain size distribution of the 3 principal cores NZ-M-2 (near river, coastal), NZ-M-4 (near river, offshore) and NZ-M-7 (far from river), colour coding gives percentage of each grain size class, varying from 11.5% (yellow) to 0% (blue).

Calibration of pXRF and XRF scanner data

To quantify the semi-quantitative pXRF and XRF Scanner data, they have been calibrated with the WD-XRF data. The correlation plots with the 28 discrete samples analysed with WD-XRF show that the scanner data provide better correlation factors than the pXRF data (Figure 4.4). For the XRF Scanner data, Pb (R^2=0.97) has a higher correlation than Zn (R^2=0.87), but both show a good fit. For pXRF, the correlations with the discrete samples are less significant, but still show a clear positive correlation for Pb (R^2=0.81) and Zn (R^2=0.72). The correlation between the XRF Scanner and the pXRF was used as additional verification for data reliability. Correlation factors for the two elements are good and show no difference between Pb (R^2=0.89) and Zn (R^2=0.89). Using the corresponding correlation equations gives higher quantitative Pb and Zn contents for calibrated XRF Scanner data than for pXRF data. This offset can be explained by the lower beam energy of the pXRF compared to the XRF Scanner, affecting the detection limits. Therefore, lower contents of Pb and Zn are only resolved in the XRF Scanner data, giving a different linear regression equation for the two applied methods. The lower beam energy results additionally in lower analytical precision of the pXRF (Young et al., 2016).

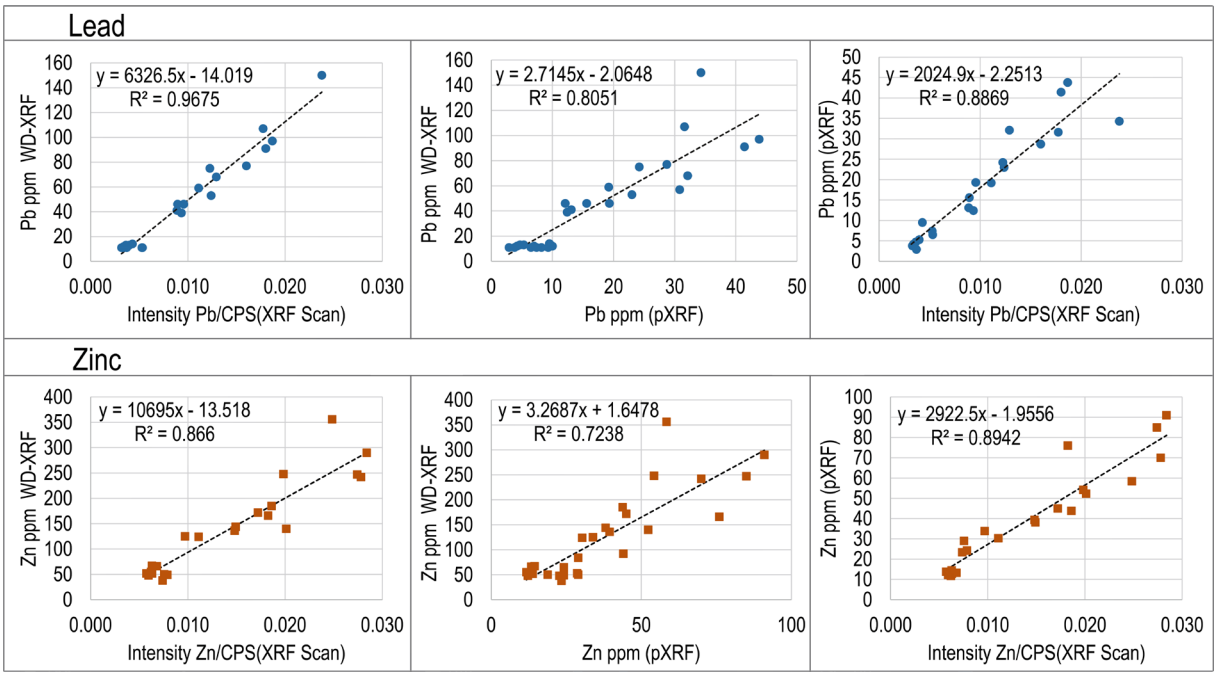

Figure 4.4 Correlation diagrams of the different XRF methods (XRF Scan, pXRF, WD-XRF) and empirically established linear equations for calibrating the XRF Scanner and the pXRF data with the quantitative WD-XRF results.

Calibrated pXRF data

Calibrated pXRF data show a distinct and sudden peak in Pb and Zn in the upper part of 6 of the 8 cores with varying contents and depths of onset (Figure 4.5). Values below the peaks are very constant within the cores as well as between the cores with values around 12 ppm for Pb and 50 ppm for Zn. Exceptions are cores NZ-M-2 and NZ-M-3 with slightly higher values of 18 ppm for Pb and 80 ppm for Zn in the lower core sections.

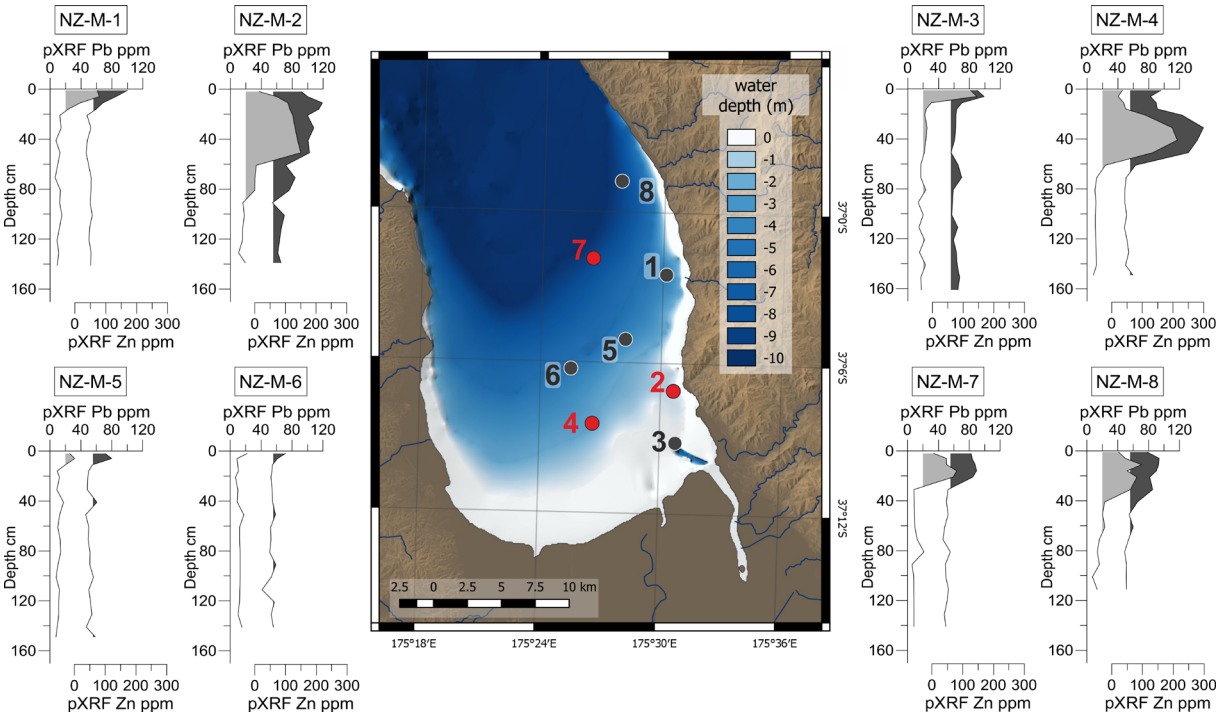

Figure 4.5 Regional and vertical distribution pattern of Pb and Zn contents in the Firth of Thames sediments obtained by calibrated portable XRF data. Light grey shading marks Pb contents >20 ppm, dark grey shadings represent Zn contents > 60 ppm. Circles represent core locations, red circles - 3 high-resolution principal cores, black circles - other cores.

Cores NZ-M-2 and NZ-M-4 display very distinct peaks in their uppermost 56 cm and 54 cm, which also show the highest Pb and Zn contents of all cores (Pb up to 90 ppm in NZ-M-2 and 120 ppm in NZ-M-4; Zn up to 190 ppm and 300 ppm respectively). The cores NZ-M-7 and NZ-M-8 located furthest north have less pronounced peaks with lower contents and onsets of the peaks higher up in sediment column. Nevertheless, all these four cores show the same pattern in peak structure with a pronounced increase and a following decrease in Pb and Zn content towards the core top. The Pb and Zn contents of cores NZ-M- 1, NZ-M-3 and NZ-M-5 increase only very close to the core tops (11-16 cm) and no increase was detected in core NZ-M-6.

Calibrated XRF-scan data (principal cores)

The temporal and spatial patterns of the pXRF data were confirmed by the calibrated XRF Scan results of the three cores NZ-M-2, NZ-M-4 and NZ-M-7 (Figure 4.6), which, however, provide a much higher temporal resolution. In the lower part of core NZ-M-4 rather constant values around 12 ppm for Pb and 57 ppm for Zn can be observed. At 54 cm core depth, both values increase steeply to a maximum at 34 cm depth and show from there a general declining trend towards the top of the core. The heavy metal content at the sediment surface is still clearly above the background values found in the lower part of the core. The average content of this peak section is 82 ppm for Pb and 236 ppm for Zn respectively. Core NZ-M-7 shows a very similar pattern, but with generally lower values (Pb = 52 ppm, Zn = 154 ppm) and the onset of the strong increase higher up in the core at 26 cm.

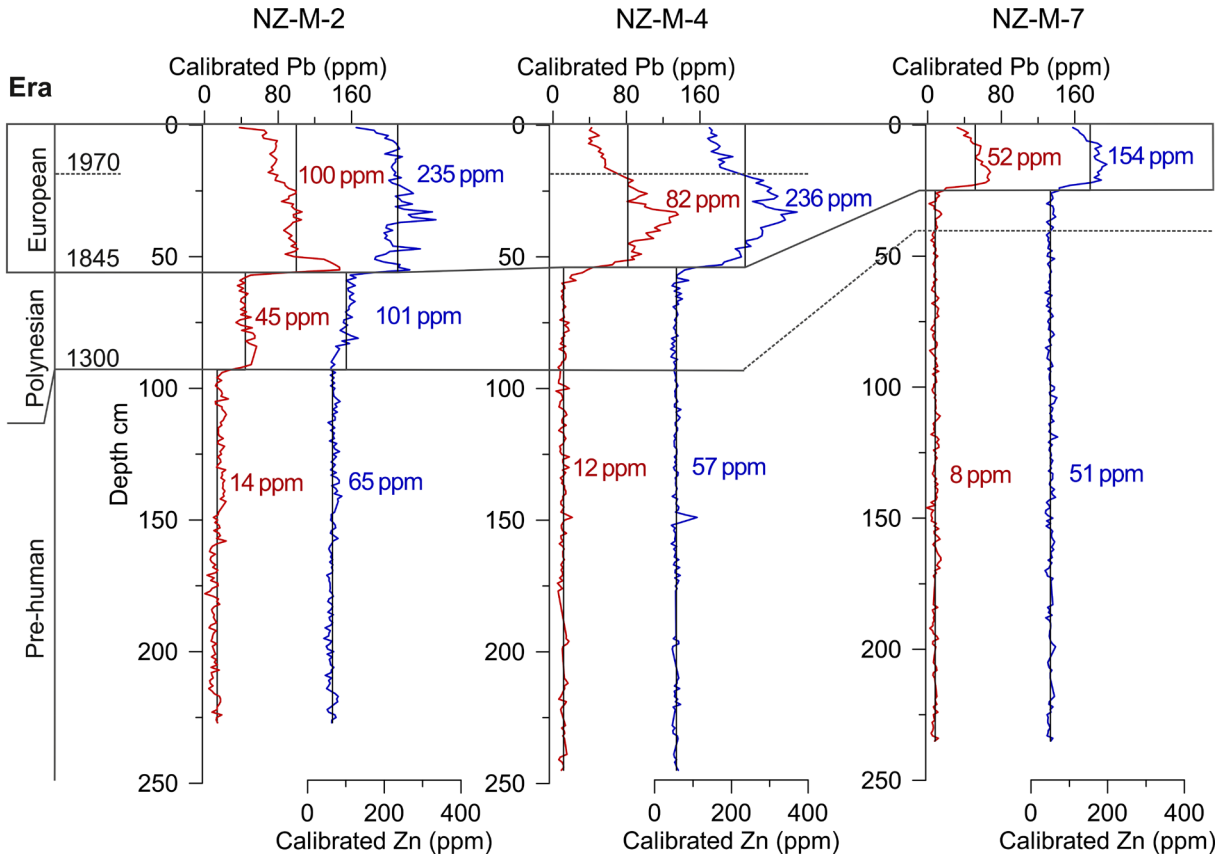

Figure 4.6 High-resolution calibrated XRF Scanner data for the 3 principal cores with the interpreted age zonation of the pre-human, Polynesian and European Era. Averaged Pb and Zn contents were calculated from all values above the peak onset and below the peak onset respectively. Solid lines are based on the stratigraphic frameworks. Dotted line in NZ-M-7 is extrapolated under the assumption of similar relative changes in sedimentation rates in all cores. Dotted line in NZ-M-4 is based on the first occurrence of olea europaea.

Core NZ-M-2 is exceptional, as a two-step increase in heavy metals was recorded in both independent XRF data sets. Heavy metal values stay very constant at 14 ppm (Pb) and 65 ppm (Zn) from the core bottom up to 93 cm depth. Above this boundary, matching with the change in grain size, the level of Pb (44 ppm) and Zn (101 ppm) is elevated abruptly. This step is followed by a second, even sharper increase to average contents of 100 ppm for Pb and 235 ppm for Zn at 56 cm. Towards the core top also in this core Pb and Zn contents decline again but stay above the lower core section values.

4.5 Discussion

Development of the stratigraphic framework

Despite the high number of available radiocarbon dates (n=33), the overall scatter of the data makes the development of a stratigraphic framework for the three principal cores focusing on the delineation of the three eras discussed above rather complex (Figure 4.7). Here, the final stratigraphic frameworks are built on three premises: (i) mixed benthic foraminifera give the most reliable ages of the different materials dated and are therefore taken as hard constraints, (ii) the first occurrence of exotic pollen is a distinct marker for the beginning of the European era, and (iii) radiocarbon dates based on organic matter can serve only to constrain maximum ages (soft constraints). Ages obtained from bulk organic matter

with a terrestrial component are known to be generally older than the time of actual deposition, as they have long residence times, depending on the size, morphology and climate of the catchment area (Blaauw et al., 2011). Shells were regarded only if their dates fitted into the overall pattern, as they were not classified and therefore the position in the sediment (epifaunal, infaunal) is uncertain. Thus, in a first step, the age-depth relationship attained from radiocarbon dating on foraminifera by interpolation is accepted as the most reliable (solid line, Figure 4.7). Minor age reversals covered by the 1σ range could be influenced by bioturbation or some disturbance related to the shallow water depth and are not considered here.

With respect to premise (ii), two additional palynological dates were established for core NZ-M-4 at 53 cm. The occurrence of *Pinus spp.* pollen in New Zealand lake and coastal sediments is widely used as a stratigraphic event that marks the onset of the European era in ~1845 CE (Augustinus et al., 2006). Consequently, the first occurrence of *Pinus spp.* pollen at 53 cm in core NZ-M-4 was dated to 1845 CE. Furthermore, the drastic increase in the content of *Pinus spp.* pollen in the sediment at 17 cm depth is interpreted as the first evidence of pine plantations, which were established in the 1970s (Hume and Dahm, 1992). This interpretation is supported by the occurrence of the only *Olea europaea* pollen found in the core, as the oldest records of this species in New Zealand are from the 1970s (Heenan et al., 1999). This allows for core NZ-M-4 to differentiate the European era into a historic and recent part (Figure 4.6). Furthermore, in the same core at 20 cm depth, a reliable shell-based date reveals a recent age (~1950 CE, Figure 4.7).

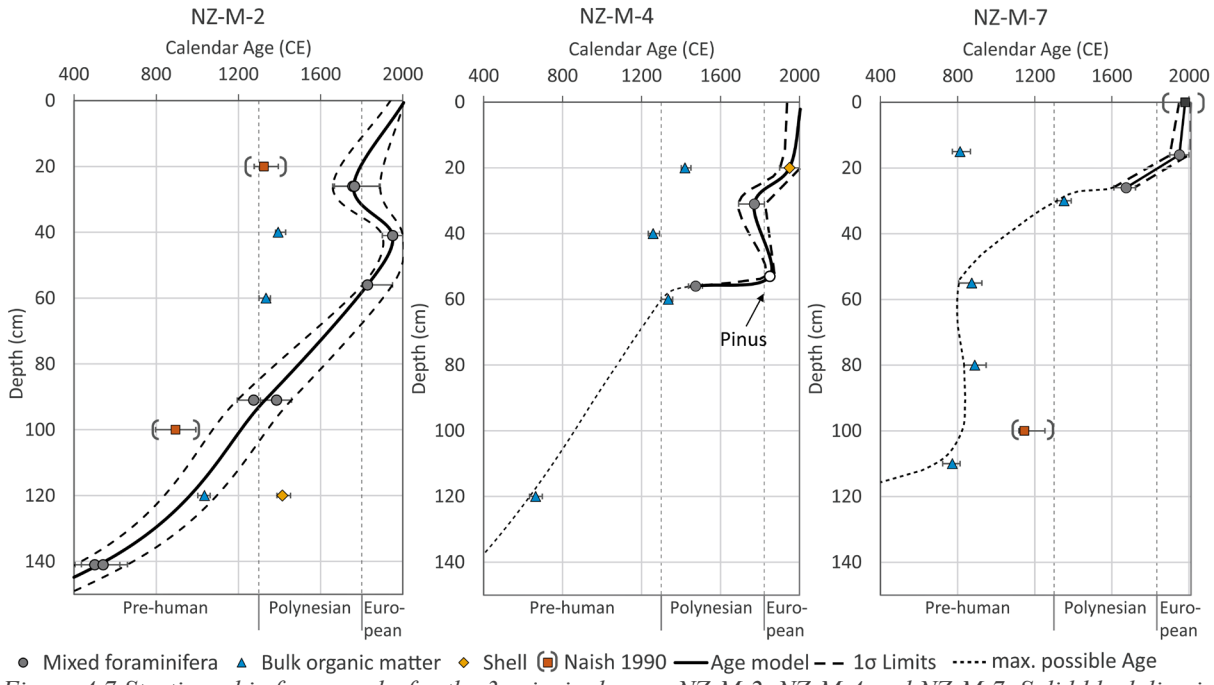

Figure 4.7 Stratigraphic frameworks for the 3 principal cores NZ-M-2, NZ-M-4 and NZ-M-7. Solid black line is the interpolation between the calibrated ages of the values considered as reliable. Dashed black lines are the upper and lower limits based on the 1σ range of reliable data. Dotted line represents the maximum possible age for the lower sections of NZ-M-4 and NZ-M-7. Orange squares in () are dates obtained on cores in less than 5 km distance from the NZ-M core sites (Naish, 1990).

All stratigraphic frameworks, interpreted here solely to differentiate between the pre-human, the Polynesian, and the European era, were forced to go through 2010 CE at the sediment surface. This assumption is supported by the foraminifera as well as pollen dates obtained in this study and reinforced by a modern radiocarbon date (CE 1950 ± 60) from Naish (1990) at the sediment surface of a core taken in less than 5 km distance from core NZ-M-7. A comparison of the stratigraphic framework of this study to published age-depth relationships based on shells and wood fragments for two cores taken within less than 5 km from the cores NZ-M-2 and NZ-M-7, respectively (orange squares in Figure 4.7; Naish, 1990) shows a reasonably good agreement of the general sedimentation rates.

Sedimentation rates

A comparison of the resulting sedimentation rates for the principal cores with rates obtained from the same area (Naish, 1990; Hume and Dahm, 1992) shows that all rates are in the same order of magnitude (Table 4.3). Even though the sedimentation rates presented here are higher than those previously reported, all three data sets document that sedimentation rates were significantly lower during the pre-European times (< 0.65 mm/yr) and increased with the onset of the European era (up to 3.2 mm/yr). On average, all data indicate an approximately fourfold increase in sedimentation rate upon the beginning of the European era. Additionally, the pollen data in core NZ-M-4 indicate, that the sedimentation rates in the recent European era are even higher than in the historic one. Acceleration of sedimentation rates during European times was already suspected by Hume and Dahm (1992) and suggested to be additionally enhanced by the establishment of pine plantations in the 1970s. The lack of reliable ages in the lower sections of the NZ-M cores does preclude any differentiation between the pre-human and Polynesian eras and, therefore no statement can be made whether the Polynesian deforestation had an impact on sedimentation rates.

Table 4.3 Comparison of sedimentation rates in the southeastern Firth of Thames in mm/yr.

		This study			**Naish (1990)**	**Hume and Dahm (1992)**
		NZ-M-2	NZ-M-4	NZ-M-7		
European	Recent		3.8			
	Historic		2.8			
	Overall	3.2	3.1	1.5	1.9-2.1	0.5 & 1.3-1.5
Polynesian		0.65	n.a.	n.a.	0.35-0.45	0.1-0.4
Pre-human		n.a.			n.a.	0.1-0.2

Timing of increase in heavy metal inputs

For the older parts of the cores, especially for the pre-human and the early Polynesian eras, a well-defined stratigraphic framework only exists for core NZ-M-2. The sedimentation rate of NZ-M-2 for the Polynesian era has been extrapolated to core NZ-M-4, which appears to be a valid assumption as both cores also have very similar sedimentation rates for the European era. Extrapolation for NZ-M-7 (dashed line in Figure 4.6) is based on the assumption, that sedimentation rates in this distal location were

constantly half of the sedimentation rates close to the Waihou River, as it is the case for the European era.

Two reliable radiocarbon ages at 91 cm depth of core NZ-M-2 give an age of ~1350 CE, which slightly post-dates the arrival of the Polynesians. This is close to the depth level of 96 cm where the sediments get significantly finer and enriched in heavy metals. Interestingly, in the other two principal cores, neither the two-step increase in heavy metal contents (Figures 4.5 and 4.6) nor the shift in grain size (Figure 4.3) is recorded. However, assuming a sedimentation rate for the Polynesian era of ~25% of that corresponding to the European era, all principal cores should cover the change from the pre-human to the Polynesian era (see correlation in Figure 4.6 for the principal cores). Consequently, the two-step increase in core NZ-M-2 is interpreted to reflect a local sedimentological change at this near-coastal site (e.g., a meandering tidal channel) that primarily affected the grain size distribution. The accompanying shift towards higher heavy metal contents probably reflects a simple grain-size effect caused by higher loadings of heavy metals of finer particles due to their larger capacity for adsorption (Förstner and Wittmann, 1981). As cores NZ-M-4 and NZ-M-7 show no changes neither in XRF nor in grain size, the precise determination of the boundary between the pre-human and Polynesian era is difficult, but obviously it is not accompanied by any significant anthropogenic impact.

The coherent pattern with continuously low heavy metal contents through the pre-human as well as the Polynesian era in all the cores (except NZ-M-2) indicates that the Polynesians did not leave any sizable impact on the heavy metal budget in the Firth of Thames. Instead, the sudden increase in heavy metal contents in 6 out of 8 investigated cores (Figure 4.5) can be correlated with the European era based on the stratigraphic information available for the three principal cores (Figure 4.6, 4.7).

In cores NZ-M-2 and NZ-M-4, both located in the inner Firth of Thames, the increase in heavy metal contents occurs at 56 cm and 54 cm core depth, respectively, corresponding to a radiocarbon age of ~1830 CE (NZ-M-2) as well as to the onset of *Pinus spp.* pollen deposition (NZ-M-4) corresponding to ~1845 CE (Augustinus et al., 2006). In core NZ-M-7 from a more distal position in the central Firth of Thames, Pb and Zn contents increase at 26 cm core depth, radiocarbon dated to ~1670 CE. Despite this somewhat older age, linking the increase in heavy metal contents (Figure 4.6) with the increase in sedimentation rate (see the slopes of the curves in Figure 4.7) clearly reflects the same pattern as in the other two cores and thus points to the impact of the European settlers causing the enhanced deposition of heavy metals also at this site. The comparably old radiocarbon age might be affected by the significantly lower average sedimentation rate at this site that likely allows for a larger bioturbation bias in the dating and/or 'smear' the onset of the Pb and Zn signal to some degree into the deeper sediment.

As the grain-size data show no change associated with the increase in heavy metals, any grain size effect can be excluded, pointing to a real input signal. Thus, based on (i) the similar pattern of the Pb and Zn contents in the cores with decreasing contents and thicknesses of the affected sediment packages from

the main sediment source, the Waihou River (not considering core NZ-M-3 due to its very different sediment texture, see above), to further offshore and (ii) the fit between the radiocarbon and the pollen data defining the onset of the increase, it is concluded that the increase in heavy metal input to the Firth of Thames correlates with the onset of the European era.

Furthermore, all three principal cores show a decline in heavy metal content towards the core top (Figure 4.6), most pronounced in core NZ-M-4 above maximum Pb and Zn contents at 34 cm. In the same core, the rapid increase in the number of *Pinus spp.* pollen and the occurrence of *Olea europaea*, at 17cm depth, roughly mark the year ~1970 CE. This indicates that, in the second half of the 20th century, the input of heavy metals into the Firth of Thames already decreased, coinciding with a decline in mining activity in the Coromandel region with main operations between the 1890s and 1930s (Kidd, 1988).

Cause of elevated heavy metal levels

The main evidence for the source of pollution is provided by the stratigraphic framework, placing the marked increase in heavy metal contents in the Firth of Thames sediments clearly into the European era. As sedimentary Pb and Zn contents were rather low and constant during the pre-human and Polynesian eras, the increase in heavy metal inputs points to a cause unique to activities of the European settlers.

The prime candidate here is mining. During the early gold mining operations (1850s to 1950s) along the Coromandel Peninsula substantial volumes of mine waste were dumped directly into the Firth of Thames and discharge of tailings into the Waihou River and its tributaries occurred (e.g., Webster, 1995; Craw and Chappell, 2000). Typical contaminants in these mine tailings are Pb and Zn as well as Cu and As (Hume and Dahm, 1992; Christie et al., 2007). As in this region the gold is associated with sulphide-rich sections of hydrothermally altered host rock, these elements were probably released to the Firth of Thames through oxidation and leaching of the mine waste (Garrels and Thompson, 1960; Livingston, 1987; Craw and Chappell, 2000). Elevated Cu and As contents were neither detected in the XRF Scan nor in the pXRF data, but there are indications from the WD-XRF that these elements show similar enrichments as Pb and Zn in the Firth of Thames sediments. Most certainly, the Cu and As contents are too low to be detected by the energy dispersive methods (B. Schnetger, pers. communication).

The strongest enrichment in heavy metals was recorded near the Waihou River (cores NZ-M-2 and NZ-M-4), which is, together with its tributaries the Tui Stream and Ohinemuri River, known to be strongly influenced by mining operations (Webster, 1995). In addition, elevated Zn and Pb levels also have been found near the coast of the Coromandel Peninsula, where small streams drain the mining areas. The sediments from these streams are also characterised by enhanced Zn (106-720 ppm) and Pb (18-85 ppm) contents (Sheppard et al., 2009).

The main period of gold mining operations in the Coromandel Range ended with the closure of the Martha mine in 1952 (Christie et al., 2007), although most of the mines were already closed by the end of the nineteenth century (Fraser, 1910; Downey, 1935; Sheppard et al., 2009). This is a likely

explanation for the observed decrease in Pb and Zn contents in the uppermost sections of the principal cores. While some mines re-opened in a recent mining phase (post-1960), these days tailings are confined by dams (Craw and Chappell, 2000).

Although the observations clearly point to mining as the most likely trigger for the elevated Zn and Pb contents in the Firth of Thames sediments, it also might be impacted by other processes. These include volcanic eruptions, changes in source area, enhanced erosion in the catchment and urban runoff. As New Zealand, part of the Pacific ring of fire, is characterised by frequently occurring volcanic eruptions also over the last millennium (Lowe et al., 2002; Lowe 2008), the sudden increase in Pb and Zn records after low and rather constant inputs for seemingly centuries (Figure 4.6) does not fit to a volcanic source of the heavy metals.

Linking the enhanced Pb and Zn inputs to a change in source area would most likely also require changes in the sediment transport and deposition processes that should be reflected in the grain-size data. However, in the principal cores (except NZ-M-2) the grain-size compositions show no major change corresponding to the increase in heavy metal contents (Figure 4.3). This is further supported by the macroscopic lithological core description of the remaining five cores, with sand sedimentation near the Waihou River mouth (NZ-M-3) and homogeneous silt grain sizes for all others (NZ-M-1, NZ-M-5, NZ-M-6, NZ-M-8).

Interestingly, the lowest Pb and Zn contents in the sand dominated lower part of core NZ-M-2 are comparable or only slightly above the ‘background’ values observed in the two other fine-grained principal cores (Figure 4.3), despite any grain-size effect. However, the coarser grained deposits in this core might derive from a different source area. Still, natural background values for Pb (45 ppm) and Zn (101 ppm) recorded in NZ-M-2 for the Polynesian era are much higher than for cores NZ-M-4 and NZ-M-7 collected further offshore (Pb: 8-12 ppm; Zn: 51-57 ppm). This offset might be due to the close proximity of core NZ-M-2 to the Thames gold deposits immediately onshore. A comparably short transport distance, thus, might have resulted in higher natural Pb and Zn inputs to this site originating from natural erosion.

The discussion if erosion in New Zealand has increased after the arrival of the first humans is controversial (e.g., Grant, 1985; McGlone, 1989; Wilmshurst, 1997; Ogden et al., 2003). Both, the Polynesian and the European settlers cleared vast stretches of land for agriculture. Nevertheless, on a regional scale around the Firth of Thames, the arrival of the Polynesians left no traces in the sediment composition (grain size, Pb and Zn contents) albeit sedimentation rates slightly increased (Table 4.3). Thus, deforestation by the Polynesians probably just mobilised more sediments from the same source area representative for the regional lithology by the same transport processes. The same can be assumed for the effects of forest clearances during the European era done in the context of farming, construction works, kauri logging, and gum digging (Sale, 1978; Hume and Dahm, 1992). Consequently, these

activities probably increased the quantity of the eroded sediments but did not affect the composition towards containing more heavy metals. Thus, deforestation probably also had no major impact on the sudden increase of Zn and Pb inputs since the 1840s. Still, it has to be acknowledged that there is conflicting evidence in core NZ-M-2, where a distinct natural background value cannot be determined with absolute certainty due to a change in grain size.

Finally, also significant urban runoff from the major settlement areas on New Zealand's North Island was identified as a source for heavy metals. However, being documented to begin in the mid-1920s for Wellington Harbour (Dickinson et al., 1996) and post-1945 in the Tamaki Estuary (Auckland area; Abrahim and Parker, 2002), urban runoff is not very likely to cause the sudden increase in Pb and Zn contents at c.1845 in the Firth of Thames that is surrounded by only lightly populated areas. In addition, by pinpointing the years around 1970 in the presented records by increasing *Pinus spp.* pollen numbers and by the occurrence of *Olea europaea*, heavy metal inputs to the Firth of Thames were already decreasing shortly after urban runoff began to affect the Auckland region. Based on these considerations, gold mining in the Coromandel Peninsula is most likely the dominant cause for an increased release of Pb and Zn during the European era.

Assessment of the human impact

Based on the dated cores, it can be concluded that the onset of enhanced heavy metal input clearly observed in 6 out of the 8 investigated cores from the Firth of Thames occurred at all sites simultaneously approximately at 1845 CE. Since then, enhanced heavy metal input, most likely due to historical gold mining in the region, had a widespread effect on sediment chemistry in the Firth of Thames. However, as the pXRF based data are considered less reliable, the heavy metal contents will be evaluated quantitatively only in the principal cores (Table 4.4).

Table 4.4 XRF Scanner contents of Pb and Zn in ppm of the surface sediments (topmost value obtained in the sediment core), the averaged peak section (all values from peak onset to core top) and the averaged background section (all values below peak onset) measured on the three principal cores. Additionally, Pb and Zn values for the Tamaki Estuary (Abrahim and Parker, 2008) and for Wellington Harbour (Dickinson et al., 1996) are listed for comparison. Values in parentheses present the conflicting potential natural baseline which are not comparable because of grain size differences. EF = enrichment factor comparing peak average and background values.

	NZ-M-2		NZ-M-4		NZ-M-7		Abrahim and Parker (2008)		Dickinson et al. (1996)	
	Pb (ppm)	Zn (ppm)	Pb (ppm)	Zn (ppm)	Pb (ppm)	Zn (ppm)	Pb (ppm)	Zn (ppm)	Pb (ppm)	Zn (ppm)
Surface Sediment	38	127	42	143	32	109				
Peak average	100	235	82	236	52	154	73	207	104	221
Background	45 (14)	101 (65)	12	57	8	51	22	72	37	128
EF	2.2	2.3	6.8	4.1	6.5	3.0	3.3	2.9	3	1.7

In the principal cores, the baseline contents for Zn and Pb are extremely stable in the pre-European era, suggesting that these reflect pristine natural background values. Except for NZ-M-2 where the natural baseline is not absolutely certain, background values in the Firth of Thames are significantly lower than those reported for Wellington Harbour (Dickinson et al., 1996) and for the Tamaki Estuary near Auckland (Abrahim and Parker, 2008) (Table 4.4). These differences in background values underline the need for baseline studies in different regions with different hydrological and geological settings.

According to the Australian and New Zealand Environment and Conservation Council (ANZECC) Sediment Quality Guidelines (Simpson et al., 2013), the Pb and Zn contents of the surface sediments are within the Sediment Quality Guideline Values (SQGV) Category 1 indicating negligible effects (Table 4.5). However, as all three cores show Zn and Pb peaks in the subsurface and decrease again towards the core top, Category 1 thresholds have been exceeded in the past. Taking the average peak values (Figure 4.6, Table 4.4), the Pb contents of all three principal cores and the Zn contents of two of them fall into category 2, meaning ecological effects are possible. Even though Pb and Zn contents in the surface sediments are below the threshold for Category 2, the higher contents in the subsurface impose potential threats for the ecosystem in case of resuspension (e.g., dredging, bioturbation). Considering the spatial-temporal pattern displayed be the pXRF data, it can be assumed that also for the wider area in the Firth of Thames in the subsurface sediments Category 2 thresholds might be passed.

Table 4.5 ANZECC Sediment Quality Guideline Values for the total content of lead and zinc

	Pb	Zn	Effects
Category 1	< 50 ppm	< 200 ppm	Negligible
Category 2	50-220 ppm	200-410 ppm	Possible
Category 3	> 220 ppm	> 410 ppm	Expected

4.6 Conclusion

From the results presented the following conclusions can be drawn:

- A significant increase of Pb and Zn contents occurred with the onset of the European era and was most likely caused by mining.
- The sedimentation rates during this time period increased simultaneously, but might not only be related to the historical gold mining operations.
- The impact on the Pb and Zn contents of the bulk sediment is widespread in the southeastern Firth of Thames.
- Most Pb and Zn surface sediment contents are according to ANZECC below the guideline values, but exceed them in the subsurface.

Acknowledgements

This project was funded by the Deutsche Forschungsgemeinschaft (DFG) through the International Research Training Group – 'Integrated Coastal Zone and Shelf-Sea Research' (GRK 1598 INTERCOAST). Funding for radiometric dating was partly provided by Waikato Regional Council, New Zealand (Funding Deed No: SAS2017/2019-1955). The authors would like to thank Dean Sandwell and Christopher Morcom for technical support during the coring campaign. Data were in parts acquired at the XRF Core Scanner Lab at the MARUM – Center for Marine Environmental Sciences, University of Bremen, Germany. The data reported in this paper will be archived in Pangaea (www.pangaea.de)

Chapter 5 Manuscript 2

Test Deformation and Chemistry of Foraminifera as Response to Anthropogenic Heavy Metal Input

S. Boehnert[1, *], A.R. Birkelund[2], G. Schmiedl[3], H. Kuhnert[1], G. Kuhn[4], H.C. Hass[5], D. Hebbeln[1]

[1] *MARUM — Centre for Marine Environmental Sciences, University of Bremen, Leobener Straße 8, 28359 Bremen, Germany*

[2] *Department of Geosciences, University of Oslo, P.O. box 1028 Blindern, 0316 Oslo, Norway*

[3] *Center for Earth System Research and Sustainability, Institute for Geology, University of Hamburg, Bundesstraße 55, 20146 Hamburg, Germany*

[4] *Alfred Wegener Institute, Am Alten Hafen 26, 27568 Bremerhaven, Germany*

[5] *Alfred Wegener Institute, Hafenstraße 43, 25992 List/Sylt, Germany*

Abstract

Near-coastal marine environments close to highly populated coastal areas are prone to the accumulation of pollutants, such as heavy metals, potentially causing negative ecological effects due to their toxicity. Benthic foraminifera are sensitive to such changes and therefore widely used as tools to monitor pollution. One characteristic often applied is the rising number of deformed tests under increasing environmental stress such as elevated levels of heavy metals, but little is known about the relation between heavy metal incorporation into foraminifera tests and the formation of test deformities. Here, two sediment cores covering the pollution history of the southeastern North Sea of the past 400 years are compared with respect to the occurrence of abnormal foraminiferal tests, foraminifera test chemistry and bulk sediment Pb content. The proportion of deformed tests shows a gently increasing trend throughout the record followed by a strong rise around the year ~1960 CE. However, the total abundance of malformed foraminiferal tests seems not to be correlated to historical heavy metal pollution. Bulk sediment Pb contents reveal a distinct increase as early as 1850 CE, while sudden increases in Pb/Ca and Cd/Ca in the calcite shells of the two benthic foraminifera species *Ammonia beccarii* and *Elphidium excavatum* occur with a temporal offset. Therefore, we suggest that foraminifera react with test deformation to environmental stressors other than the studied heavy metals. Test chemistry reflects bulk sediment chemistry very well, but we propose that Pb and Cd are only incorporated after a yet to be defined threshold of pollution is exceeded. This makes test chemistry a suitable tool for monitoring polluted areas above a certain limit only but offers the potential to quantify contaminant concentration.

5.1 Introduction

Near-coastal marine environments close to urbanised areas are prone to accumulation of pollutants, such as heavy metals. These put high anthropogenic pressure on the local ecosystem because of their toxicity and persistence. Benthic foraminifera are widely used as a monitoring tool for pollution as well as for

the recovery of marine ecosystems (e.g., Alve, 1991, 2000; Yanko et al., 1994; Geslin et al., 2000; Scott et al., 2005; Bergin et al., 2006; Frontalini and Coccioni, 2008; Jayaraju et al., 2008; Caruso et al., 2011; Alve et al., 2016; Vidović et al., 2016). The main advantages of foraminifera as indicators of the ecological state of an area are that they (i) are found in nearly all marine environments, (ii) have short reproductive cycles and therefore respond fast to changes, (iii) provide paleo records due to their calcitic tests often preserved in sediments, and (iv) allow for statistical analyses due to their small size and high abundance in the sediment (Boltovskoy, 1964; Yanko et al., 1999; Murray, 2006; Schönfeld, 2012; Jones, 2014).

Over the past decades a growing number of studies focused on foraminifera as bioindicators for environmental change, natural or man-made (e.g., Alve, 1995; Henderson, 2002; Jorissen et al., 2007; Katz et al., 2010). Such studies are either laboratory-based culturing studies (e.g., Munsel et al., 2010; Havach et al., 2001; Hintz et al., 2006; Nardelli et al., 2016; Brouillette Price et al., 2019) or field studies (e.g., Alve, 1991; Geslin et al., 2002; Scott et al., 2005; Frontalini et al., 2009; Caruso et al., 2011; Elshanawany et al., 2018). For instance, culturing studies investigating the effect of elevated levels of particular metals mainly focussed on cytological changes in organic tissue (Bresler and Yanko-Hombach, 2000; Le Cadre and Debenay, 2006; Frontalini et al., 2015, 2016, 2018) or the incorporation of specific heavy metals into the calcite structure of the tests (Havach et al., 2001; Hintz et al., 2006; Munsel et al., 2010; Nardelli et al., 2016). The degree of incorporation of heavy metals into the calcite lattice of foraminiferal tests is proportional to their concentration in the ambient seawater as described by the so-called partition coefficient (e.g., Lea and Boyle, 1989). Such element- and species-specific partition coefficients have been established for various elements (e.g., Cd, Ba, Ni, Cu, Mn, Zn) and foraminifera species (e.g., Havach et al., 2001; de Nooijer et al., 2007; Munsel et al., 2010; Nardelli et al., 2016) and provide the potential to calculate past element concentrations in ambient waters from fossil foraminiferal tests.

Research on organic tissue gives information on the biological response of specific foraminifera species exposed to various concentrations of a heavy metal and its bioavailability (e.g., Le Cadre and Debenay, 2006; Frontalini et al., 2015, 2016, 2018). However, as organic tissue can only be investigated in living foraminifera, this approach precludes analyses of historical trends in pollution. Most monitoring field studies on the other hand, focus on parameters such as foraminiferal assemblages and test deformation using numerous surface sediment samples distributed over a specific area in order to evaluate the current state of pollution on regional scales (Yanko et al., 1998; Coccioni, 2000; Geslin et al., 2002; Scott et al., 2005; Bergin et al., 2006; Caruso et al., 2011; Elshanawany et al., 2018).

As foraminiferal shells, and thus, information on faunal assemblages (including population density, diversity and proportion of deformed tests) are preserved in the sediment record, such data allow to reconstruct historical ecological changes (Alve, 1991; Hayward et al., 2004; Scott et al., 2005; Vidović et al., 2016). However, the ecological dynamics of foraminifera communities are complex and not yet

fully understood. The main reasons are that (i) pollution often occurs in coastal marine areas that are marked by highly variable temporal and spatial small-scale environmental conditions causing significant natural stress, (ii) different environments can get differently affected by the same kind of pollution, and (iii) usually not only one pollutant but a combination of several contaminants (multiple stressors) impact the environment (Alve, 1995; Jayaraju et al., 2008).

Foraminifera display varying tolerances towards pollutants, depending on their species (e.g., Alve, 1991; Le Cadre and Debenay, 2006) as well as on the kind of pollutant (Jayaraju et al., 2008; Nardelli et al., 2016; Brouillette Price et al., 2019). It is assumed that biological defence mechanisms, like inhibited cell metabolism or detoxifying enzymes (Ganote and Van der Heide, 1987; Yanko et al., 1994; Bresler and Yanko-Hombach, 2000; Frontalini et al., 2009) or cytological changes (Frontalini et al., 2016) protect foraminifera from toxins. It was concluded that such cytological changes may cause test deformation (Yanko et al., 1998). Le Cadre and Debenay (2006) conducted a culturing study with graded Cu concentrations and observed cytological changes only in deformed specimens. This indicates that deformed tests could be a suitable qualitative proxy for environmental impact. A recent culturing study on benthic foraminifera and elevated concentrations of Cd, Pb and Zn found that only Zn produced abundant aberrant tests (Brouillette Price et al., 2019).

Studies combining quantitative test chemistry and test deformation are sparse. Sharifi et al. (1991) reported increased heavy metal concentrations in deformed foraminifera compared to undeformed specimens, whereas Samir and El Din (2001) used a qualitative approach to examine heavy metal contents in abnormal foraminifera tests. Thus, although increased heavy metal pollution is widely accepted as a major cause for abnormal foraminiferal tests (Alve, 1991; Yanko et al., 1994, 1998; Le Cadre and Debenay, 2006; Polovodova and Schönfeld, 2008; Jayaraju et al., 2008; Caruso et al., 2011), quantitative analytical evidence is scarce. Consequently, a combined approach of test deformities and test chemistry could hold valuable information on the historical ecological impacts.

This study aims to evaluate the response of benthic foraminifera to increasing heavy metal deposition in the North Sea over the past 400 years by such an integrated approach, providing quantitative data on heavy metal contents in foraminiferal shells and on the amount of shell deformities. It is based on two sediment cores collected close to each other in the southeastern North Sea. One core provides the rate of abnormal test occurrence, whereas the other yielded Cd/Ca and Pb/Ca ratios in foraminiferal shells. Excellent correlation of both cores was obtained by XRF-based semi-quantitative estimates of Pb and Zn contents in the bulk sediment as well as by $\delta^{15}N$ data in combination with the available stratigraphies. Comparing XRF-derived bulk sediment elemental composition, ICP-MS determined Cd/Ca and Pb/Ca ratios in the calcite tests of *A. beccarii* and *E. excavatum* and proportions of aberrant tests, addresses the questions, (i) whether the chemical signature of benthic foraminiferal calcite reflects the chemistry of the bulk sediment, (ii) whether the bulk sediment chemistry and foraminiferal test deformation are related and (iii) whether there is a correlation between test deformation and test chemistry.

5.2 Regional Setting

The North Sea is a shallow marginal sea of the North Atlantic with a predominantly counter-clockwise circulation (Otto et al., 1990) (Figure 5.1). Substantial input of suspended fine particles from the often densely populated and industrialized hinterland is transported into the North Sea by several big rivers, including the Elbe and Weser in its southeastern part (e.g., Puls et al., 1997), close to the study area. The total runoff entering the North Sea region amounts to 296-354 km³/yr from a catchment area covering 841,500 km² (OSPAR, 2000). The sink for many of the contained pollutants is the North Sea.

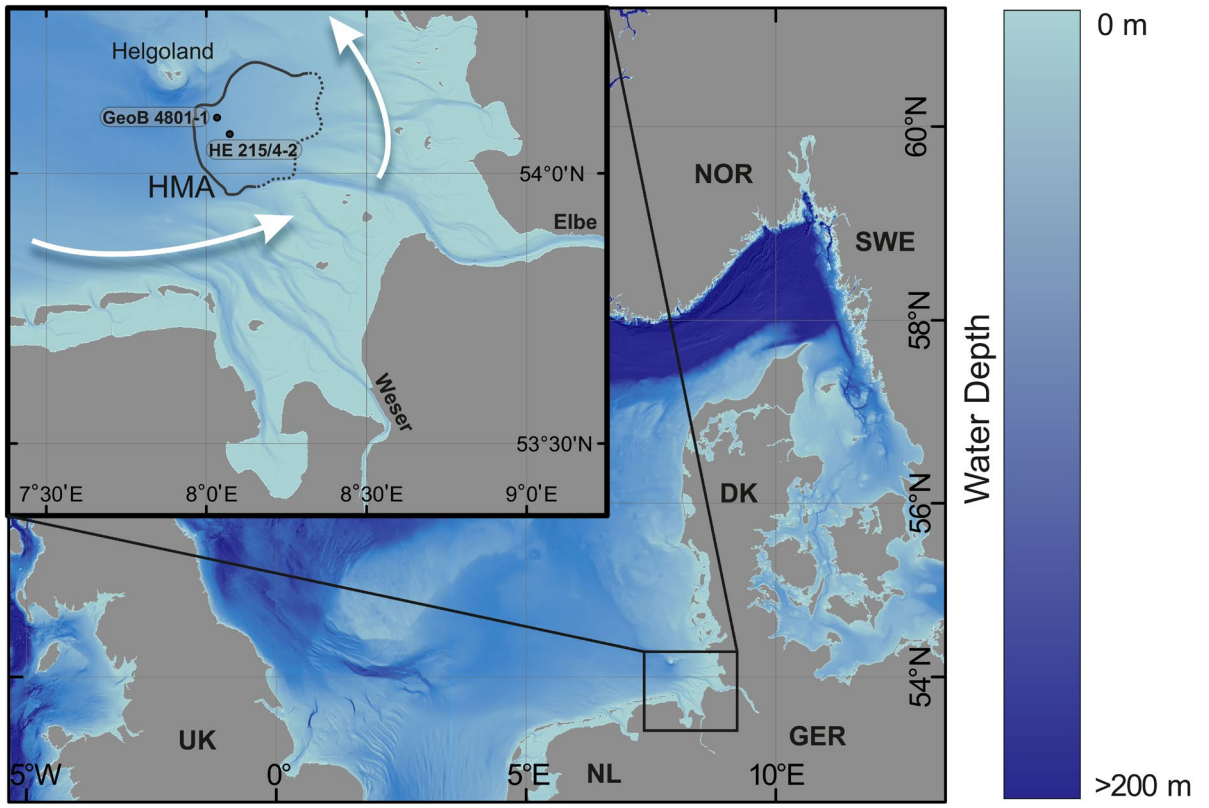

Figure 5.1 Map of the North Sea with an inset zooming into the study area, the Helgoland Mud Area (HMA; outlined by the solid (confirmed limit) and stippled (estimated limit) black line according to von Haugwitz et al., 1988). The locations of the two sediment cores used are indicated together with the residual currents (white arrows).

A prominent depocentre for fine sediments in the southern North Sea is the Helgoland Mud Area (HMA), with an extent of ~500 km² and a mean water depth of 20 m (Figge, 1981; Eisma and Kalf, 1987). A small-scale eddy triggered the filling of the underlying depression with up to 30 m of Holocene sediments (Hertweck, 1983; von Haugwitz et al., 1988). The history of anthropogenic pollution of the HMA has already been subject to several studies (e.g., Förstner and Reineck, 1974; Irion et al., 1987; Boxberg, 2017). Estimates of the temporal onset of man-made pollution in the Helgoland Mud Area vary from around 1770 CE (Förstner and Reineck, 1974) to post-war times (Irion et al., 1987). A more recent study postulates that the enrichment in heavy metals in the study area already started around 760 CE in the southeastern depocentre, but extended into the northwestern part only in 1850 CE (Boxberg, 2017). Generally, the ancient anthropogenic heavy metal release is mainly attributed to

mining activities, while increased levels from the mid-19th century are ascribed to the onset of industrialisation (Nriagu, 1996; Hebbeln et al., 2003). Besides heavy metal contamination, the area has also been impacted by increased riverine nitrate contributions since the late 19th century, resulting in increasing eutrophication of the German Bight (Serna et al., 2010).

5.3 Materials & Methods

Two gravity cores from the Helgoland mud area have been analysed (Table 5.1 and Figure 5.1). Gravity core (GC) GeoB 4801-1 was collected during expedition RV Meteor M40/0 in 1997 and sub-sampled at 2 cm intervals throughout the upper 44 cm of the core for chemical analysis of the foraminiferal tests of *Ammonia beccarii* and *Elphidium excavatum*. GC HE 215/4-2 was collected on expedition RV Heincke-215 in 2004 and sampled as 1 cm thick slices every 2 to 5 cm in the uppermost 23 cm of the core and every 10 cm below. These samples were used for foraminifera faunal analyses (including investigation of test deformations). The element composition of the bulk sediment has been determined by XRF scanner analysis. The age models of both cores are based on AMS ^{14}C and ^{210}Pb dating and have been published before (HE 215/4-2: Serna et al., 2010; GeoB 4801-1: Hebbeln et al., 2003). In addition, the age model for core GeoB 4801-1 has been further improved by linking the record to instrumental (Scheurle and Hebbeln, 2003) and historical (Scheurle et al., 2005) data.

Table 5.1 Meta-data of the two sediment cores used in this study.

Core no.	Latitude	Longitude	Water depth (m)	Core length (cm)
HE 215/4-2	54.072°N	8.074°E	23	486 cm
GeoB 4801-1	54.102°N	8.034°E	25	1141 cm

X-Ray fluorescence core scanner (energy-dispersive)

XRF Core Scanner data were collected on GC HE 215/4-2 every 1 cm down-core over a 1.2 cm^2 area with down-core slit size of 12 mm using generator settings of 10 (30) kV and 300 (700) mA current. The sampling time was 30 seconds directly at the split core surface of the archive half with XRF Core Scanner I (AVAATECH Model Nr.: 41240, Serial No. 005) at the Alfred-Wegener-Institut Helmholtz-Zentrum für Polar- und Meeresforschung, Bremerhaven. The split core surface was covered with a 4-micron thin SPEXCerti Prep Ultralene1 foil to avoid contamination of the XRF measurement unit and desiccation of the sediment. The reported data were acquired by a Silicon-PIN Amptek XR-100CR Detector with 139eV X-ray resolution (at 5.9keV, Fe), a MCA8000A multi-channel analyser and an Oxford Instruments 50W X-Ray tube with rhodium (Rh) target material. Raw data spectra were processed by the analysis of X-ray spectra by Iterative Least square software (WIN AXIL) package and interpreted for Pb and Zn. The net intensities for Pb and Zn in counts per second (cps) measured with the XRF Core Scanner were divided by the total cps from the run to normalise the data (i.e. for deviations resulting from varying water content, grain size variations and others).

ICP-MS

For Pb/Ca and Cd/Ca analyses, the foraminifera tests of *A. beccarii* and *E. excavatum* (about 30 tests per species and sample) were crushed and cleaned following the protocol described by Barker et al. (2003). The shells were dissolved in diluted nitric acid and the elemental concentrations were measured on a Thermo Finnigan Element 2 sector field ICPMS. The isotopes ^{111}Cd, ^{208}Pb, ^{27}Al, ^{43}Ca, ^{55}Mn, and ^{89}Y, have been used and Y served as internal standard, whereas Al and Mn were used to monitor contaminations from clay minerals and iron-manganese crusts. Al/Ca was usually below 0.2 mmol/mol, and samples with >0.5 mmol/mol were discarded. Mn/Ca was below 0.2 mmol/mol, with 2 exceptions, and no correlation of Pb/Ca and Cd/Ca with either Al/Ca or Mn/Ca was observed, suggesting that heavy metal values were not adversely affected by mineral coatings. The instrument calibration was based on four matrix-matched standard solutions as well as two blanks. Repetitive analyses of an in-house standard allowed the offline correction of the instrument drift and ensured consistency between measurements carried out on different days.

Average analytical precision (1 standard deviation based on 50 replicates per measurement of a standard solution) was 1.4E-05 % for Pb/Ca, 4.6E-06 % for Cd/Ca, 3.5E-03 % for Al/Ca and 2.8E-03 % for Mn/Ca. Because of a lack of material, no replicate samples were analysed.

Test deformation

Samples of GC HE 215/4-2 were freeze-dried, weighed and wet-sieved over 63 µm. Subsequently, the coarse residue was dry-sieved to obtain the > 125 µm fraction for foraminiferal assemblage analysis. On average, 300 specimens per sample were identified on the species level. *E. excavatum* and its variant forms were lumped together (Feyling-Hanssen, 1972). Test deformations exceeding the natural morphological variability were determined according to the morphological abnormality modes described by Alve (1991) and Geslin et al. (2000), following a conservative approach in order to avoid overestimation of deformation rates. The relative amount of test deformations are presented as abnormal test percentages with respect to the total amount of foraminifera per sample. For quantification of foraminiferal diversity, the Shannon – Wiener index H(S) was calculated according to Buzas and Gibson (1969).

5.4 Results and Discussion

In this section, the data are presents in a stratigraphic framework. All data versus core depth can be found in the supplementary material.

Core correlation

Independent stratigraphies for both gravity cores already exist (GeoB 4801-1: Scheurle et al., 2005; HE 215/4-2: Serna et al., 2010) and their accuracy is confirmed by the excellent correlation of normalised Zn and Pb intensities from XRF scanner data presented here (Figure 5.2). The simultaneous

increase of elevated levels of Zn and Pb in the younger sediments in these two cores but also in other cores from the HMA is used as an indicator of heavy metal pollution (see also Irion et al., 1987; Boxberg, 2017). The first increase in Zn occurs in both cores at around 1850 CE followed by a major increase at 1900 CE (Figure 5.2). Focusing on Pb in this study, core GeoB 4801-1 also recorded the first increase already around 1850 CE likewise followed by a more distinct increase around 1900 CE (Boxberg, 2017). In core HE 215/4-2 the onset of increased normalised Pb intensities at ~1850 CE is not so well expressed due to the high noise level in the data, but the distinct increase at around 1900 CE becomes obvious also in this core (Figure 5.2). The overall very good fit between both cores is supported by the $\delta^{15}N$ data (Serna et al., 2010). The values for both cores vary between 5.5 to 7‰ prior to 1880 CE, when eutrophication in the southeastern North Sea caused a sudden increase to values between 7 and 8 ‰ occurs (Serna et al., 2010; 2014). The very good correlation of the two sediment cores, best exemplified by the Zn data (Figure 5.2), justifies to directly compare the proportion of deformed tests and the benthic foraminiferal diversity obtained on core HE 215/4-2 with the Cd/Ca and Pb/Ca ratios in foraminiferal tests from core GeoB 4801-1.

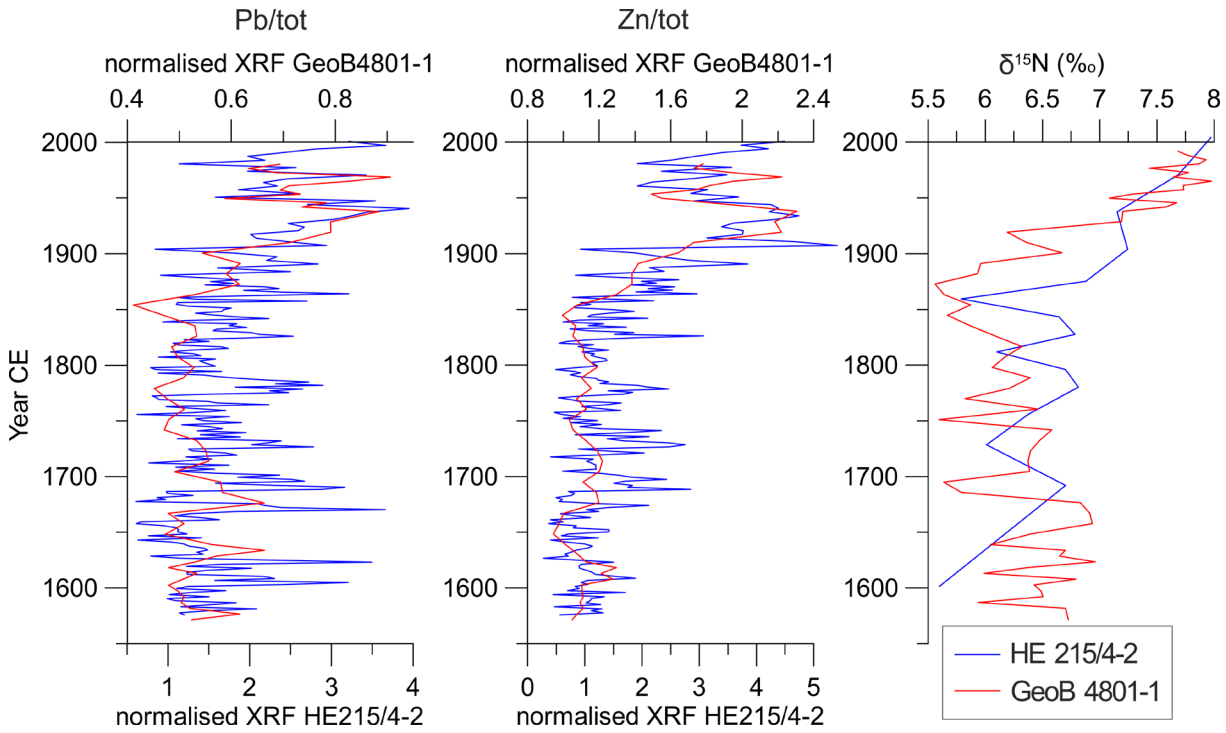

Figure 5.2 Correlation of the gravity cores HE 215/4-2 (blue line) and GeoB 4801-1 (red line) based on normalised XRF Scanner data of Pb (left) and Zn (middle) normalised intensities (HE 215/4-2: this study; GeoB 4801-1: Boxberg, 2017) and on $\delta^{15}N$ values (Serna et al., 2010, 2014) (right). The difference in normalised XRF Intensities for both cores is caused by the use of two different core scanners for data acquisition.

To what extent does the chemical signature of foraminiferal calcite reflect the chemistry of the bulk sediment?

Comparing the GeoB 4801-1 time-series record of calibrated Pb contents in bulk sediment (Boxberg, 2017) with the Pb/Ca values measured in the foraminiferal tests reveals a distinct series of events. The initial rise in bulk sediment Pb levels at ~1850 CE has no corresponding signal in the test chemistry

(Figure 5.3). Only in accordance with the second and major increase of Pb in the sediments, also Pb contents in the foraminiferal shells increased. However, a close examination shows slight temporal offsets. First, the XRF record reveals a marked increase of the Pb content in the bulk sediment around 1900 CE. This is followed by a sudden increase of the Pb/Ca ratios of *A. beccarii* from continuously low values of around 0.3 µmol/mol to rather high levels of ~1.0 µmol/mol at ~1920 CE. With another delay of ~20 years, the Pb/Ca ratios of *E. excavatum* rose from 0.2 to an average of 0.8 (and a maximum of 1.6) µmol/mol at ~1940 CE (Figure 5.3).

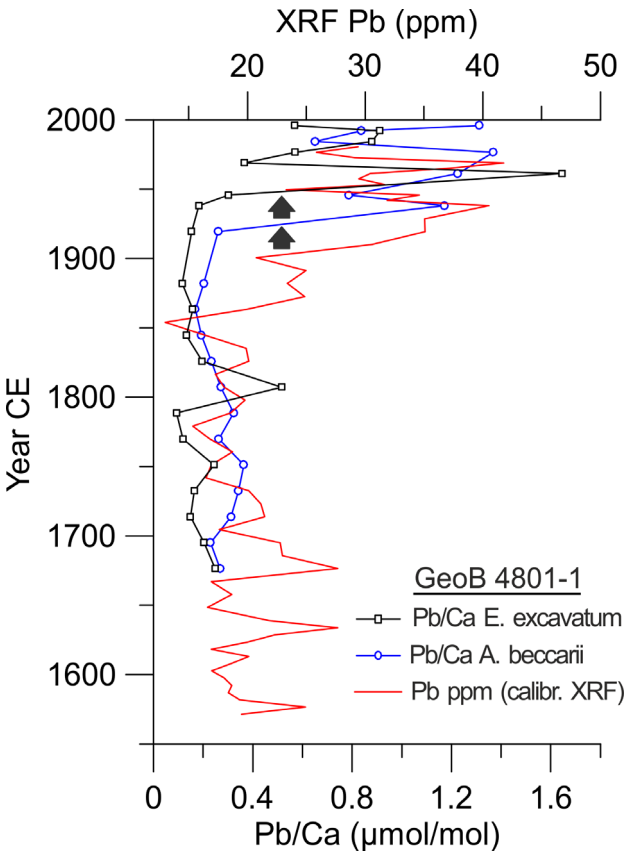

Figure 5.3 Temporal pattern of normalised bulk sediment Pb intensities based on the XRF Scanner data (red line; upper x-axis; Boxberg, 2017) and the Pb/Ca ratios (lower x-axis) in the tests of A. beccarii (blue line) and E. excavatum (grey line), all obtained in core GeoB 4801-1. The black arrows indicate the ~20 year-offsets between the individual parameters mentioned in the text.

The later onset of the relative increase of Pb in foraminiferal tests in comparison to the bulk sediment XRF data could be explained in several ways. A simple mechanistic explanation could be the effect of bioturbation, allowing for deeper penetration of the pollution signal in the clay and silt fraction (i.e., the dominant signal carrier in the bulk sediments) compared to the sand-sized and less dense foraminifera shells (Murray, 2006). Another explanation could be a delayed biologically controlled incorporation of heavy metals into the foraminiferal shells. De Nooijer et al. (2014) reviewed the processes of biomineralisation of foraminifera, referring to their ability to change the chemical composition of seawater in their cell and microenvironment for the test calcification. Such a biological control implies that foraminifera could also inhibit the incorporation of heavy metals into the calcite structure at least until the concentration is getting too high. The infaunal habitat of *A. beccarii* and *E. excavatum* (Moodley, 1990) could result in a seemingly earlier onset of the shell signal in comparison to the heavy metal signal in the ambient sediment. However, as the shell signal still occurs a few decades after the rise in heavy metals in the bulk sediments, the observed delay is assumed to be a true signal.

In a biochemical sense, the delay in Pb enrichment in the foraminifera versus the sediment potentially indicates species-specific biological defence mechanisms defining the tolerances to pollution. Such biological defence mechanisms have been described in several studies (Bresler and Yanko-Hombach, 2000; Le Cadre and Debenay, 2006; Frontalini et al., 2015, 2016, 2018). Investigating the cytological

response of *Ammonia parkinsoniana* to Pb pollution, Frontalini et al. (2015) found several cytological changes like the thickening of the inner organic lining and mitochondrial degeneration. The probably most remarkable observation was the increase of the number of lipid droplets and the fact that these were characterised by a more electron-dense core in comparison to the control group, which was interpreted as a detoxification mechanism. This means, that the lipid droplets could serve as storage for immobilising heavy metal cations (Frontalini et al., 2015, 2016), potentially prohibiting their incorporation into the calcite tests. Some authors concluded that such cytological changes also could cause deformed test (Yanko et al., 1998; Le Cadre and Debenay, 2006).

The temporal offset between rising Pb/Ca ratios in *A. beccarii* and *E. excavatum* might indicate more effective biological defence mechanisms of the latter species with slower incorporation of Pb into its calcite lattice. This agrees with observations showing a higher degree of tolerance to heavy metals for *E. excavatum* than for *A. beccarii* (Alve, 1995). However, potential differences in habitat depth of the two species (Moodley, 1990) could also be a possible explanation for the seemingly earlier onset of Pb incorporation in the tests of *A. beccarii*. Both possibilities also apply to the Cd/Ca ratios of *A. beccarii* and *E. excavatum*, which show the same temporal development (see below).

Taken together, we assume that the observed temporal offset in the Pb signals associated with the bulk sediment, *A. beccarii*, and *E. excavatum* rather reflects a biological response in the Pb incorporation process than a bioturbation effect. The lacking response in test chemistry to the first increase in sedimentary Pb contents around 1850 CE probably indicates that incorporation only reflects changing heavy metal availability after (species-) specific thresholds have been overcome. Nevertheless, the good agreement between bulk sediment and foraminiferal test Pb contents is a clear hint that foraminifera shells mirror changes in the bulk sediment chemistry very well, once such a threshold has been surpassed (Figure 5.3).

Are the chemistry of the bulk sediment and foraminiferal test deformation related?

In core HE 215/4-2 the occurrence of abnormal tests shows a slow but continuous increase from around 1650 CE until 1810 CE (average ~4%) over this time interval (Figure 5.4). Starting from ~1810 CE we observe an increasing variability on a higher average level of ~7% deformed tests. Finally, in the sediments younger than 1960 CE, a substantial increase in abnormal tests above the former range to values of up to 20% occurred.

The benthic foraminiferal fauna in this core is dominated by *Elphidium excavatum*, *Ammonia beccarii, Nonion depressulum, Haynesina germanica*, and *Elphidium magellanicum*, representing a characteristic fauna of the outermost Elbe estuary (Wang, 1983; Schönfeld et al., 2013). The most obvious change in the diversity record is a decrease in diversity during the first part of the 19th century (Figure 5.4) associated with the increasing dominance of *E. excavatum* (Rotstigen, 2009).

The initial increase in test deformation already began around 1650 CE, i.e. much earlier than the occurrence of elevated Pb levels in the bulk sediment and the incorporation of heavy metals into the calcitic foraminiferal shells. As in the post-1650 CE record the suggested 'natural background' of ~1% abnormal test (Yanko et al., 1999; Geslin et al., 2000) is already exceeded in, we postulate that the increasing proportions after 1650 CE (and possibly already before) are a reaction to increasing environmental stress. Whether this is caused by natural or anthropogenic environmental change is difficult to separate. Supporting arguments for man-made induced stress are an even earlier onset of anthropogenic heavy metal input to the southeastern Helgoland mud area, possibly as early as ~760 CE (Boxberg, 2017), and that reconstructed changes in salinity in the HMA (Scheurle et al., 2005) – as a possible natural driver – do not correlate with the test deformation record. However, the XRF Pb data in the cores HE-215/4-2 and GeoB 4801-1 from the northwestern HMA are elevated only from 1850 CE onward, excluding lead concentrations as the driver of the early rise in deformed tests.

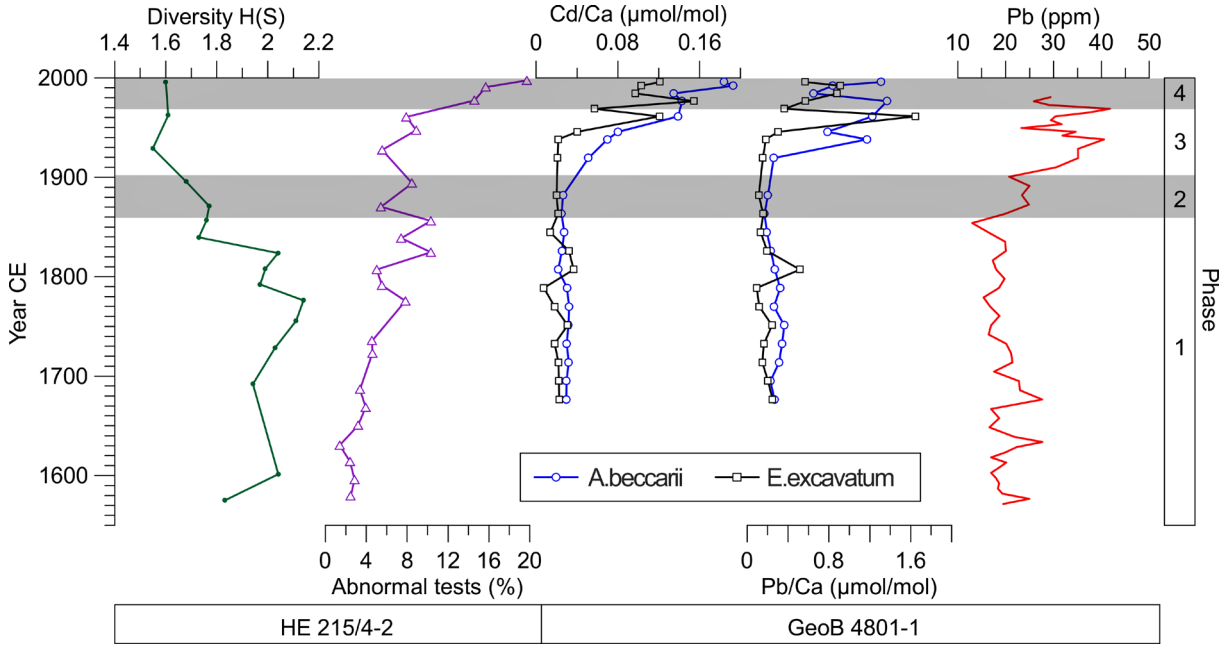

Figure 5.4 Comparison of the benthic foraminifera diversity (green line) and the proportion of abnormal benthic foraminiferal tests (purple line) in gravity core HE 215/4-2 with the Pb/Ca and Cd/Ca ratios in tests of A. beccarii (blue line) and E. excavatum (black line) and bulk sediment Pb contents (red line) (Boxberg, 2017) from gravity core GeoB 4801-1. Grey and white background shading marks the different temporal phases described in the text.

Low benthic foraminiferal diversity in the early 19th century (Figure 5.4), another indicator for environmental stress on the community (Frontalina and Coccioni, 2008) accompanies high average proportions of deformed tests. Yet, declining diversity also pre-dates the elevated levels in Pb accumulation in the sediments. Furthermore, the final increase in test deformation at ~1960 CE is not correlated with further increasing heavy metal content in the sediments, which showed the second major rise already at ~1900 CE.

These observations indicate that deformed benthic foraminiferal tests cannot be used as a first indicator for increasing Pb (and Zn) loads in the sediments of the HMA. There seems to be no general relation

between the proportion of deformed tests and bulk sediment Pb content as changes in either of the two parameters in the 20th century are not reflected in the other. This is in line with observations in Brazilian waters, where the abundance of deformed foraminiferal tests was lower in polluted areas than in unpolluted or hypersaline environments, questioning their applicability as heavy metal indicators (Geslin et al., 2002).

Is there a correlation between test deformation and test chemistry?

Similar to the Pb/Ca ratios presented above, the Cd/Ca ratios for *E. excavatum* and *A. beccarii* are constantly low (<0.04 µmol/mol) before 1900 CE (Figure 5.4), comparable to the minimum range of Cd incorporation in benthic foraminifera shells previously reported (Lea, 1999). After 1940 CE, Cd/Ca values for both species rose to >0.08 µmol/mol, corresponding to about half of the maximum of Cd/Ca ratios previously observed in benthic foraminifera (Lea, 1999). Thus, for both ratios used here to assess the chemical biomineralisation response of the benthic foraminifera to increased ambient heavy metal load, the prime signal over the past centuries was a 4- to 5-fold increase between ~1920 and ~1950 CE. However, this significant rise in heavy metals in the foraminiferal shells does not correlate with any major change in the proportions of deformed tests, which only show major increases in the first part of the 19th century and around 1960 CE (Figure 5.4). Thus, the benthic foraminifera do not seem to react with enhanced proportions of deformed test and enhanced integration of heavy metals into their shells at the same time, i.e. to the same kind/level of environmental stress, further supporting the conclusions made above, that test deformation is no indicator for heavy metal pollution.

The temporal sequence of foraminiferal responses to environmental stress

Based on the observations made in the HMA outlined above, we postulate the following sequence of causes and effects. In response to a not yet specified increasing environmental pressure prior to the first part of the 19th century, the benthic foraminifera community (i) produced higher proportions of deformed shells and (ii) decreased in diversity. This event cannot be linked to the temporal onset of elevated levels of the heavy metals Pb and Zn in the investigated cores (Boxberg, 2017; this study). A potential candidate is eutrophication caused by land use changes and increased riverine nutrient fluxes. However, for the HMA, sedimentary nitrogen isotope records revealing increasing eutrophication only since the second half of the 19th century (Serna et al., 2010). Furthermore, changes in salinity were reported to be able to cause test deformation (e.g., Alve, 1995). Yet, the temporal pattern of salinity changes in the German Bight (Scheurle et al., 2005) is asynchronous to the occurrence of test malformation. Therefore, the cause of this initial environmental stress remains unidentified.

The onset of elevated Pb contents is only evident from 1850 CE onwards. However, at this stage neither Pb nor Cd were incorporated in higher amounts into the shells of *E. excavatum* and *A. beccarii*. This is in line with observations of cytological changes in culturing studies under elevated metal concentrations interpreted as defence and neutralising mechanisms (e.g., Frontalini et al., 2015). Such cytological

changes might be sufficient to inhibit the incorporation of foreign cations during the calcification process until a specific threshold is reached.

This threshold obviously has been crossed in the early 20th century, when *E. excavatum* and *A. beccarii* responded to a further strong increase in environmental Pb levels, as recorded in the sediment, with the incorporation of Pb (and Cd) into their calcite shells. This delayed response to rising ambient Pb levels indicates that heavy metal incorporation into the foraminiferal shells is biologically controlled and only occurred after specific thresholds for Pb and Cd availability at the seafloor were overcome. Whether the ~20 years offset in Pb and Cd signal between both foraminifera species is caused by species-specific tolerances resulting in a delayed response by *E. excavatum* or by a slightly deeper habitat of *A. beccarii* (Moodley, 1990) cannot be solved based on the available data. This change in test chemistry in the early 20th century was not accompanied by an increase in test deformation. The sudden increase in sedimentary Pb at this time probably resulted in a fast crossing of the threshold, forcing the foraminifera to incorporate Pb and Cd into their shells.

The final rise in test deformation some decades later at ~1960 CE was once more neither related to higher bulk sediment Pb levels nor to changes in Pb and Cd incorporation into the shells of *E. excavatum* and *A. beccarii*. This points to another environmental stress factor to which the foraminifera responded with producing higher amounts of deformed tests. However, from the low diversity as well as elevated Pb/Ca and Cd/Ca ratios, it can be assumed that this additional stressor impacted an environment already under anthropogenic pressure. A potential candidate is the contamination with polycyclic aromatic hydrocarbons (PAHs), a constituent in crude oil and petroleum products (e.g., lubricant oil) (Nisbet and LaGoy, 1992). Offshore oil exploration in the North Sea started in the 1960s (Larminie, 1987). Studies indicate a strong influence of oil pollution on the proportion of abnormal foraminiferal tests (Ernst et al., 2006; Lei et al., 2015). Romano et al. (2008) found a strong correlation between the percentages of abnormal tests and PAH concentrations near a non-oil producing industrial site in Italy. Another possible stressor could be the contamination with radioactive material from nuclear testing fallout and/or the reprocessing of nuclear waste, for example in Sellafield (UK) and LaHague (France). Bogutskaya et al. (2011) reported a strong increase in skeletal malformation in fish due to radioactive contamination. However, to what extent the only slightly elevated levels of radioactive substances found in the sediments in the German Bight (BSH, 2016) can exert such stress is not clear. Also, leaching of increasingly used agrochemicals, such as pesticides and fertilisers since the mid-20th century (Carvalho, 2017) could be a potential cause. Finally, other heavy metals not considered in this study, such as e.g., mercury (Hylander and Melli, 2003), most likely affect foraminifera and potentially can result in test deformation.

5.5 Summary

Benthic foraminifera in the HMA seem to respond to environmental stress, in this case likely man-made, in a stepwise manner (Figure 5.4):

1. Phase: Increasing stress of unknown cause resulted in rising proportions of deformed foraminiferal tests as well as a decline in foraminiferal diversity.
2. Phase: Foraminifera compensated increasing pollution with Pb (and other heavy metals) using cytological changes as biological defence mechanisms, without any incorporation of Pb in the test calcite or increase in test deformities.
3. Phase: After exceeding a threshold upon which they could no longer neutralise or store heavy metal in their cells, they began to incorporate Pb (and Cd) into the test calcite – without any accompanying increase in test deformation.
4. Phase: Foraminifera reacted with forming more abnormal tests to additional environmental stress factors (e.g., radioactive or persistent organic pollutants) that obviously did not affect the incorporation of Pb and Cd into the test calcite.

Triggering the different steps may occur at slightly different times for individual species, as the respective thresholds can be species-specific depending on the tolerances to environmental stress. The close temporal links between pollution and foraminiferal response point to a significant role of human activities as the main driver for the above steps, although other factors might also have influenced the biomineralisation of the benthic foraminifera.

To understand the processes involved in the response of benthic foraminifera to environmental stress, future culturing studies should develop from only looking on a single response mechanism to considering a combination of test deformities, cytological changes and test chemistry. Only with such a comprehensive approach, the complex interplay between environmental stress factors and foraminiferal response mechanisms might be disentangled. In addition, test chemistry provides the potential to quantify historical levels of heavy metal pollution on the base of (to be) established species- and element-specific partition coefficients.

Acknowledgements

This project was funded by the Deutsche Forschungsgemeinschaft (DFG) through the International Research Training Group – ‘Integrated Coastal Zone and Shelf-Sea Research’ (GRK 1598 INTERCOAST). Sample material has been partially provided by the GeoB Core Repository at the MARUM – Center for Marine Environmental Sciences, University of Bremen, Germany. The data reported in this paper will be archived in Pangaea (www.pangaea.de).

Chapter 6 Manuscript 3

Evaluation of Zn Pollution in the Skagerrak applying the OSPAR Assessment Criteria

S. Boehnert[1] and D. Hebbeln[1]

[1] MARUM — Centre for Marine Environmental Sciences, University of Bremen, Leobener Straße 8, 28359 Bremen, Germany

Abstract

Heavy metals pose a potential threat to the environment and humans' health, because of their toxic and persistent character. In the North Sea, a marginal sea bordered by highly industrialised countries and with densely populated coasts, most studies on the history of pollution focused on near-shore areas like estuaries, fjords and harbours. In contrast, the most important sediment depocentre of the North Sea, the 700 m deep Skagerrak, has only experienced little attention with respect to the reconstruction of historical heavy metal contamination. In this study we analyse, if and to what extent human impact, exemplified by Zn contents, is recorded in the sediments of the central Skagerrak by applying X-ray fluorescence (XRF), grain size and CN elemental analysis to an SW-NE transect of three short sediment cores (~40 cm). The quantitative XRF data indicate an increase in Zn contents at c.1920 CE solely in the southwesternmost core. The other two cores show no increase but contain generally higher values, leading to the conclusion that pre-industrial background was not reached. To obtain better comparability, normalisation of the Zn contents to 5% Al was performed according to the OSPAR guidelines, revealing values between 54 and 95 ppm normalised Zn for bulk sediment. Higher Zn values correlate with greater contents of total organic carbon. Based on the comparison with previous studies we suggest that the potential source area of the contamination is rather of local than regional origin. According to the OSPAR background contents, the heavy metal enrichment in the Skagerrak takes place on a relatively low level. However, there are indications that these suggested background contents might overestimate the actual background levels by about 50%, meaning a potentially much higher degree of pollution than previously assumed. Therefore, this study adds an important piece to the puzzle for evaluating the environmental state of the whole North Sea, a fundamental base for ecological conservation and recovery, as well as fishery and mariculture.

6.1 Introduction

Humans changed the appearance of the landscape over the past millennia and had a big influence on the environment. One of the major impacts is the contamination with chemicals, posing a severe threat on ecosystems and human health. Especially in marine environments, such input of pollutants is not necessarily affecting only on a local scale, but can be spread to regional or even global scales. One of

the biggest concerns relates to the contamination with heavy metals, because of their toxicity, persistence and bioaccumulation in the food chain. The history of heavy metal release into the environment can be traced back up to ~4,500 yrs (e.g., Leblanc et al., 2000; Monna et al., 2000, Kienlin et al., 2006) deriving from smelting and mining activities, coal burning and later on industrialization (petrochemical industry, chemical industry, pulp and paper, automobile emission etc.).

These anthropogenic activities also threaten the North Sea, a marginal sea surrounded by highly industrialised countries (e.g., Emeis et al., 2015). Studies reconstructing historical heavy metal inputs focus mainly on near-shore areas, such as estuaries (Croudace and Cundy, 1995), intertidal flats (Berry and Plater, 1998; Spencer et al., 2003), fjords (Pederstad et al., 1993; Polovodova Asteman et al., 2015) and harbours (Lepland et al., 2010). Their close proximity to a point source of pollution or a mix of pollutants from a wider catchment area discharged by rivers into the sea often leads to relatively severe enrichment of heavy metals in the sediments. An overview of some studies in the North Sea is provided in Table 6.1 and Figure 6.1.

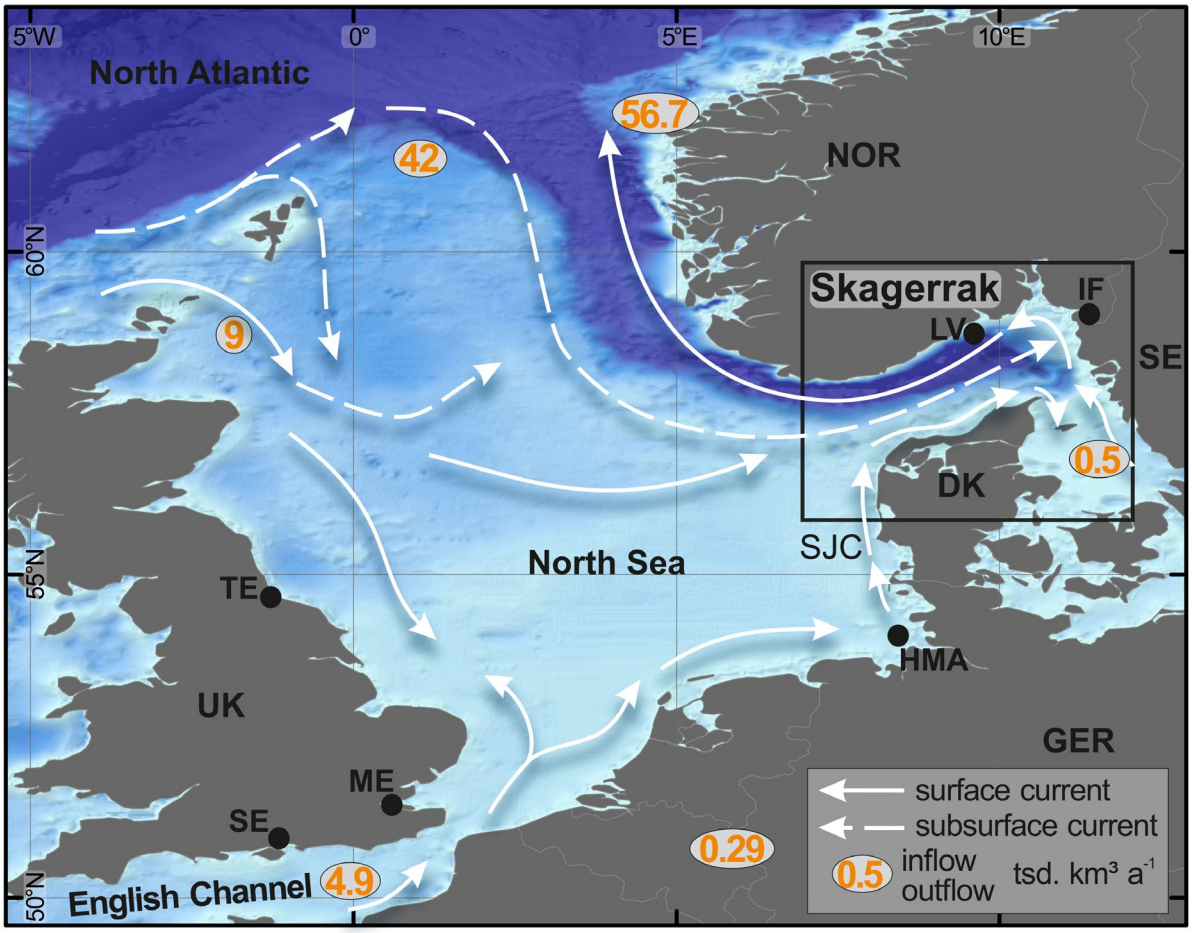

Figure 6.1 Bathymetric map of the North Sea with indicated counter-clockwise surface (solid arrows) and subsurface currents (dashed arrows), inflow and outflow volumes of water and locations of previous near-coastal studies (see also Table 6.1). Countries: DK – Denmark, GER – Germany, NOR – Norway, SE – Sweden, UK – United Kingdom; Study sites: HMA – Helgoland Mud Area (Boxberg, 2017), IF – Idefjord (Polovodova Asteman et al., 2015), LV – Larvik (Pederstad et al., 1993), ME – Medway Estuary (Spencer et al., 2003), SE – Southampton Estuary (Croudace and Cundy, 1995), TE – Tees Estuary (Berry and Plater, 1998). Modified from Eisma and Kalf (1987) and Nordberg (1991).

For example, Berry and Plater (1998) found an increase in heavy metals (up to 600 ppm Zn) in the Tees estuary (UK) related to mining operations (1880 CE) or the industrial development (1970 CE). In the Southampton Estuary (UK) the onset of increased pollution by Pb, Zn and Cu occurred 1950-1960 CE. The very high enrichment in Cu (maximum content of 1022 ppm) resulted from a nearby oil refinery, whereas Pb contamination was related to a mix of coal burning, automobile emission and other industrial uses (Croudace and Cundy, 1995). Very high Zn contamination (maximum of 935 ppm) caused by the pulp and paper industry was found in the Idefjord, setting on in ~ 1940 CE and peaking in ~ 1975 CE (Polovodova Asteman et al., 2015). All studies are based on short cores, covering only the past few centuries.

The concentration of the studies in the near-shore region is due to the fact that the open North Sea does not provide many natural sediment traps where continuous sedimentation allows the reconstruction of historical developments. Besides the Skagerrak, the only other main depocentre off the coast is the Helgoland mud area (HMA) in the German Bight (Eisma and Kalf, 1987). For this region, Förstner and Reinick (1974) reported an anthropogenically caused enrichment in Pb, Zn, Hg and Cd. A more recent study proposes an onset of increased Zn accumulation in the Helgoland mud area as early as ~750 CE in the southeast, whereas in the northwestern part anthropogenic heavy metal inputs can only be recorded around ~1850 CE (Boxberg, 2017). In comparison to the previously mentioned studies focusing on near coastal sites, the polluted sediment in the HMA has relatively low Zn contents (see Table 6.1).

*Table 6.1 Overview of some other studies on pollution history with heavy metals in the North Sea. *- marks studies with extractable heavy metal contents, () indicate maximum Zn contents recorded*

Site	Average elevated Zn (ppm)	Average background Zn (ppm)	Peak onset (yrs CE)	Authors
Tees Estuary*	~250 (600)	/	1880 or 1970	Berry and Plater, 1998
Medway Estuary	202	61-92	~1870	Spencer et al., 2003
Southampton	146 (169)	75	~1950	Croudace and Cundy, 1995
Helgoland	79-132 (200)	41-46	~750 to ~1850	Boxberg, 2017
Skagerrak	75-109 (126)	66	~1920	This study
Larvik*	50-100 (160)	20	~1860	Pederstad et al., 1993
Idefjord*	350 (935)	121	~1940	Polovodova Asteman et al., 2015

The Skagerrak, being the main sediment depocentre of the North Sea, receives suspended matter input from entire northwest Europe through the river drainage system (van Weering et al., 1993). Because of high sedimentation rates, it provides high-resolution sedimentary records (Hebbeln et al., 2006). This led to various studies concerning suspended matter (Eisma, 1981, Eisma and Kalf, 1987), sedimentation processes (van Weering et al., 1987; Hass, 1993), climate forcing and reconstruction (Hass, 1996; Brückner and Mackensen, 2006), as well as organic carbon accumulation (Anton et al., 1993, de Haas and van Weering, 1997).

To our knowledge, only two studies dealt with heavy metal distribution in the Skagerrak. Kuijpers et al. (1993) analysed sediment surface samples all over the Skagerrak and Kattegat for their content of Hg, Pb, Zn, Cu and organic carbon. Based on these data, they postulated that Zn contents derive mainly from three sources, namely the Varberg and Uddevalla area (both in Sweden), as well as the southern North Sea. Pederstad et al. (1993) also investigated the distribution of Zn and Cu in surface sediment samples spread over the Skagerrak area as well as the Zn content in two near-shore sediment cores. The authors concluded that, besides some near coastal zones (Oslo harbour ~100 ppm Zn), the pollution in the Skagerrak is with maximum 50 ppm extractable Zn rather low.

However, these two studies are not comparable to one another because of different methodologies. Besides, heavy metal contents are dependent on sediment properties, such as grain size, mineralogy and total organic carbon (TOC), making a North Sea wide assessment rather complex. In order to evaluate the current ecological status of the entire North Sea, a coherent approach for the determination of historical pollution degrees is needed.

A criterion for the assessment of heavy metals in the sediment is the background content (BC) of a specific element established for the OSPAR Coordinated Environmental Monitoring Programme. BCs were determined by down-core metal contents from or prior to 1850 CE and normalised to 5% Al for comparability between different sediments in different regions (OSPAR, 2008). Adding more pre-industrial background content data of heavy metals from various marine settings is important for the verification of these guideline classifications.

In order to assess the status of the anthropogenic impact on the deeper Skagerrak exemplified by Zn contents, we are using quantitative X-ray fluorescence (XRF) and grain size analysis as well as total-carbon and total-nitrogen data on a transect of three multicores (MUCs). Our scientific objectives are to answer if: (i) the Skagerrak is affected by anthropogenic pollution, (ii) a regional trend along the transect can be detected, and (iii) the signal derives from a local or regional source. Furthermore, the anthropogenic impact will be evaluated based on the OPSAR BC. Zn contents normalised to 5% Al will be marked as Zn* throughout this article for easier differentiation from Zn contents without this normalisation.

6.2 Regional Setting

The North Sea is characterised by a counter-clockwise circulation pattern, primarily driven by North Atlantic waters entering between Scotland and Norway (Figure 6.1). While the largest portion of the Atlantic water masses flows directly into the Skagerrak, about 20 per cent follow the coastline around the entire North Sea (Eisma and Kalf, 1987). Trough mixing with waters passing into the North Sea through the English Channel and freshwater discharged by rivers (e.g., Thames, Rhine, Weser, Elbe), the water masses are modified, for example with regards to the suspended matter and pollutant loads. The altered North Sea water continues along the Danish Coast as South Jutland Current (SJC) and North

Jutland Current (NJC) and eventually reaches the Skagerrak (Figure 6.1, Figure 6.2). Further water mass modifications occur through mixing with the less saline Baltic Current (BC) in the eastern Skagerrak. The resulting water deviates counter-clockwise towards northwest and west, following the Norwegian coast as Norwegian Coastal Current (NCC) (Svansson, 1975; Rodhe, 1987; Longva and Thorsnes, 1997; Rodhe, 1998) (Figure 6.1, Figure 6.2).

The Skagerrak is the deepest area of the North Sea (maximum water depth 700 m) and part of the Norwegian Trench, serving as a natural sediment trap. It is asymmetrically shaped, with a relatively gentle southern and a steep northern slope, indicating that the main sediment supply is deriving from the south (e.g., Svansson, 1975; van Weering, 1981, Kuijpers et al., 1993). Resulting from the net-sedimentation and the counter-clockwise circulation pattern, the Skagerrak has the potential to record the history of pollution of the North Sea on a regional scale.

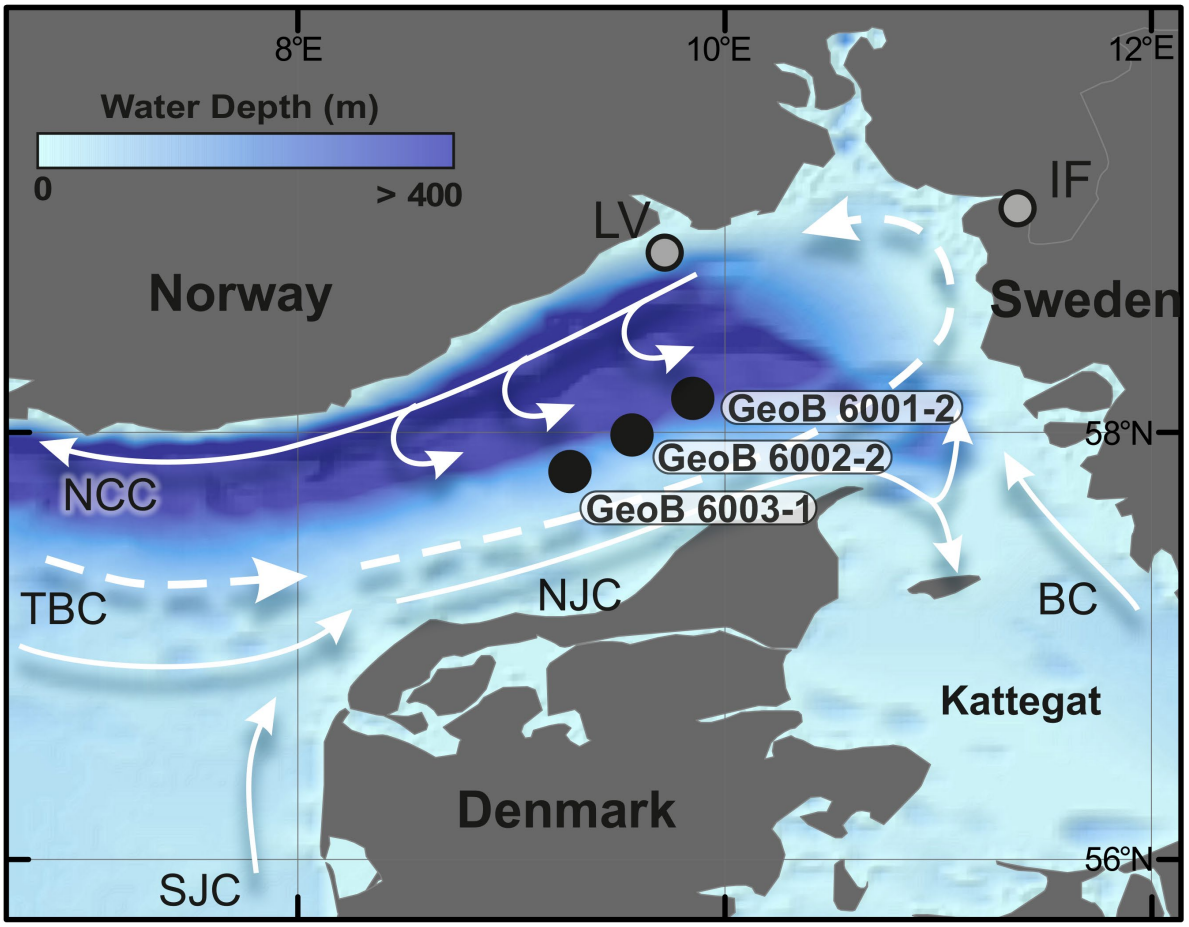

Figure 6.2 Bathymetric map of the Skagerrak with arrows indicating circulation pattern (Nordberg, 1991) and core locations (black dots) as well as previous studies (grey dots). BC – Baltic Current, NCC – Norwegian Continental Current, NJC – North Jutland Current, SJC – South Jutland Current, TBC – Tampen Bank Current; IF – Idefjord (Polovodova Asteman et al., 2015), LV – Larvik (Pederstad et al., 1993) (see also Table 6.1).

6.3 Material & Methods

During research cruise RV Meteor M45-5 in 1999 three multicores (MUCs) were obtained from water depths of 308 m to 460 m in the central Skagerrak (Table 6.2). The age-depth relationship for

GeoB 6003-1 is based on a sedimentation rate of 1.8 mm/yr obtained by ^{210}Pb dating on the corresponding gravity core GeoB 6003-2 (Hebbeln et al., 2006).

Table 6.2 Sampling stations of multicores (MUCs) used in this study specifying water depth and core length.

Core no.	Latitude [N]	Longitude [E]	Water depth [m]	MUC length [cm]
GeoB 6001-2	58° 09.4`	09° 48.3`	460	42
GeoB 6002-2	58° 04.8`	09° 37.2`	428	43
GeoB 6003-1	57° 58.3`	09° 23.2`	308	36

Grain size analysis

Grain-size measurements on 115 samples taken from the three MUCs were performed in the Particle-Size Laboratory at MARUM, University of Bremen, with a Beckman Coulter Laser Diffraction Particle Size Analyzer LS 13320. Prior to the measurements, the terrigenous sediment fractions were isolated by removing organic carbon, calcium carbonate, and biogenic opal by boiling the samples (in about 200 ml water) with 10 ml of H_2O_2 (35%; until the reaction stopped), 10 ml of HCl (10%; 1 min) and 6 g NaOH pellets (10 min), respectively. After every preparation step the samples were diluted (dilution factor: >25). Finally, remaining aggregates were disaggregated prior to the measurements by boiling the samples with ~0.3 g tetra-sodium diphosphate decahydrate ($Na_4P_2O_7$ * $10H_2O$, 3 min) (see McGregor et al., 2009). Sample preparation and measurements were carried out with deionized, degassed and filtered water (filter mesh size: 0.2 µm) to reduce the potential influence of gas bubbles or particles within the water. The obtained results provide the particle-size distribution of a sample from 0.04 to 2000 µm divided into 116 size classes. The calculation of the particle sizes relies on the Fraunhofer diffraction theory and the Polarization Intensity Differential Scattering (PIDS) for particles from 0.4 to 2000 µm and from 0.04 to 0.4 µm, respectively. The reproducibility was checked regularly by replicate analyses of three internal glass-bead standards and is found to be better than ± 0.7 µm for the mean and ± 0.6 µm for the median particle size (1σ). The average standard deviation integrated overall size classes is better than ± 4 Vol-% (note that the standard deviation of the individual size classes is not distributed uniformly). All provided statistic values are based on a geometric statistic.

Energy-dispersive X-ray fluorescence

After grain size analysis, the remains of the MUC samples were dried in a drying cabinet at 40°C for 48 hours and ground to a homogeneous fine powder with an agate mortar and pestle. Then approximately 4 g of the sample were filled in a sampling cuvette with a prolene thin-film base and compressed with a stamp to obtain a smooth surface for measuring with an EPSILON 3 from PANalytical. The following major and trace elements were detected: Al, Br, Ca, Cl, Fe, K, Mg, Mn, Si, Sr, Ti, Zr, Rb, Zn, however, only Zn and Al contents are discussed in this study. Instrumental set-up for Zn detection (50kV, 200µA, silver filter, in air) differs from the settings for the lighter element Al (5kV, 1004µA, no filter, in He atmosphere). Calibration was performed with the certified marine sediment standard MAG-1. The precision of Al is 0.19% and 0.94% for Zn.

CN analysis

For organic carbon analysis, 35 mg dried and homogenised sample material was weighed into silver cups, acidified with 10% HCl to remove carbonate, dried at 50-60°C and pressed into pellets. For total nitrogen analysis, the same procedure was applied using tin cups and no acidification was necessary. The measurement was performed using the *Vario EL III Element Analyzer* by *elementar*, operated in CN mode and a combustion temperature of 950°C. The instrument is equipped with an autosampler and a thermal conductivity detector. Measuring duration for one sample was between 6 to 12 minutes (self-optimising). As calibration check the two standards wst4 (internal standard) and acetanilide (NIST141D) as well as empty cups (tin and silver respectively) as blanks were analysed every morning and after a batch of samples in the evening. Further calibration checks were conducted after every 10 samples, using the wst4 and empty cup only. The precision of the analysis is < 0.1% absolute.

6.4 Results

XRF Analysis

For GeoB 6003-1 Zn contents of the bulk sediment show relatively stable values around 66 ppm in the deeper sediment (15 – 36 cm), while for the topmost 15 cm an average level of 74 ppm Zn was measured (Figure 6.3, Table 6.3). In contrast, GeoB 6002-2 and GeoB 6001-2 display no sudden increase with average overall values of 106 and 109 ppm, respectively. The observed pattern consists of a slight continuous increase in the lower section towards a maximum (GeoB 6002-2: 121 ppm at 31 cm depth, GeoB 6001-2: 126 ppm at 17 cm depth), followed by a decreasing trend towards the sediment surface.

Table 6.3 Averaged peak and background contents as well as maximum Zn contents and the according Zn (normalised to 5% Al) values. Standard deviations of the Zn and Zn* distribution are reported in parentheses.*

		GeoB 6003-1	GeoB 6002-2	GeoB 6001-2
Zn bulk (ppm)	Ø peak	74 (± 3)	106 (± 9)	109 (± 8)
	Ø background	66 (± 2)	/	/
	max peak	80	121	126
Zn* (ppm)	Ø peak	68 (± 2)	86 (± 4)	86 (± 5)
	Ø background	57 (± 2)	/	/
	max peak	72	93	96

In order to ensure comparability within the cores as well as between the cores despite differences in clay contents, a normalisation to 5% Al was conducted (OSPAR, 2008). The resulting data (Zn*) still show the same pattern within each core, but on a generally lower level (Figure 6.3, Table 6.3). For the cores GeoB 6001-2 and GeoB 6002-2 the Zn* values have an average of 86 ppm both, while GeoB 6003-1 displays Zn* contents around 68 ppm in the upper section and 57 ppm in the section below 15 cm depth.

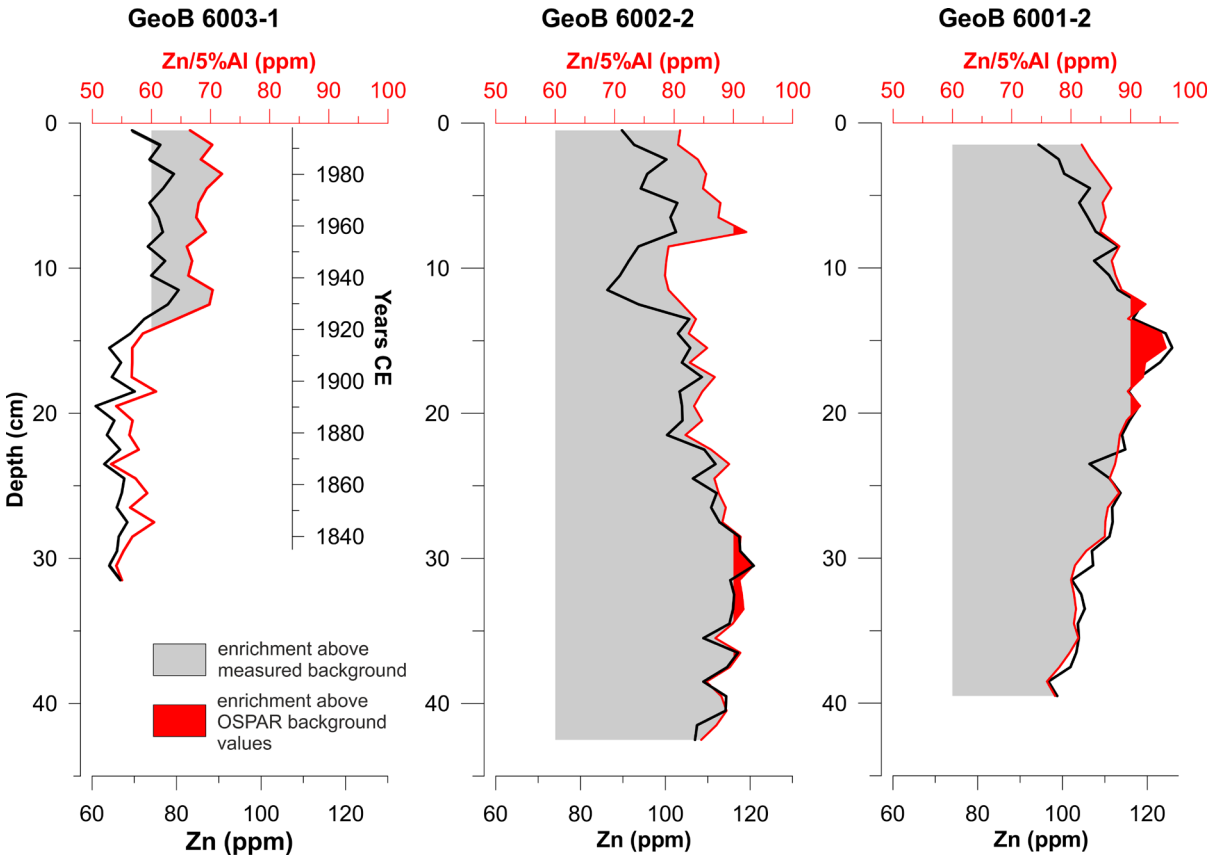

Figure 6.3 Zn contents (black line) and Zn (normalised to 5% Al) contents (red line) of the sediment cores from the Skagerrak, displayed on the two accordingly coloured axes. Gray shading marks Zn* values above 60 ppm; Red shading marks Zn* values above 90 ppm, both apply to the red Zn* plot only.*

Grain Size Analysis

All three MUCs consist of fine sediments without major changes in grain size distribution throughout the core (Figure 6.4). The sediment of cores GeoB 6002-2 and 6001-1 consist dominantly of clay and silt. In comparison, MUC GeoB 6001-2 (mean ~5 µm, mode ~7 µm) is insignificantly finer than MUC GeoB 6002-2 (mean ~6 µm, mode ~10 µm). Both cores show a remarkably consistent particle size distribution with depth.

GeoB 6003-1 is considerably coarser and the only core containing a sandy component. In addition, it is the only core displaying a minor shift in grain size. In the deeper section, from 32 to 14 cm the sediment is in the silt range (mean ~10 µm, mode ~54 µm), whereas from 14 cm to the core top the proportion of fine sand increases (mean ~12 µm, mode ~71 µm). Nonetheless, all analysed sediment samples contain a considerable amount of clay (and fine silt), evident from the low mean grain sizes in the three cores.

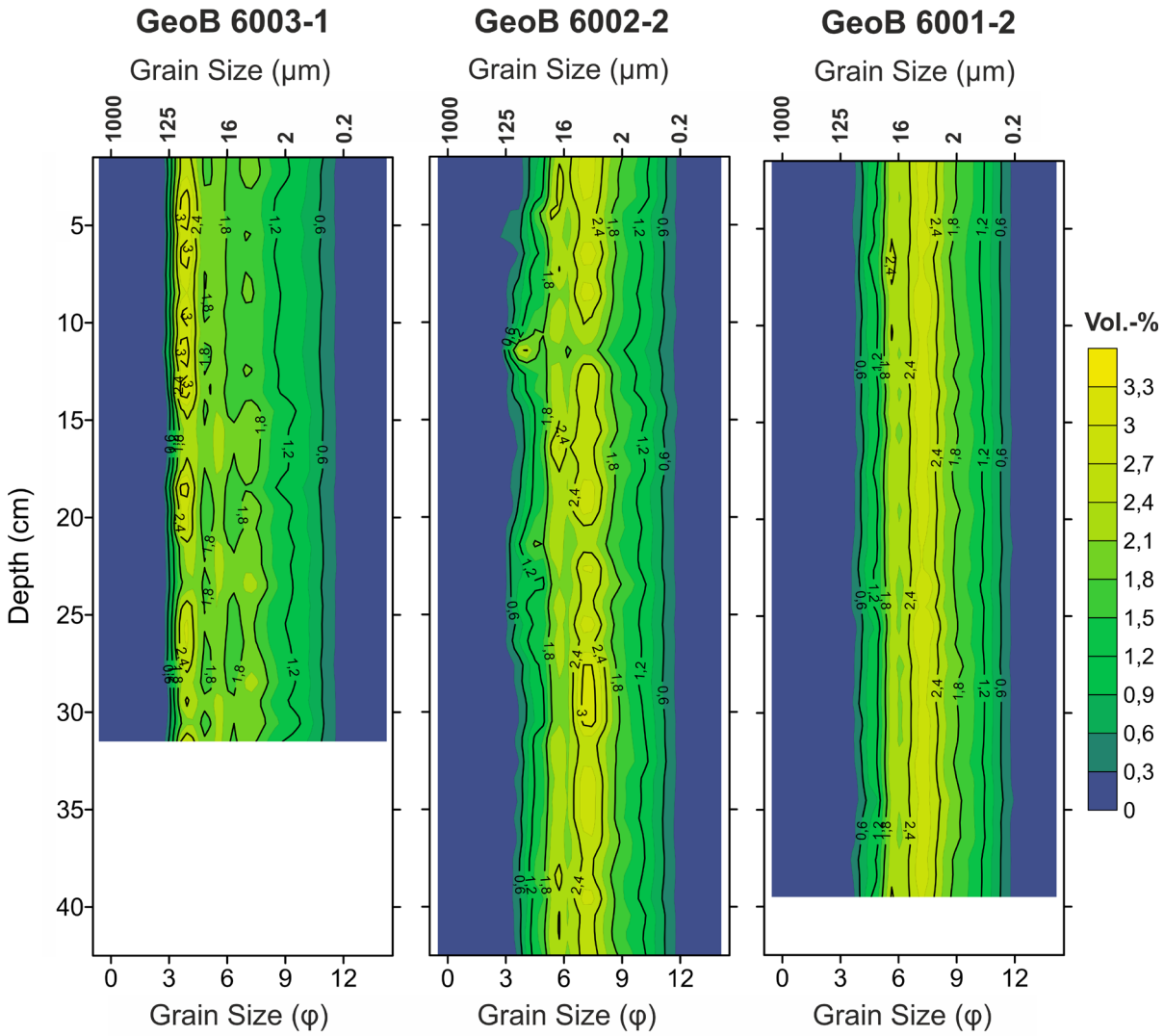

Figure 6.4 Grain size distribution of the 3 cores GeoB 6003-1 (farthest southwest), GeoB 6002-2 and GeoB 6001-2 (farthest northeast), colour coding gives a percentage of each grain size class, varying from 0 vol.-% (blue) to 3.3 vol.-% (yellow).

CN Analysis

Average total organic carbon (TOC) values for GeoB 6001-2 and GeoB 6002-2 are very similar with 25.8 mg/g and 25.3 mg/g respectively (Figure 6.5). However, both cores show a relatively wide range of values, fluctuating between 21.9 and 30.6 in GeoB 6001-2, while GeoB 6002-2 alternate between 15.6 and 36.3 mg/g TOC. In contrast, GeoB 6003-1 contains comparably little TOC on average (16.5 mg/g), with minimum contents of 13.3 mg/g and maximum values of 19.0 mg/g.

The similarity of GeoB 6001-2 and GeoB 6002-2 is also reflected in carbon-to-nitrogen (C/N) ratios, showing with average ratios of 7.4 and 7.3 almost identical values. The principal pattern follows that of the TOC data. The minimum and maximum ratio for GeoB 6001-2 are 6.2 and 8.1, whereas GeoB 6002-2 varies between 5.0 and 9.0. For GeoB 6003-1 a slightly lower average C/N ratio of 6.7 was obtained, with the lowest value throughout the core being 5.4 and the highest 7.7. None of the cores shows a marked internal trend concerning TOC contents nor C/N ratios (Figure 6.5).

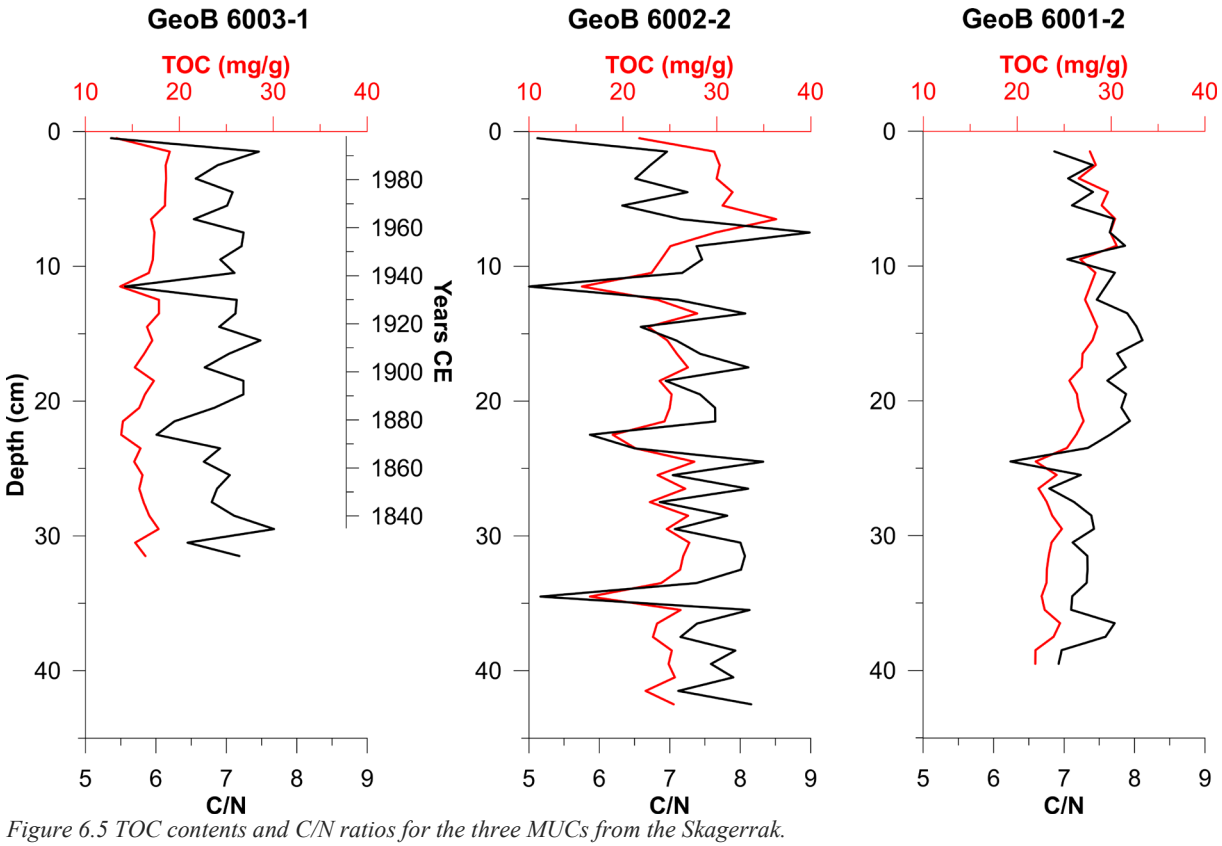

Figure 6.5 TOC contents and C/N ratios for the three MUCs from the Skagerrak.

6.5 Discussion

Is there an indication of anthropogenic pollution in the Skagerrak?

The quantitative XRF data show a sudden increase in Zn* contents (* - normalised to 5% Al) by 19% from 57 to 68 ppm in the southwesternmost MUC (GeoB 6003-1). This is the only core with stratigraphic information and therefore the onset of this increase can be determined to ~1920 CE (Figure 6.3), which is in good agreement with reported onsets in most other studies (Table 6.1). Further support for the temporal onset of heavy metal enrichment in the study area is given by core 'Station 53' (near the location of GeoB 6002-2), where Zn started to clearly increase c.1900 CE (Longva and Thorsnes, 1997). Simultaneously with the increase in Zn in core GeoB 6003-1, the grain size shifts towards a slightly coarser fraction in this core (Figure 6.4). Because of the generally accepted inverse correlation of grain size and heavy metal content (e.g., Horowitz, 1991), this coarsening potentially masks in parts the degree of the rising content (without normalisation only +15% Zn), verifying the usefulness of the normalisation to 5% Al.

The two other cores (GeoB 6001-2 and GeoB 6002-2) are very similar to one another and both display overall Zn* values of 86 ppm (± 5 ppm) that are about 40% higher in comparison to the average 62 ppm Zn* of GeoB 6003-1. Additionally, both cores show a different temporal Zn* distribution pattern, with the highest Zn* contents further downcore (GeoB 6002-2: >90 ppm in ~31 cm; GeoB 6001-2: >90 ppm in ~17 cm) and therefore reveal rather a decreasing than increasing tendency in the younger sediments.

We have to acknowledge a minor peak at 7 cm depth for GeoB 6002-2. However, we argue that this is not recording the onset of anthropogenic Zn* enrichment, as the values are barely exceeding the overall measured contents throughout the core.

As no independent age model is available for the two MUCs GeoB 6001-2 and GeoB 6002-2, an estimation of sedimentation rates has been derived from the two nearby cores 15535-1 (Hass, 1993) and GC 225510 (Dähnke et al., 2008). For 15535-1, located only 0.5 km northwest of GeoB 6002-2, the age-depth correlation was determined by ^{210}Pb and ^{226}Ra dating, resulting in a sedimentation rate of 7 mm/yr (Hass, 1993). The gravity core 225510, approximately 5 km south of GeoB 6002-2, confirms the high sedimentation rate, indicating sedimentation of 8 mm per year (Dähnke et al., 2008). Extrapolating this relatively high sedimentation rate to the nearby 42 cm long MUC GeoB 6002-2, the sediment record would cover only 50 to 60 years, reaching back until ~1940 CE. Consequently, the onset of pollution in c.1920 CE and pre-industrial background values would not be covered.

For core GeoB 6001-2 (furthest northeast) no nearby dated core could be found. However, the depositional environment at this core location was most likely very similar to MUC GeoB 6002-2, concerning water depth (and therefore current speeds), grain size, Zn* contents, TOC values and C/N ratios, suggesting that this location experienced probably similar sedimentation rates. Assuming similar sedimentation rates for both MUCs results in maximum Zn* contents in c.1960 CE for GeoB 6002-2, while maximum values in GeoB 6001-2 would date back to c.1980 CE. Yet, it has to be noted, that the maximum values barely exceed the overall range of Zn* contents measured. Therefore, it is reasonable to assume that these two MUCs do not reach pre-industrial background at all and represent only the Zn* enriched topmost sediments. In summary, there are good arguments that the top decimetres of the sediments in the Skagerrak are enriched with anthropogenic Zn* while only one core (GeoB 6003-1) captured as well the pre-industrial background (prior ~1920 CE).

Can we see a regional trend between the cores?

The three MUCs seem to represent two slightly different depositional settings. While GeoB 6003-1 contains the coarsest observed sediments and lower TOC contents as well as C/N ratios, the cores further to the northeast show very similar results amongst each other. By normalising the Zn contents to 5% Al, the cores can be compared despite the differences in grain size. This way, it becomes obvious that the average Zn* contents of GeoB 6003-1 once more differ from the two MUCs GeoB 6002-2 and GeoB 6001-2. As potential grain size effects are minimised by the normalisation, a reason for the higher Zn* contents in the two MUCs from a greater water depth could be attributed to the higher TOC contents. It is well known that heavy metals contents correlate with the TOC content of the sediments, but also that higher TOC contents are commonly attributed to finer grain sizes (Horowitz, 1991; and references therein). However, while van Weering (1981) demonstrated the association of TOC with the clay fraction, Anton et al. (1993) state an inverse correlation between grain size and TOC for the southern

slope of the Skagerrak. Previously reported TOC and Zn data of surface sediment samples from the Skagerrak and Kattegat confirm that these values correlate very well with one another (R^2 = 0.83) (Kuijpers et al., 1993). Comparing the data obtained for this study with these previous results from the wider study area reveals a very good agreement for non-normalised Zn values, while the normalisation to 5% Al results in a similar trend but with generally lower Zn*/TOC ratios (Figure 6.6).

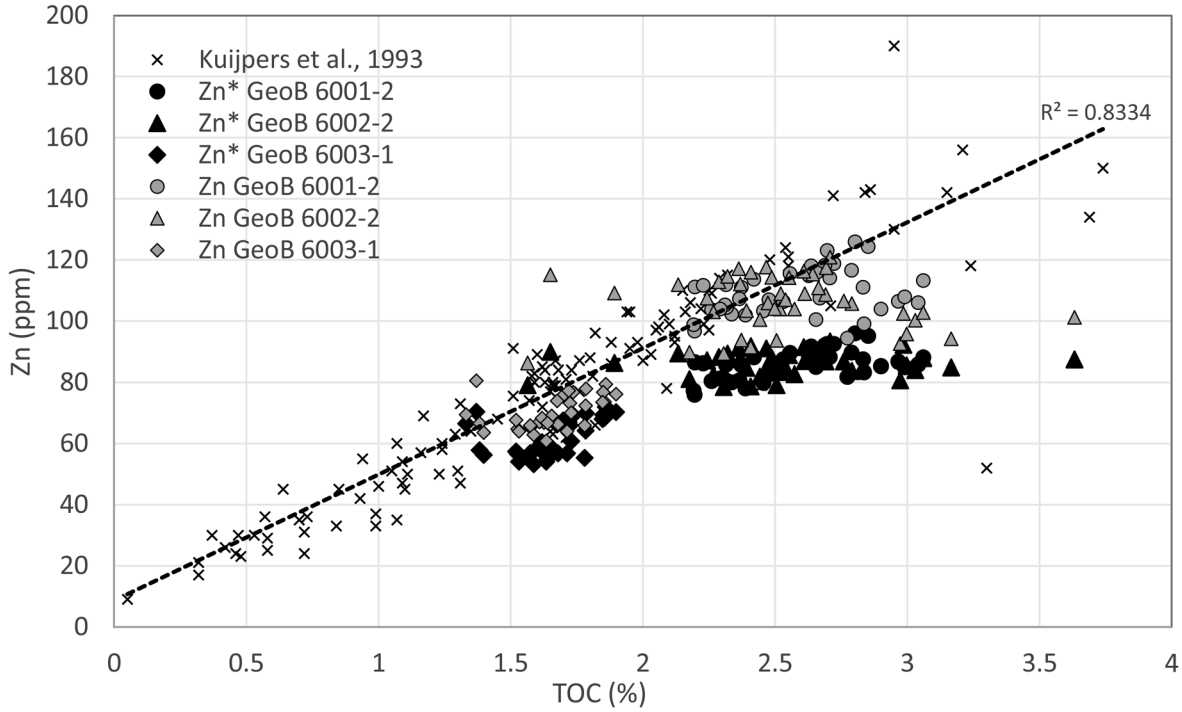

Figure 6.6 Published Zn and TOC data in surface sediments from Kuijpers et al. (1993) for the Skagerrak-Kattegat area, on which the linear regression line is based. Zn/TOC (grey symbols) and Zn/TOC (black symbols) of the three investigated Skagerrak MUCs in this study are added to the correlation plot.*

However, once more the difference between GeoB 6003-1 on the one hand, and GeoB 6001-2 and GeoB 6002-2 on the other hand, becomes visible. While the farther southwest located core (GeoB 6003-1) plots in the lower section of the linear regression, the two other cores display higher TOC and Zn* contents. This indicates that TOC indeed has a considerable effect on Zn load, despite the potential grain size dependence. In surface sediments in the Skagerrak, the organic carbon contents increase with water depth (van Weering, 1981). Therefore, the differences in the depositional settings (i.e. water depth) provide a possible explanation for the observed regional trend. An alternative reason could be that for the different core locations Zn derives from a different source area.

Can we tell whether the signal is local or regional?

Possible sources for heavy metal input into the North Sea are located more or less along its entire coast. The counter-clockwise circulation pattern has the potential to collect the different inputs from the UK and the Netherlands towards the German Bight following the Danish coast and ending up as a mixed regional signal in the Skagerrak.

It is estimated that 40 million tons (dry weight) of suspended matter is transported through the North Sea annually, half of it sourced from the southern North Sea (English Channel 10 Mio. tons, seafloor erosion 6-7.5 Mio. tons, rivers 4.8 Mio. tons) (Eisma and Kalf, 1987). These authors estimate that 50-70% of the suspended matter is deposited in the Kattegat-Skagerrak-Norwegian Channel. When comparing the averaged absolute Zn contents of the polluted sediments along the coast of the North Sea (Table 6.1), we can see, that the values become less pronounced along the path, seemingly indicating continuous dilution of the signal. However, this comparison is not justified, because almost all of these studies were conducted in very coastal settings and are no analogy to the deep marine Skagerrak. Additionally, a comparison would only be valid, if no other sources supply additional heavy metals into the mix. It is a fair assumption that the differences in heavy metal contents are rather correlated with the distance to the shoreline (and therefore source) than with the distance the signal was carried with the regional circulation. The studies published from the coasts of the UK were all conducted in very shallow estuaries (Spencer et al., 2003) or intertidal flats (Berry and Plater, 1998; Ridgway and Shimmield, 2002). For the Helgoland mud area (HMA) in the German Bight, a time-transgressive onset of heavy metal pollution is postulated, starting ~1250 CE in the SE, while the NW of the HMA was only impacted in ~1850 CE (Boxberg, 2017). This very early onset is certainly not captured in the Skagerrak MUCs analysed here nor does it explain the observed enrichment since c.1920 CE, as radionuclides indicate that the North Sea wide water transport time is only a few years (Kautsky, 1985).

The annual turnover of 40 million tons suspended matter in the North Sea is largely sourced by the English Channel and the North Atlantic with 30% contribution each. Rivers account for only ~15%, with the remaining suspended matter deriving from the Baltic, seafloor and coastal erosion, the atmosphere and primary production (Eisma and Kalf, 1987). Even though the waters from the southern North Sea display the highest suspended matter concentration (i.e. from rivers), the major proportion in the Skagerrak derives from the large volume of low concentrated Atlantic inflow (Eisma and Kalf, 1987, Gyllencreutz et al., 2006). This means that river derived anthropogenic Zn contents from the southern North Sea are most likely diluted by mixing with suspended matter form North Atlantic water masses. Therefore, local sources on the shores of the Skagerrak would potentially contribute more to the heavy metal increase than a mixed regional signal. A direct comparison with previous studies is of little use because of different analytical methods applied (extractable or bulk sediment Zn) and parameters for normalisation (Al, TOC) are not available. Only the study by Kuijpers et al. (1993) justifies the comparison as the Zn (not normalized) and TOC values obtained in the present study fit very well to their extractable Zn data (Figure 6.6). The authors report the highest contents of extractable Zn in surface sediments along the Swedish coast north of Gothenburg (140 ppm), from where they significantly decrease towards the central Skagerrak (~30 ppm). Three main sources for Zn in the Skagerrak were identified by comparing the ratios of Zn to organic carbon: two Swedish fjords and, to a lesser degree, the Jutland Current from the southern North Sea (Kuijpers et al., 1993).

Other potential sources with reportedly high anthropogenic Zn contents are the Oslo Fjord in Norway (Pederstad et al., 1993) and the Idefjord at the Norwegian-Swedish border (Polovodova Asteman et al., 2015). For the latter, very high heavy metal contents (including Zn), as well as TOC values, are reported and pollution is attributed to the pulp and paper industry (since c.1900 CE), with a declining degree of pollution recorded since 1975 CE. Today, the surface sediment in the fjord is considered as almost completely recovered (Polovodova Asteman et al., 2015), which would be a possible explanation for the decreasing trend in the two northeastern cores. We suggest that, especially to the northeast of the investigated transect, the Zn enrichment is rather locally sourced and regionally transported Zn (by the Jutland current) is of minor significance, which is in line with the assumptions by Kuijpers et al. (1993).

Evaluation of the impact

This is the first study applying the recommended normalisation to 5% Al for evaluation of results from different regions. The background contents (BCs) are defined as contaminant content at a 'pristine' site and an important tool in assessing anthropogenic pollution. The suggested BC for Zn* is 90 ppm (Figure 6.3) (OSPAR, 2008).

For the southeastern core location of the transect (GeoB 6003-1), obtained Zn* contents are well below this baseline regardless of the increase at c.1920 CE. In contrast, the two MUCs farther northeast (GeoB 6001-2, GeoB 6002-2) contain, on average, values that are close to or even above the recommended BC but showing a decreasing trend towards the youngest sediments. We also have to acknowledge, that the exceedance of the OSPAR BC in these cores is less than 10% and therefore the overall pollution recorded in the studied transect has to be considered low.

However, the obtained pre-industrial baseline values for Zn* in core GeoB 6003-1 (57 ppm) question the suggested OSPAR background contents (90 ppm). Assessing the Zn* pollution based on the background values obtained in this study, GeoB 6003-1 would, with the previously discussed increase of 19% in 1920 CE, still be the least polluted core. However, the two MUCs farther towards the northeast would be 50% above the background, with maximum values exceeding 60% of additional Zn* (GeoB 6001-2 = 68%, GeoB 6002-2 = 63%). This suggests that the impact of heavy metal pollution on the sediment quality especially in the deeper Skagerrak is much more severe than previously assumed.

Furthermore, based on the comparison with the surface sediment samples analysed by Kuijpers et al. (1993) (Figure 6.6), there is evidence that the spatial distribution of Zn covers a wide range of values. This gives rise to the concern that the anthropogenic impact recorded in this study cannot be generalised to the whole Skagerrak area and might be exceeded locally. Unfortunately, Zn is not included in the OSPAR List of Chemicals for Priority Action and therefore the OSPAR commission reports no Zn* values (OSPAR, 2009).

6.6 Conclusions

The topmost sediments of the study area in the Skagerrak are elevated with respect to Zn contents and the onset of increased anthropogenic release can be dated to c.1920 CE. Subsequent to the normalisation of Zn to 5% Al for comparability, it can be confirmed that the sampling site in the southwest (GeoB 6003-1) is impacted less than the two cores farther northeast (GeoB 6001-2, GeoB 6002-2). We relate this to the different contents of TOC. Furthermore, it is assumed that local sources (e.g., from the Swedish coast) have a greater influence on Zn input into the Skagerrak than the North Sea wide signal deriving from the southern North Sea.

The application of the OSPAR BCs points to overall low pollution in all three cores. However, these suggested natural background contents might be overestimating the true natural background values by 50%. Using the pre-industrial Zn* contents obtained in this study, the degree of pollution has to be evaluated significantly higher.

A direct comparison to other studies in the North Sea was not possible because of the different methods regarding analysis (measuring bulk sediment versus extractable Zn) and normalisation. Therefore, we hope that future studies will profit from the comparability of results by using the normalisation applied here.

Acknowledgements

This project was funded by the Deutsche Forschungsgemeinschaft (DFG) through the International Research Training Group – 'Integrated Coastal Zone and Shelf-Sea Research' (GRK 1598 INTERCOAST).

Chapter 7 Synthesis & future research

7.1 Synthesis

The scientific objectives of this study (Chapter 1.3) were to decipher the heavy metal pollution history in near-coastal regions in order to (i) define pristine background levels and estimate the degree of pollution, (ii) establish an ecotoxicological link between sediment pollution and foraminiferal response and, (iii) evaluate the anthropogenic impact on the deep marine setting applying the existing OSPAR assessment criteria. To answer these questions, two shallow marine study areas (Firth of Thames, New Zealand, and Helgoland Mud Area, SE North Sea) were selected and complemented with a deep marine site in the Skagerrak, NE North Sea (Chapter 2). Through a predominantly geochemical approach, a wide array of techniques, such as radiocarbon dating, inductively coupled plasma mass spectrometry, X-ray fluorescence and grain size analysis, was applied to a total of 13 marine sediment cores (Chapter 3).

The study in the Firth of Thames (Chapter 4) proved a substantial increase of Pb and Zn contents occurring simultaneously with the onset of the European era (~1845 CE) which was most likely related to the mining activities in the nearby Coromandel region. Prior to this onset, background values for Pb (~10 ppm) and Zn (~60 ppm) were extremely stable throughout the pre-human and Polynesian era. In addition to elevated heavy metal values, a synchronous increase in the sedimentation rates could not clearly be attributed to the historical gold mining but possibly results from changes in land use. The increase of Pb and Zn contents in the bulk sediment is widespread in the southeastern Firth of Thames. All Pb and Zn surface sediment contents are below the values recommended in the ANZECC sediment quality guideline, but exceed them in the subsurface. These sediments therefore serve as a potential source of heavy metals, implying a possible threat when sediments are disturbed (e.g., by dredging, severe storm events).

The ecotoxicological effects of increased heavy metal pollution were studied in the Helgoland Mud Area (Chapter 5), where a baseline study on Pb and Zn already existed (Boxberg, 2017). The benthic foraminifera *E. excavatum* and *A. beccarii* were chosen as indicator species and seem to respond to progressive environmental stress in a stepwise manner. This response comprises an increase in abnormal test morphologies, decrease in foraminiferal diversity and the incorporation of heavy metals into the calcitic foraminifera tests. With respect to Pb, test chemistry reflects bulk sediment chemistry very well. An observed temporal offset is attributed to species-specific defence mechanisms, resulting in the incorporation of heavy metals only after a yet to be quantified threshold of pollution is exceeded. Elevated ratios of Pb/Ca and Cd/Ca in foraminiferal calcite were measured in samples younger than 1920 CE (*A. beccarii*) and 1940 CE (*E. excavatum*). However, Pb in bulk sediment and foraminifera tests could not be linked to the increased occurrence of aberrant tests, giving room for speculations on other causes. A strong increase in the proportion of abnormal tests since 1960 CE points towards a

significant role of human activities as the main driver (e.g., levels of radioactive and/or persistent organic pollutants, other heavy metals not detected in this study), although other factors might also have influenced the biomineralisation of the benthic foraminifera.

The study area in the Skagerrak was chosen to complement the two shallow marine study sites with a deeper site and to investigate the impact of heavy metals in a near-coastal but deep marine setting (Chapter 6). In a transect of three short cores it was discovered that elevated Zn contents in bulk sediments are present in the topmost sediments, with the onset dated to c. 1920 CE. The degree of pollution was assessed applying the OSPAR background contents (BCs), including the recommended normalisation of Zn to 5% Al for comparability. All three cores display overall low pollution according to OSPAR BCs, despite a regional trend in the degree of pollution with less impact in the southwest (GeoB 6003-1) than in the two cores farther to the northeast. Possible explanations for this trend are differences in depositional settings (i.e. TOC contents) and the varying influence of local Zn sources. However, the natural Zn contents in pre-industrial sediments obtained in this study strongly question the OSPAR BCs and suggest that they might overestimate natural background contents by 50%. Using the pre-industrial Zn contents obtained in this study, the degree of pollution has to be re-evaluated as being significantly higher than previously suggested by Pederstad et al., (1993).

The combined investigation of the three study areas in the Firth of Thames, Helgoland Mud Area and the Skagerrak unravelled some remarkable characteristics regarding the historical heavy metal release despite the different development of human settlements and locations on either side of the globe.

First, all study areas show a significant increase in the heavy metal contents of the marine sediments only during industrial times, even though the North Sea region has been influenced by anthropogenic activity considerably longer and at a more gradual rate than the Firth of Thames. However, there are some slight differences in the temporal onset between the study sites. An almost simoultaneous increase in Pb and Zn contents of the bulk sediment was recorded ~1845 CE in the Firth of Thames (Chapter 4) and ~1850 CE in the Helgoland Mud Area (Boxberg, 2017), with a second major increase for the latter site around 1900 CE. Both study areas are shallow marine settings in relatively close proximity to the coast. The increase of bulk sediment Zn contents in the Skagerrak occurs around 1920 CE. In contrast to the Firth of Thames and Helgoland Mud Area, this comparably late onset of elevated heavy metal levels might be explained by the greater water depth and more distal location from the coast, i.e. the source.

In addition to this temporal distribution pattern, there seems to be a general trend towards a decreasing degree of pollution with increasing distance to the source. The background contents of bulk sediment Zn in the shallow marine Firth of Thames and the deep marine Skagerrak are surprisingly similar (~60 ppm Zn), despite the different settings (water depth, distance to coast, lithology of the hinterland). However, with the onset of the anthropogenic signal, Zn increased by a factor of 2-3 in the sediments of

the Firth of Thames, while the Skagerrak experiences an enrichment of only 1.2. Interestingly, the enrichment factor of Zn contents in the sediments of the Helgoland Mud Area is with 2-3 (Boxberg, 2017) quite similar to that of the Firth of Thames. A potential explanation is, once again, the distance from the source. The further a pollution signal is carried away from the source area in the marine environment, the more it is subject to mixing with signals from other water masses and therefore - potentially - dilution. It has to be pointed out that other factors, such as an actually lower degree of pollution, can also result in the observed pattern.

The heavy metal increase in the New Zealand study area occurred contemporaneous with the beginning of the European era and was seemingly linked to the mining activity in the nearby Coromandel Range, drained by the Waihou River into the Firth of Thames. With no reported mining operations conducted by the Polynesian settlers and very stable Pb and Zn contents in the pre-European sediments, these sediment values are regarded as truly natural background. In contrast, mining in the catchment areas of the two main rivers draining into the German Bight (Elbe and Weser) already started hundreds and even thousands of years earlier (Monna et al., 2000). Thus, although the two studied cores from the Helgoland Mud Area show a distinct heavy metal increase only around ~1850 CE, the heavy metal contents in the older pre-industrial sediments probably cannot be considered as real natural baseline values, which is in contrast to the Firth of Thames. The increasing occurrence of deformed foraminiferal tests and decreasing diversity in the Helgoland Mud Area sediments underline these non-pristine conditions. Nevertheless, the chemical signal of heavy metals in foraminiferal test, examplified by Pb/Ca and Cd/Ca, indicates no response of foraminifera with respect to the incorporation of heavy metals during the biomineralisation process in pre-industrial times. Increased levels of Pb/Ca and Cd/Ca in foraminiferal tests were only recorded following a second major increase in bulk sediment Pb contents in ~1900 CE with a slight temporal offset.

For the reconstruction of the contents of Pb and Zn in the bulk sediment, X-ray fluorescence analysis demonstrates to be a suitable tool. Yet, for the investigation of heavy metals impact on biota, other elements of importance (e.g., Cd, Hg) cannot be detected in the sediment and limit the applicability of XRF. The effects of increased levels of heavy metals on the biota prove to be rather complex. While foraminiferal test chemistry appears to reflect sediment heavy metal load very well above a certain threshold, test deformation seems to be insufficient as an indicator for heavy metal pollution.

Taken together, the conducted studies confirm the importance of near-coastal sediments as an archive for historical heavy metal pollution caused by human activity. All three study areas recorded an increase in heavy metal accumulation during industrial times, with the shallow marine sites located closer to the coast (Firth of Thames, Helgoland Mud Area) seeming to be affected more readily and to a higher degree than the deep marine Skagerrak. The need for baseline studies was highlighted by the study in the Firth of Thames in New Zealand, where the natural background levels of Pb and Zn were previously unknown, and the Skagerrak, where the currently used OSPAR assessment criterion was evaluated and questioned.

Furthermore, new knowledge about the response of foraminifera to increasing historical levels of heavy metals in the marine sediments was gathered, confirming the demand for an intensification of studies on ecotoxicological aspects.

7.2 Future research

This study contributed to the knowledge needed for the assessment of the environmental impact of historical heavy metal input on coastal regions, which is essential to minimise the potential threat to the marine environment and subsequently human health. Generally, the improvement of the environmental state in these sensitive areas, needs addressing of the following questions:

i) What is the current degree of pollution?
ii) What are the implications for the ecosystem?
iii) Where exactly are the 'additional' heavy metals coming from?

While significant improvements in answering these questions were made, the following aspects should guide further research:

The baseline study in the Firth of Thames indicated an onset of elevated Pb and Zn levels at the same time as the beginning of the European era. Furthermore, the detection of the elevated Pb and Zn signal in six out of eight sediment cores pointed to a Firth-wide contamination. In the course of this research we assume a contemporaneous increase in Pb and Zn in all sediment records. Nevertheless, a time-transgressive pattern can only be excluded by stratigraphic frameworks for each individual core. To better determine the pathways and accumulation patterns of heavy metals within the Firth of Thames, it would prove useful to also establish independent age-depth relationships for the remaining five cores by radiocarbon dating, preferably on foraminifera.

The study in the Skagerrak was conducted on three short cores, exhibiting the onset of increased Zn contents in the bulk sediment at c. 1920 CE. The observed discrepancy between the pre-industrial background values determined in this thesis (~60 ppm) and the suggested OSPAR BCs (~90 ppm) questions the validity of the assessment criteria currently in use and shows the necessity to validate existing guideline BCs. However, pre-industrial background was only captured in the southwesternmost core GeoB 6003-1, while the two other MUCs showed generally higher Zn contents, but did not display this marked onset. For all three MUCs, the corresponding longer gravity cores exist, which should be analysed quantitatively for their heavy metal composition, especially in the pre-industrial sediments. The determination of the temporal onset in the cores GeoB 6001-2 and 6002-2 would additionally require the establishment of an independent stratigraphy by radiometric dating. The determination of the pre-industrial background values for the GCs would be a valuable contribution to verify or contradict the OSPAR BCs.

Due to a lack of implementation in other studies, no conclusions regarding the improved comparability by applying the OSPAR normalisation could be drawn on a North Sea wide scale. Yet, with so many different approaches for heavy metal analysis (e.g., measuring bulk sediment Zn versus extractable Zn) and normalisation (e.g., to grain size, TOC or 5%Al) it would be beneficial to the scientific community and society to conduct a comparative study with the aim of obtaining conversion factors between different methods.

Following the reconstruction of the temporal and spatial pollution history in near-coastal sediments, it is important to gain an understanding of the ecological consequences resulting from these changes. The study of ecotoxicological effects on the local biota are a complex issue because of the number of variables influencing the status of an ecosystem (e.g., temperature, salinity, oxygenation, turbidity, multiple contaminants), even in modern settings. However, benthic foraminifera offer the potential to improve our understanding of these effects throughout the past, because of the preservation of their tests in the geological record. The test chemistry reflects the increased contents of the heavy metals Pb (and most likely Cd) very well, as the study in the Helgoland Mud Area showed. However, the cause of the increased proportions of deformed tests remains unidentified, even though timing points to a most likely anthropogenic cause.

Previous studies on certain species of foraminifera assumed a connection between some heavy metals and test deformation (e.g., Brouillette Price et al., 2019) or cytological changes (e.g., Frontalini et al., 2015), while other authors suggest natural variability (e.g., salinity, periodical acidification) as a major driver for aberrant tests (Geslin et al., 2002). Culturing experiments with graded heavy metal concentrations should combine the observations of cytological changes and malformed tests with the subsequent analysis of test chemistry. This way, a holistic understanding of the relationship between cytological changes, abnormal tests and test chemistry could be obtained. In a time-resolved manner, this could also answer the question if biological defence mechanisms inhibit the incorporation of specific heavy metals and, if so, what the element- and species-specific thresholds are. This combined approach would improve the understanding of the relationship between foraminiferal “health” and characteristics of their shells, allowing to draw more robust conclusions about the historical “health” of foraminiferal communities as an indicator for the ecosystem.

Alternatively, a field study in a transect with increasing distance from a specific heavy metal point source could replace graded concentrations in the laboratory. Besides living (stained) foraminifera, surface sediment and pore water should be analysed for heavy metals. In combination with a down core record, this holds the potential to (i) observe how the load of heavy metals changes with the distance to the point source, (ii) investigate the reaction of recent benthic foraminifera to the sediment and water quality (chemically and morphologically) and (iii) relate this to a downcore record, where the gained knowledge can be applied to unravel the historical development.

Knowing the degree of heavy metal pollution and its effects on the ecosystem is fundamental to a good environmental management and protection plan. Undoubtedly, the reduction of heavy metal release to the environment, i.e. the coastal areas, is the best mitigation strategy. To do this most efficiently, it needs to be known what the major sources of heavy metals in a specific area are and (ideally) which sources contribute to what extent to the pollution. Once again, the reconstruction of the historical development and temporal determination of the pollution onset helps to narrow down on the (some) most likely major source(s). For example, based on the temporal pattern and the proximity to the source, mining could be identified as most likely source in the Firth of Thames. However, this conclusion still needs to be verified. A powerful tool for source identification is isotopic fingerprinting.

The principle behind isotopic fingerprinting relies on the comparison of the isotopic ratio found in a sample to the isotopic ratio of a potential source. It can be differentiated between radiogenic (e.g., Pb) and stable (e.g., Zn) isotope systems.

For the purpose of tracing heavy metal pollution mainly through Pb and Zn, it would be beneficial to use these elements as tracers. Pb has four isotopes occurring in nature (^{204}Pb, ^{206}Pb, ^{207}Pb, ^{208}Pb), with only ^{204}Pb being non-radiogenic and basically constant in abundance (Cheng and Hu, 2010). The three other Pb isotopes derive from U and Th through radioactive decay over geological time-scales (Faure, 1986). The individual isotopic Pb fingerprint is dependent on the relative proportion of U-Th-Pb in the geogenic source material, with no fractionation occurring during environmental or anthropogenic processes (Ault et al., 1970). Therefore, samples retain the Pb isotopic signatures of the rock they derive from and are only modified by mixing with other Pb sources (Cheng and Hu, 2010).

In contrast, the stable isotopes of Zn (^{64}Zn, ^{66}Zn, ^{67}Zn, ^{68}Zn, ^{70}Zn) are subject to mass-dependent fractionation during natural and anthropogenic processes (Bermin et al., 2006; John et al., 2007; Mattielli et al., 2009). For example, the high-temperature smelting process of a specific ore result in air emissions, effluents and slags with each having different Zn isotopic signatures (Yin et al., 2016, and references therein).

In summary, the Pb isotopic signature only depends on the geogenic source, while the Zn isotope ratio reflects the fractionation during environmental or industrial processes. In combination it might be possible to determine the origin of the pollution in great detail (e.g., not only which smelting plant, but also if the tailings or air emissions are the major problem). Nevertheless, it needs to be acknowledged that this idealised approach might face some limitations caused by mixing of many different sources (e.g., in the Skagerrak) and analytical precision. However, for study sites near a potential major source, as is the case for the Firth of Thames, this approach seems to be promising.

This shows that, even though the studies presented in this thesis shed new light on the spatial and temporal development of heavy metal accumulation in near-coastal areas and their effects on benthic foraminifera, future research is still needed.

Chapter 8 References

Abrahim, G. M. S., & Parker, R. J. (2008). Assessment of heavy metal enrichment factors and the degree of contamination in marine sediments from Tamaki Estuary, Auckland, New Zealand. Environmental monitoring and assessment, 136(1), 227-238.

Abrahim, G. M. S., Parker, R. J., & Horrocks, M. (2013). Pollen core assemblages as indicator of polynesian and european impact on the vegetation cover of Auckland Isthmus catchment, New Zealand. Estuarine, Coastal and Shelf Science, 131, 162–170.

Abrahim, G., & Parker, R. (2002). Heavy metal contaminants in Tamaki Estuary: Impact of city development and growth, Auckland, New Zealand. Environmental Geology, 42, 883–890.

Adams, C. J., Graham, I. J., Seward, D., Skinner, D. N. B., Adams, C. J., Skinner, D. N. B., & Moore, P. R. (1994). Geochronological and geochemical evolution of late Cenozoic volcanism in the Coromandel Peninsula, New Zealand, New Zealand Journal of Geology and Geophysics, 37(3), 359-379.

Alve, E. (1991). Benthic foraminifera in sediment cores reflecting heavy metal pollution in Sorfjord, western Norway. The Journal of Foraminiferal Research, 21(1), 1–19.

Alve, E. (1995). Benthic foraminiferal responses to estuarine pollution; a review. The Journal of Foraminiferal Research, 25(3), 190–203.

Alve, E. (2000). Environmental stratigraphy: A case study reconstructing bottom water oxygen conditions in Frierfjord, Norway, over the past five centuries. In: Martin, R.E. (Ed.), Environmental Micropaleontology. Topics in Geobiology, 15, 323-350.

Alve, E., Korsun, S., Schönfeld, J., Dijkstra, N., Golikova, E., Hess, S., Husum, K., & Panieri, G. (2016). Foram-AMBI: A sensitivity index based on benthic foraminiferal faunas from North-East Atlantic and Arctic fjords, continental shelves and slopes. Marine Micropaleontology, 122, 1-12.

Anton, K. K., Liebezeit, G., Rudolph, C., & Wirth, H. (1993). Origin, distribution and accumulation of organic carbon in the Skagerrak. Marine Geology, 111, 287–297.

Arz, H. W., Pätzold, J., & Wefer, G. (1999). Climatic changes during the last deglaciation recorded in sediment cores from the northeastern Brazilian Continental Margin. Geo-Marine Letters, 19(3), 209–218.

Atkinson, I. A. E., & Cameron, E. K. (1993). Human influence on the terrestrial biota and biotic communities of New Zealand. Trends in Ecology & Evolution, 8(12), 447–451.

Augustinus, P., Reid, M., Andersson, S., Deng, Y., & Horrocks, M. (2006). Biological and Geochemical Record of Anthropogenic Impacts in Recent Sediments from Lake Pupuke, Auckland City, New Zealand. Journal of Paleolimnology, 35(4), 789–805.

Ault, W. U., Senechal, R. G., & Erlebach, W. E. (1970). Isotopic Composition as a Natural Tracer of Lead in the Environment. Environmental Science and Technology, 4(4), 305–313.

Badr, N. B. E., El-Fiky, A. A., Mostafa, A. R., & Al-Mur, B. A. (2009). Metal pollution records in core sediments of some Red Sea coastal areas, Kingdom of Saudi Arabia. Environmental monitoring and assessment, 155, 509-526.

Bard, E. (1998). Geochemical and geophysical implications of the radiocarbon calibration. Geochimica et Cosmochimica Acta, 62(12), 2025–2038.

Barker, S., Greaves, M., & Elderfield, H. (2003). A study of cleaning procedures used for foraminiferal Mg/Ca paleothermometry. Geochemistry, Geophysics, Geosystems, 4(9), 1–20.

Barkla, C. G. (1911). The spectra of the fluorescent Röntgen radiations. The London, Edinburgh, and Dublin Philosophical Magazine and Journal of Science, 22(129), 396–412.

Baskaran, M. (2011). Po-210 and Pb-210 as atmospheric tracers and global atmospheric Pb-210 fallout: A Review. Journal of Environmental Radioactivity, 102(5), 500–513.

Behre, K.-E. (1988). The rôle of man in European vegetation history. In: Huntley, B., & Webb, T. (Eds.), Vegetation history (pp. 633–672). Springer Netherlands, Dordrecht.

Benninghoff, W.S. (1962). Calculation of pollen and spores density in sediments by addition of exotic pollen in known quantities. Pollen spores, 4(2), 332-333.

Bergin, F., Kucuksezgin, F., Uluturhan, E., Barut, I. F., Meric, E., Avsar, N., & Nazik, A. (2006). The response of benthic foraminifera and ostracoda to heavy metal pollution in Gulf of Izmir (Eastern Aegean Sea). Estuarine, Coastal and Shelf Science, 66(3–4), 368–386.

Bermin, J., Vance, D., Archer, C., & Statham, P. J. (2006). The determination of the isotopic composition of Cu and Zn in seawater. Chemical Geology, 226(3–4), 280–297.

Berry, A., & Plater, A. J. (1998). Rates of tidal sedimentation from records of industrial pollution and environmental magnetism: The Tees estuary, north-east England. Water, Air, and Soil Pollution, 106, 463–479.

Bienfang, P. K. (1980). Phytoplankton sinking rates in oligotrophic waters off Hawaii, USA. Marine Biology, 61(1), 69–77.

Blaauw, M., van Geel, B., Kristen, I., Plessen, B., Lyaruu, A., Engstrom, D. R., von der Plicht, J., & Verschuren, D. (2011). High-resolution 14C dating of a 25,000-year lake-sediment record from equatorial East Africa. Quaternary Science Reviews, 30(21–22), 3043–3059.

Black, K. P., Bell, R. G., Oldman, J. W., Carter, G. S., & Hume, T. M. (2000). Features of 3-dimensional barotropic and baroclinic circulation in the Hauraki Gulf, New Zealand. New Zealand Journal of Marine and Freshwater Research, 34(1), 1–28.

Blanchet, C. L., Thouveny, N., & Vidal, L. (2009). Formation and preservation of greigite (Fe3S4) in sediments from the Santa Barbara Basin: Implications for paleoenvironmental changes during the past 35 ka. Paleoceanography, 24(2), 1–15.

Bogutskaya, N. G., Zuykov, M. A., Naseka, A. M., & Anderson, E. B. (2011). Normal axial skeleton structure in common roach Rutilus rutilus (Actinopterygii: Cyprinidae) and malformations due to radiation contamination in the area of the Mayak (Chelyabinsk Province, Russia) nuclear plant. Journal of Fish Biology, 79(4), 991–1016.

Boltovskoy, E. (1964). Seasonal Occurrences of some Living Foraminifera in Puerto Deseado (Patagonia, Argentina). ICES Journal of Marine Science, 29(2), 136–145.

Boxberg, F. (2017). Anthropogenic input of heavy metals to near-coastal sediment depocenters in the eastern North Sea and the Hauraki Gulf in historical times. PhD Thesis, University of Bremen, Bremen.

Boyle, J.F., Chiverrell, R.C., & Schillereff, D. (2015). Approaches to Water Content Correction and Calibration for µXRF Core Scanning: Comparing X-ray Scattering with Simple Regression of Elemental Concentrations. In: Rothwell, R. G., & Croudace, I. W. (Eds.), Micro-XRF Studies of Sediment Cores: A Perspective on Capability and Application in the Environmental Sciences (pp. 373–391). Springer, Dordrecht.

Bradl, H. B. (2005). Sources and origins of heavy metals. In: H. B. Bradl (Ed.), Heavy Metals in the Environment: Origin, Interaction and Remediation (pp. 1–27). Elsevier Academic Press, Amsterdam, Boston.

Brathwaite, R. L. (1989). Geology and exploration of the Karangahake gold-silver deposit. Australasian Institute of Mining and Metallurgy Monograph, 13, 73–78.

Brathwaite, R. L., & Rabone, S. D. C. (1985). Heavy metal sulphide deposits and geochemical surveys for heavy metals in New Zealand. Journal of the Royal Society of New Zealand, 15(4), 363–370.

Brathwaite, R. L., Cargill, H. J., Christie, A. B., & Swain, A. (2001). Lithological and spatial controls on the distribution of quartz veins in andesite- and rhyolite-hosted epithermal Au-Ag deposits of the Hauraki Goldfield, New Zealand. Mineralium Deposita, 36, 1-12.

Bresler, V.M., & Yanko-Hombach, V.V. (2000). Chemical ecology of foraminifera: Parameters of health, environmental pathology, and assessment of environmental quality. In: Martin, R.E. (Ed.), Environmental Micropaleontology. Topics in Geobiology, 15, 217-254.

Brouillette Price, E., Kabengi, N., & Goldstein, S. T. (2019). Effects of heavy-metal contaminants (Cd, Pb, Zn) on benthic foraminiferal assemblages grown from propagules, Sapelo Island, Georgia (USA). Marine Micropaleontology, 147, 1–11.

Brückner, S., & Mackensen, A. (2006). Deep-water renewal in the Skagerrak during the last 1200 years triggered by the North Atlantic Oscillation: evidence from benthic foraminiferal δ8O. The Holocene, 16(3), 331–340.

Bryan, G. W. (1971). The effects of heavy metals (other than mercury) on marine and estuarine organisms. Proceedings of the Royal Society of London. Series B. Biological Sciences, 177(1048), 389–410.

BSH (2016). Nordseezustand 2008-2011, Berichte des BSH, Nr. 54, 311 pp., Bundesamt für Seeschifffahrt und Hydrographie, Hamburg und Rostock.

Burdige, D. J. (2005). Burial of terrestrial organic matter in marine sediments: A re-assessment. Global Biogeochemical Cycles, 19(4), 1–7.

Buzas M. A., & Gibson T. G. (1969). Species Diversity: Benthonic Foraminifera in Western North Atlantic. Science, 163, 72-75.

Byrami, M., Ogden, J., Horrocks, M., Deng, Y., Shane, P., & Palmer, J. (2002). A palynological study of Polynesian and European effects on vegetation in Coromandel, New Zealand, showing the variability between four records from a single swamp. Journal of the Royal Society of New Zealand, 32(3), 507–531.

Carbonell, E., Mosquera, M., Rodríguez, X. P., & Sala, R. (1996). The First Human Settlement of Europe. Journal of Anthropological Research, 52(1), 107–114.

Caruso, A., Cosentino, C., Tranchina, L., & Brai, M. (2011). Response of benthic foraminifera to heavy metal contamination in marine sediments (Sicilian coasts, Mediterranean Sea). Chemistry and Ecology, 27(1), 9–30.

Carvalho, F. P. (2017). Pesticides, environment, and food safety. Food and Energy Security, 6(2), 48–60.

Cheng, H., & Hu, Y. (2010). Lead (Pb) isotopic fingerprinting and its applications in lead pollution studies in China: A review. Environmental Pollution, 158(5), 1134–1146.

Cheshire, H., Thurow, J., & Nederbragt, A. J. (2005). Late Quaternary climate change record from two long sediment cores from Guaymas Basin, Gulf of California. Journal of Quaternary Science, 20(5), 457–469.

Christie, A. B., Simpson, M. P., Brathwaite, R. L., Mauk, J. L., & Simmons, S. F. (2007). Epithermal Au-Ag and Related Deposits of the Hauraki Goldfield, Coromandel Volcanic Zone, New Zealand. Economic Geology, 102, 785–816.

Clement, A. J., Nováková, T., Hudson-Edwards, K. A., Fuller, I. C., Macklin, M. G., Fox, E. G., & Zapico, I. (2017). The environmental and geomorphical impacts of historical mining in the Ohinemuri and Waihou river catchments, Coromandel, New Zealand. Geomorphology, 295, 159-175.

Coccioni, R. (2000). Benthic foraminifera as bioindicators of heavy metal pollution: A case study from the Goro Lagoon (Italy). In: Martin, R.E. (Ed.), Environmental Micropaleontology. Topics in Geobiology, 15, 71-103.

Craw, D., & Chappell, D. A. (2000). Metal redistribution in historic mine wastes, Coromandel Peninsula, New Zealand. New Zealand Journal of Geology and Geophysics, 43(2), 187-198.

Croudace, I. W., & Cundy, A. B. (1995). Heavy Metal and Hydrocarbon Pollution in Recent Sediments from Southampton Water, Southern England: A Geochemical and Isotopic Study. Environmental Science and Technology, 29(5), 1288–1296.

Dähnke, K., Serna, A., Blanz, T., & Emeis, K. C. (2008). Sub-recent nitrogen-isotope trends in sediments from Skagerrak (North Sea) and Kattegat: Changes in N-budgets and N-sources? Marine Geology, 253(3–4), 92–98.

Damon, P. E., & Peristykh, A. N. (2000). Radiocarbon calibration and application to geophysics, solar physics, and astrophysics. Radiocarbon, 42(1), 137–150.

De Haas, H., & van Weering, T. C. E. (1997). Recent sediment accumulation, organic carbon burial and transport in the northeastern North Sea. Marine Geology, 136, 173–187.

De Nooijer, L. J., Reichart, G. J., Dueñas-Bohórquez, A., Wolthers, M., Ernst, S. R., Mason, P. R. D., & Van Der Zwaan, G. J. (2007). Copper incorporation in foraminiferal calcite: Results from culturing experiments. Biogeosciences, 4(4), 493–504.

De Nooijer, L. J., Spero, H. J., Erez, J., Bijma, J., & Reichart, G. J. (2014). Biomineralization in perforate foraminifera. Earth-Science Reviews, 135, 48–58.

Dellwig, O., Hinrichs, J., Hild, A., & Brumsack, H.-J. (2000). Changing sedimentation in tidal flat sediments of the southern North Sea from the Holocene to the present: a geochemical approach. Journal of Sea Research, 44(3–4), 195–208.

Dickinson, W. W., Dunbar, G. B., & McLeod, H. (1996). Heavy metal history from cores in Wellington Harbour, New Zealand. Environmental Geology, 27, 59-69.

Dominik, J., Förstner, U., Mangini, A., & Reineck, H. E. (1978). 210Pb and 137Cs chronology of heavy metal pollution in a sediment core from the German Bight (North Sea). Senckenbergiana Maritima, 10, 213–227.

Downey, J. F. (1935). Gold mines of the Hauraki district, New Zealand. Govt. Printer, Wellington N.Z.

Dredge, M. (2014). Natural hazard risk assessment for Matamata Piako District. Waikato Regional Council Technical Report 2014/01, Waikato Regional Council, Hamilton.

Duffus, J. H. (2002). “Heavy metals” a meaningless term? (IUPAC Technical Report). Pure and Applied Chemistry, 74(5), 793–807.

Duruibe, J. O., Ogwuegbu, M. O. C., & Egwurugwu, J. N. (2007). Heavy metal pollution and human biotoxic effects. International Journal of Physical Sciences, 2(5), 112–118.

Eglinton, T. I., Aluwihare, L. I., Bauer, J. E., Druffel, E. R. M., & McNichol, A. P. (1996). Gas chromatographic isolation of individual compounds from complex matrices for radiocarbon dating. Analytical Chemistry, 68(5), 904–912.

Eisma, D. (1981). Supply and deposition of suspended matter in the North Sea. Special Publication of the International Association of Sedimentologists, 5,415-428.

Eisma, D., & Kalf, J. (1987). Dispersal, concentration and deposition of suspended matter in the North Sea. Journal of the Geological Society, London, 144, 161–178.

Elberling, B., & Langdahl, B. R. (1998). Natural heavy-metal release by sulphide oxidation in the High Arctic. Canadian Geotechnical Journal, 35(5), 895–901.

Elenga, H., Schwartz, D., & Vincens, A. (1994). Pollen evidence of late Quaternary vegetation and inferred climate changes in Congo. Palaeogeography, Palaeoclimatology, Palaeoecology, 109(2–4), 345–356.

Elliot, M. B., Flenley, J. R., & Sutton, D. G. (1998). A late Holocene pollen record of deforestation and environmental change from the Lake Tauanui catchment, Northland, New Zealand. Journal of Paleolimnology, 19(1), 23–32.

Elshanawany, R., Ibrahim, M. I., Frihy, O., & Abodia, M. (2018). Foraminiferal evidence of anthropogenic pollution along the Nile Delta coast. Environmental Earth Sciences, 77(444), 1-33.

Emeis, K. C., van Beusekom, J., Callies, U., Ebinghaus, R., Kannen, A., Kraus, G., Kröncke, I., Lenhart, H., Lorkowski, I., Matthias, V., Möllmann, C., Pätsch, J., Scharfe, M., Thomas, H., Weisse, R., & Zorita, E. (2015). The North Sea - A shelf sea in the Anthropocene. Journal of Marine Systems, 141, 18–33.

Ernst, S. R., Morvan, J., Geslin, E., Le Bihan, A., & Jorissen, F. J. (2006). Benthic foraminiferal response to experimentally induced Erika oil pollution. Marine Micropaleontology, 61(1–3), 76–93.

Faegri K., & Iversen J. (1989). Textbook of pollen analysis, 4th Edition. Wiley, Chichester.

Fält, L.M. (1982). Late Quaternary sea-floor deposits off the Swedish west coast. Ph.D. Thesis, Chalmers Univ. Technol., Univ. Gothenburg, Publ. A37, 259 pp.

Faure, G. (1986). Principles of isotope geology, 2nd Edition. New York, Chichester, Brisbane, Toronto, Singapore: John Wiley & Sons.

Feyling-Hanssen, R.W. (1972). The foraminifer Elphidium excavatum (Terquem) and its variant forms. Micropaleontology, 18(3), 337-354.

Figge, K. (1981). Sedimentverteilung in der Deutschen Bucht (No: 2900, Maßstab: 1:250.000). Deutsches Hydrographisches Institut, Hamburg.

Förstner, U., & Reineck, H. E. (1974). Die Anreicherung von Spurenelementen in den rezenten Sedimenten eines Profilkerns aus der Deutschen Bucht. Senckenbergiana Maritima, 6(2), 175–184.

Förstner, U., & Wittmann, G. T. W. (1981). Metal pollution in the aquatic environment, 2nd Edition. Springer, Berlin, Heidelberg, New York, pp 121-131.

Fraser, C. (1910). The geology of the Thames subdivision, Hauraki, Auckland. New Zealand Geological Survey Bulletin, 10.

Frontalini, F., & Coccioni, R. (2008). Benthic foraminifera for heavy metal pollution monitoring: A case study from the central Adriatic Sea coast of Italy. Estuarine, Coastal and Shelf Science, 76(2), 404–417.

Frontalini, F., Buosi, C., Da Pelo, S., Coccioni, R., Cherchi, A., & Bucci, C. (2009). Benthic foraminifera as bio-indicators of trace element pollution in the heavily contaminated Santa Gilla lagoon (Cagliari, Italy). Marine Pollution Bulletin, 58(6), 858–877.

Frontalini, F., Curzi, D., Cesarini, E., Canonico, B., Giordano, F. M., De Matteis, R., Bernhard, J. M., Pieretti, N., Gu, B., Eskelsen, J. R., Jubb, A. M., Zhao, L., Pierce, E. M., Gobbi, P., Papa, S., & Coccioni, R. (2016). Mercury-pollution induction of intracellular lipid accumulation and lysosomal compartment amplification in the benthic foraminifer ammonia parkinsoniana. PLoS ONE, 11(9), 1–14.

Frontalini, F., Curzi, D., Giordano, F. M., Bernhard, J. M., Falcieri, E., & Coccioni, R. (2015). Effects of lead pollution on Ammonia parkinsoniana (foraminifera): ultrastructural and microanalytical approaches. European Journal of Histochemistry, 59(1), 1–8.

Frontalini, F., Greco, M., Di Bella, L., Lejzerowicz, F., Reo, E., Caruso, A., Cosentino, C., Maccotta, A., Scopelliti, G., Nardelli, M. P., Losada, M. T., Armynot du Châtelet, E., Coccioni, R., & Pawlowski, J. (2018). Assessing the effect of mercury pollution on cultured benthic foraminifera community using morphological and eDNA metabarcoding approaches. Marine Pollution Bulletin, 129(2), 512–524.

Fukue, M., Nakamura, T., Kato, Y., & Yamasaki, S. (1999). Degree of pollution for marine sediments. Engineering Geology, 53(2), 131-137.

Ganote, C. E., & Van der Heide, R. S. (1987). Cytoskeletal lesions in anoxic myocardial injury. A conventional and high-voltage electron-microscopic and immunofluorescence study. American Journal of Pathology, 129(2), 327–344.

Garrels, R. M., & Thompson, M. E. (1960). Oxidation of pyrite in iron sulfate solutions. American Journal of Science, 258A, 57-67.

Ge, C., Lao, F., Li, W., Li, Y., Chen, C., Qiu, Y., Mao, X., Li, B., Chai, Z., & Zhao, Y. (2008). Quantitative Analysis of Metal Impurities in Carbon Nanotubes: Efficacy of Different Pretreatment Protocols for ICPMS Spectroscopy. Analytical Chemistry, 80(24), 9426–9434.

Geslin, E., Debenay, J. P., Duleba, W., & Bonetti, C. (2002). Morphological abnormalities of foraminiferal tests in Brazilian environments: Comparison between polluted and non-polluted areas. Marine Micropaleontology, 45(2), 151–168.

Geslin, E., Stouff, V., Debenay, J.-P., & Lescourd, M. (2000). Environmental variation and foraminiferal test abnormalities. In: Martin, R.E. (Ed.), Environmental Micropaleontology. Topics in Geobiology, 15, 191-215.

Godwin, H. (1962). Half-life of Radiocarbon. Nature, 195, 984.

Goullé, J.-P., Mahieu, L., Castermant, J., Neveu, N., Bonneau, L., Lainé, G., Bouige, D., & Lacroix, C. (2005). Metal and metalloid multi-elementary ICP-MS validation in whole blood, plasma, urine and hair. Forensic Science International, 153(1), 39–44.

Grant, P. J. (1985). Major periods of erosion and alluvial sedimentation in New Zealand during the late Holocene. Journal of the Royal Society of New Zealand, 15(1), 67–121.

Green, M., & Zeldis, J. (2015). Firth of Thames Water Quality and Ecosystem Health – A Synthesis. NIWA Client Report No. HAM2015-016, prepared for Waikato Regional Council and DairyNZ.

Guiot, J., Pons, A., de Beaulieu, J. L., & Reille, M. (1989). A 140.000-year climatic reconstruction from two European pollen records. Nature, 338, 309–313.

Guyard, H., Chapron, E., St-Onge, G., Anselmetti, F. S., Arnaud, F., Magand, O., Francus, P., & Mélières, M.-A. (2007). High-altitude varve records of abrupt environmental changes and mining activity over the last 4000 years in the Western French Alps (Lake Bramant, Grandes Rousses Massif). Quaternary Science Reviews, 26(19–21), 2644–2660.

Gyllencreutz, R., Backman, J., Jakobsson, M., Kissel, C., & Arnold, E. (2006). Postglacial palaeoceanography in the Skagerrak. The Holocene, 16(7), 975–985.

Hall, G. E. M., Bonham-Carter, G. F., & Buchar, A. (2014). Evaluation of portable X-ray fluorescence (pXRF) in exploration and mining: Phase 1, control reference materials. Geochemistry: Exploration, Environment, Analysis, 14(2), 99–123.

Hass, H. C. (1993). Depositional processes under changing climate: Upper Subatlantic granulometric records from the Skagerrak (NE-North Sea). Marine Geology, 111(3–4), 361–378.

Hass, H. C. (1996). Northern Europe climate variations during late Holocene: evidence from marine Skagerrak. Palaeogeography, Palaeoclimatology, Palaeoecology, 123, 121–145.

Havach, S.M., Chandler, G.T., Wilson-Finelli, A., & Shaw, T.J. (2001). Experimental determination of trace element partition coefficients in cultured benthic foraminifera. Geochimica et Cosmochimica Acta, 65, 1277–1283.

Hayward, B. W., Grenfell, H. R., Nicholson, K., Parker, R., Wilmhurst, J., Horrocks, M., Swales, A., & Sabaa, A. T. (2004). Foraminiferal record of human impact on intertidal estuarine environments in New Zealand's largest city. Marine Micropaleontology, 53(1–2), 37–66.

Healy, T. (2002). Muddy coasts of mid-latitude oceanic islands on an active plate margin – New Zealand. In: Healy, T., Wang, Y., & Healy, J.-A. (Eds.), Muddy coasts of the world: processes, deposits and function (pp. 347-374). Proceedings in Marine Science 4, Elsevier Science, Amsterdam.

Hebbeln, D., Knudsen, K., Gyllencreutz, R., Kristensen, P., Klitgaard-Kristensen, D., Backman, J., Scheurle, C., Jiang, H., Gil, I., Smelror, M., Jones, P.D., & Sejrup, H.-P. (2006). Late Holocene coastal hydrographic and climate changes in the eastern North Sea. The Holocene, 16(7), 987–1001.

Hebbeln, D., Scheurle, C., & Lamy, F. (2003). Depositional history of the Helgoland mud area, German Bight, North Sea. Geo-Marine Letters, 23(2), 81–90.

Heenan, P. B., de Lange, P. J., Glenny, D. S., Breitwieser, I., Brownsey, P. J., & Ogle, C. C. (1999). Checklist of dicotyledons, gymnosperms, and pteridophytes naturalised or casual in New Zealand: Additional records 1997–1998. New Zealand Journal of Botany, 37(4), 629–642.

Henderson, G. M. (2002). New oceanic proxies for paleoclimate. Earth and Planetary Science Letters, 203(1), 1–13.

Hertweck, G. (1983). Das Schlickgebiet in der inneren Deutschen Bucht. Aufnahme mit dem Sedimentechographen. Senckenbergiana Maritima, 15, 219–249.

Hicks, D., Shankar, U., McKerchar, A., Basher, L., Lynn, I., Page, M., & Jessen, M. (2011). Suspended sediment yields from New Zealand rivers. Journal of Hydrology (New Zealand), 50(1), 81–142.

Hintz, C., J. Shaw, T., Chandler, G., Bernhard, J., McCorkle, D., & Blanks, J. (2006). Trace/minor element:calcium ratios in cultured benthic foraminifera. Part I: Inter-species and inter-individual variability. Geochimica et Cosmochimica Acta, 70(8), 1952–1963.

Hirabayashi, S., Yokoyama, Y., Suzuki, A., Miyairi, Y., & Aze, T. (2017). Multidecadal oceanographic changes in the western Pacific detected through high-resolution bomb-derived radiocarbon measurements on corals. Geochemistry, Geophysics, Geosystems, 18(4), 1608–1617.

Hochstein, M. P., & Nixon, I. M. (1979). Geophysical study of the Hauraki depression, North Island, New Zealand. New Zealand Journal of Geology and Geophysics, 22(1), 1–19.

Hong, S., Candelone, J.-P., Patterson, C. C., & Boutron, C. F. (1996). History of Ancient Copper Smelting Pollution During Roman and Medieval Times Recorded in Greenland Ice. Science, 272(5259), 246–249.

Horowitz, A. J. (1991). A Primer on sediment-trace element chemistry, 2nd Edition. Open-File Report 91-76, 136p, U.S. Geological Survey. Lewis Publishing, Chelsea.

Horrocks, M., Deng, Y., Ogden, J., Alloway, B. V., Nichol, S. L., & Sutton, D. G. (2001). High spatial resolution of pollen and charcoal in relation to the c. 600 yr B.P. Kaharoa Tephra: implications for Polynesian settlement of Great Barrier Island, northern New Zealand. Journal of Archaeological Science, 28, 153-168.

Hume, T. M., & Dahm, J. (1992). An Investigation of the Effects of Polynesian and European Land Use on Sedimentation in Coromandel Estuaries. Prepared for the Department of Conservation, Hamilton Regional Office.

Hunt, A. M. W., & Speakman, R. J. (2015). Portable XRF analysis of archaeological sediments and ceramics. Journal of Archaeological Science, 53, 626–638.

Hurrell, J. W. (1995). Decadal Trends in the North Atlantic Oscillation: Regional Temperatures and Precipitation. Science, 269(5224), 676–679.

Hylander, L. D., & Meili, M. (2003). 500 Years of mercury production: Global annual inventory by region until 2000 and associated emissions. Science of the Total Environment, 304(1–3), 13–27.

Injuk, J., & van Grieken, R. (1995). Atmospheric concentrations and deposition of heavy metals over the North Sea: A literature review. Journal of Atmospheric Chemistry, 20(2), 179–212.

Irion, G., Wunderlich, F., & Schwedhelm, E. (1987). Transport of clay minerals and anthropogenic compounds into the German Bight and the provenance of fine-grained sediments SE of Helgoland. Journal of the Geological Society, 144(1), 153–160.

Ishizawa, T., Goto, K., Yokoyama, Y., Miyairi, Y., Sawada, C., Nishimura, Y., & Sugawara, D. (2017). Sequential radiocarbon measurement of bulk peat for high-precision dating of tsunami deposits. Quaternary Geochronology, 41, 202–210.

Jakimska, A., Konieczka, P., Skóra, K., & Namieśnik, J. (2011). Bioaccumulation of Metals in Tissues of Marine Animals, Part II: Metal Concentrations in Animal Tissues. Polish Journal of Environmental Studies, 20(5), 1127–1146.

Jansen, J. H. F., Van Der Gaast, S. J., Koster, B., & Vaars, A. J. (1998). CORTEX, a shipboard XRF-scanner for element analyses in split sediment cores. Marine Geology, 151(1–4), 143–153.

Jayaraju, N., Sundara Raja Reddy, B. C., & Reddy, K. R. (2008). The response of benthic foraminifera to various pollution sources: A study from Nellore Coast, East Coast of India. Environmental Monitoring and Assessment, 142(1–3), 319–323.

John, S. G., Park, G. J., Zhang, Z., & Boyle, E. A. (2007). The isotopic composition of some common forms of anthropogenic zinc. Chemical Geology, 245(1–2), 61–69.

Jones, R.W.J. (2014). Foraminifera and their applications. Cambridge University Press, Cambridge, 391 pp.

Jorissen, F. J., Fontanier, C., & Thomas, E. (2007). Paleoceanographical proxies based on deep-sea benthic foraminiferal assemblage characteristics. In: Hillaire-Marcel, C., & De Vernal, A. (Eds.), Proxies in Late Cenozoic paleoceanography. Developments in Marine Geology, 1, 277-328.

Kaplan, J. O., Krumhardt, K. M., & Zimmermann, N. (2009). The prehistoric and preindustrial deforestation of Europe. Quaternary Science Reviews, 28(27–28), 3016–3034.

Katz, M. E., Cramer, B. S., Franzese, A., Honisch, B., Miller, K. G., Rosenthal, Y., & Wright, J. D. (2010). Traditional and Emerging Geochemical Proxies in Foraminifera. The Journal of Foraminiferal Research, 40(2), 165–192.

Kautsky, H. (1985). Distribution and content of different artificial radio nuclides in the water of the North Sea during the years 1977 to 1981 (complemented with some results from 1982 to 1984). Deutsche Hydrographische Zeitschrift, 38(5), 193–224.

Kawahara, N., & Shoji, T. (2006). Wavelength Dispersive XRF and a Comparison with EDS. In: Beckhoff, B., Kanngießer, B., Langhoff, N., Wedell, R., & Wolff, H. (Eds.), Handbook of Practical X-Ray Fluorescence Analysis (pp. 284–308). Springer, Berlin, Heidelberg, New York.

Kersten, M., Dicke, M., Kriews, M., Naumann, K., Schmidt, D., Schulz, M., Schwikowski, M., & Steiger, M. (1988). Distribution and fate of heavy metals in the North Sea. In: Salomons, W., Bayne, B. L., Duursma, E. K., & Förstner, U. (Eds.), Pollution of the North Sea (pp. 300–347). Springer-Verlag, Berlin, Heidelberg.

Kidd, C. H. (1988). Prediction of Solute Transport from Gold Mine Wastes, Coromandel, New Zealand. IMWA Proceedings 1988, 173–184.

Kido, Y., Koshikawa, T., & Tada, R. (2006). Rapid and quantitative major element analysis method for wet fine-grained sediments using an XRF microscanner. Marine Geology, 229(3-4), 209–225.

Kienlin, T. L., Bischoff, E., & Opielka, H. (2006). Copper and bronze during the Eneolithic and Early Bronze Age: A metallographic examination of axes from the Northalphine region. Archaeometry, 48(3), 453–468.

Kuhnert, H., & Mulitza, S. (2011). Multidecadal variability and late medieval cooling of near-coastal sea surface temperatures in the eastern tropical North Atlantic. Paleoceanography, 26(4), 1–11.

Kuijpers, A., Dennegård, B., Albinsson, Y., & Jensen, A. (1993). Sediment transport pathways in the Skagerrak and Kattegat as indicated by sediment Chernobyl radioactivity and heavy metal concentrations. Marine Geology, 111(3–4), 231–244.

Larminie, F. G., Clark, R. B., Rudd, J. K., & Tasker, M. L. (1987). The History and Future of North Sea Oil and Gas: An Environmental Perspective. Philosophical Transactions of the Royal Society of London. Series B, Biological Sciences, 316(1181), 487–493.

Le Cadre, V., & Debenay, J. P. (2006). Morphological and cytological responses of Ammonia (foraminifera) to copper contamination: Implication for the use of foraminifera as bioindicators of pollution. Environmental Pollution, 143(2), 304–317.

Lea, D. W. (1999). Incorporation of trace elements in foraminiferal calcite. In: Sen Gupta, B. K. (Ed.), Modern Foraminifera (pp. 259–277). Kluwer Academic Publishers, Dordrecht.

Lea, D., & Boyle, E. (1989). Barium content of benthic foraminifera controlled by bottom-water composition. Nature, 338, 751.

Leblanc, M., Morales, J. A., Borrego, J., & Elbaz-Poulichet, F. (2000). 4,500-year-old mining pollution in southwestern Spain: Long-term implications for modern mining pollution. Economic Geology, 95(3), 655–662.

Lei, Y. L., Li, T. G., Bi, H., Cui, W. L., Song, W. P., Li, J. Y., & Li, C. C. (2015). Responses of benthic foraminifera to the 2011 oil spill in the Bohai Sea, PR China. Marine Pollution Bulletin, 96(1–2), 245–260.

Lepland, A., Andersen, T. J., Lepland, A., Arp, H. P. H., Alve, E., Breedveld, G. D., & Rindby, A. (2010). Sedimentation and chronology of heavy metal pollution in Oslo harbor, Norway. Marine Pollution Bulletin, 60(9), 1512–1522.

Li, Y. Y., Zhou, L. P., & Cui, H. T. (2008). Pollen indicators of human activity. Chinese Science Bulletin, 53(9), 1281–1293.

Livingston, M. E. (1987). Preliminary studies on the effects of past mining on the aquatic environment, Coromandel Peninsula. Water & Soil Miscellaneous Publication Number 104, Water and Soil Directorate, Ministry of Works and Development, Wellington, New Zealand.

Lohse, L., Malschaert, J. F. P., Slomp, C. P., Helder, W., & van Raaphorst, W. (1995). Sediment-water fluxes of inorganic nitrogen compounds along the transport route of organic matter in the North Sea. Ophelia, 41(1), 173–197.

Longva, O., & Thorsnes, T. (1997). Skagerrak in the past and at the present: An integrated study of geoloy, chemistry, hydrography and microfossil ecology. Geological Survey of Norway Special Publication 8, 99pp.

Lowe, D. J. (2008). Polynesian settlement of New Zealand and the impacts of volcanism on early Maori society: an update. In: Lowe, D. J. (Ed.), Guidebook for Pre-conference North Island Field Trip A1 ‘Ashes and Issues’ (28-30 November 2008). Australian and New Zealand 4th Joint Soils Conference, Massey University, Palmerston North (1-5 Dec. 2008). New Zealand Society of Soil Science, 142–147.

Lowe, D. J., Newnham, R. M., & McCraw, J. D. (2002). Volcanism and early Maori society in New Zealand. In: Torrence, R., & Grattan. J. (Eds.), Natural Disasters and Cultural Change (pp. 126–161). Routledge, London.

Mackay, K.A., Mackay, E.J., Neil, H.L., Mitchell, J.S., & Bardsley, S.A. (2012). Hauraki Gulf. NIWA Chart, Miscellaneous Series 91.

Martin, J. M., & Brun-Cottan, J. C. (1988). Estuaries. In: Salomons, W., Bayne, B. L., Duursma, E. K., & Förstner, U. (Eds.). Pollution of the North Sea (pp. 88–99). Springer-Verlag, Berlin, Heidelberg.

Mattielli, N., Petit, J. C. J., Deboudt, K., Flament, P., Perdrix, E., Taillez, A., Rimetz-Planchon, J., & Weis, D. (2009). Zn isotope study of atmospheric emissions and dry depositions within a 5 km radius of a Pb–Zn refinery. Atmospheric Environment, 43(6), 1265–1272.

May, T. W., & Wiedmeyer, R. H. (1998). A Table of Polyatomic Interferences in ICP-MS. Atomic Spectroscopy, 19(5), 150–155.

McFadgen, B. G. (1994). Coastal stratigraphic evidence for human settlement. In: Sutton, D. G. (Ed.), The Origins of the First New Zealanders (pp. 195–207). Auckland University Press, Auckland.

McGlone, M. S. (1983). Polynesian deforestation of New Zealand: a preliminary synthesis. Archaeology of Oceania, 18, 1–10.

McGlone, M. S. (1989). The polynesian settlements of New Zealand in relation to environmental and biotic changes. New Zealand Journal of Ecology, 12, 115–129.

McGlone, M. S., & Wilmshurst, J. M. (1999). Dating initial Maori environmental impact in New Zealand. Quaternary International, 59, 5–16.

McGlone, M. S., Anderson, A. J., & Holdaway, R. N. (1994). An ecological approach to the settlement of New Zealand. In: Sutton, D.G. (Ed.), The Origins of the First New Zealanders (pp. 136–163). Auckland University Press, Auckland.

McGregor, H. V., Dupont, L., Stuut, J. B. W., & Kuhlmann, H. (2009). Vegetation change, goats, and religion: a 2000-year history of land use in southern Morocco. Quaternary Science Reviews, 28(15–16), 1434–1448.

Mitchell, J. S., Mackay, K. A., Neil, H. L., Mackay, E. J., Pallentin, A., & Notman P. (2012). Undersea New Zealand, 1:5,000,000.

Monien, D., Kuhn, G., von Eynatten, H., & Talarico, F. M. (2012). Geochemical provenance analysis of fine-grained sediment revealing Late Miocene to recent Paleo-Environmental changes in the Western Ross Sea, Antarctica. Global and Planetary Change, 96–97, 41–58.

Monna, F., Hamer, K., Lévêque, J., & Sauer, M. (2000). Pb isotopes as a reliable marker of early mining and smelting in the Northern Harz province (Lower Saxony, Germany). Journal of Geochemical Exploration, 68, 201–210.

Moodley, L. (1990). Southern North Sea seafloor and subsurface distribution of living benthic foraminifera. Netherlands Journal of Sea Research, 27(1), 57–71.

Moseley, H. G. J. (1913). XCIII. The high-frequency spectra of the elements. The London, Edinburgh, and Dublin Philosophical Magazine and Journal of Science, 26(156), 1024–1034.

Müller, P. J. (1977). C/N vatios in pacific deep-sea sediments: effect of inorganic ammonium and organic nitrogen compounds sorbed by clays. Geochimica et Cosmochimica Acta, 41(1975), 765–776.

Müller, P. J., & Suess, E. (1979). Productivity, sedimentation rate, and sedimentary organic matter in the oceans - I. Organic carbon preservation. Deep Sea Research Part A, Oceanographic Research Papers, 26(12), 1347–1362.

Munsel, D., Kramar, U., Dissard, D., Nehrke, G., Berner, Z., Bijma, J., Reichart, G. J., & Neumann, T. (2010). Heavy metal incorporation in foraminiferal calcite: Results from multi-element enrichment culture experiments with Ammonia tepida. Biogeosciences, 7(8), 2339–2350.

Murozumi, M., Chow, T. J., & Patterson, C. (1969). Chemical concentrations of pollutant lead aerosols, terrestrial dusts and sea salts in Greenland and Antarctic snow strata. Geochimica et Cosmochimica Acta, 33(10), 1247–1294.

Murray, J.W. (2006). Ecology and applications of benthic foraminifera. Cambridge University Press, Cambridge, 426 pp.

Naish, T. R. (1990). Late Holocene mud sedimentation and diagenesis in the Firth of Thames: bentonite in the making. M.SC. Thesis, University of Waikato, New Zealand.

Naish, T. R., Nelson, C. S., & Hodder, A. P. W. (1993). Evolution of Holocene sedimentary bentonite in a shallow-marine embayment, Firth of Thames, New Zealand. Marine Geology, 109, 267–278.

Nardelli, M. P., Malferrari, D., Ferretti, A., Bartolini, A., Sabbatini, A., & Negri, A. (2016). Zinc incorporation in the miliolid foraminifer Pseudotriloculina rotunda under laboratory conditions. Marine Micropaleontology, 126, 42–49.

Newnham, R. M., de Lange, P. J., & Lowe, D. J. (1995a). Holocene, vegetation, climate and history of a raised bog complex, northern New Zealand based on palynology, plant macrofossils and tephrochronology. The Holocene, 5, 262–282.

Newnham, R. M., Lowe, D. J., & Wigley, G. N. A. (1995b). Late Holocene palynology and palaeovegetation of tephra-bearing mires at Papamoa and Waihi Beach, western Bay of Plenty, North Island, New Zealand. Journal of the Royal Society of New Zealand, 25, 283–300.

Newnham, R. M., Lowe, D. J., McGlone, M. S., Wilmshurst, J. M., & Higham, T. F. G. (1998). The Kaharoa tephra as a critical datum for earliest human impact in northern New Zealand. Journal of Archaeological Science, 25(6), 533–544.

Newnham, R., Lowe, D. J., Gehrels, M., & Augustinius, P. (2018). Two-step human–environmental impact history for northern New Zealand linked to late-Holocene climate change. The Holocene, 28(7), 1-14.

Nigst, P. R., Haesaerts, P., Damblon, F., Frank-Fellner, C., Mallol, C., Viola, B., Götzinger, M., Niven, L., Trnka, G., & Hublin, J.-J. (2014). Early modern human settlement of Europe north of the Alps occurred 43,500 years ago in a cold steppe-type environment. Proceedings of the National Academy of Sciences, 111(40), 14394–14399.

Nisbet, I. C. T., & LaGoy, P. K. (1992). Toxic Equivalency Factors (TEFs) for Polycyclic Aromatic Hydrocarbons (PAHs). Regulatory Toxicology and Pharmacology, 16, 290–300.

Nordberg, K. (1991). Oceanography in the Kattegat and Skagerrak over the past 8000 years. Paleoceanography, 6(4), 461–484.

Nriagu, J. O. (1996). A History of Global Metal Pollution. Science, 272(5259), 223–224.

Nydal, R. (1963). Increase in radiocarbon from the most recent series of thermonuclear tests. Nature, 200, 212–214.

Ogden, J., Basher, L., & McGlone, M. (1998). Fire, forest regeneration and links with early human habitation: evidence from New Zealand. Annals of Botany, 81, 687–696.

Ogden, J., Deng, Y., Boswijk, G., & Sandiford, A. (2003). Vegetation changes since early Maori fires in Waipoua Forest, Northern New Zealand. Journal of Archaeological Science, 30(6), 753–767.

OSPAR Commission (2000). Quality Status Report 2000, Region II – Greater North Sea. OSPAR Commission, London. 136 + xiii pp.

OSPAR Commission (2008) CEMP Assessment Manual - Co-ordinated Environmental Monitoring Programme Assessment Manual for contaminants in sediment and biota. Monitoring and Assessment Series.

OSPAR Commission (2009) CEMP assessment report : 2008/2009 Assessment of trends and concentrations of selected hazardous substances in sediments and biota. Monitoring and Assessment Series.

Otto, L., Zimmerman, J. T. E., Furnes, G. K., Mork, M., Saetre, R., & Becker, G. (1990). Review of the Physical Oceanography of the North Sea. Netherlands Journal of Sea Research, 26(2-4), 161-238.

Pache, T., Brockamp, O., & Clauer, N. (2008). Varied pathways of river-borne clay minerals in a near-shore marine region: A case study of sediments from the Elbe- and Weser rivers, and the SE North Sea. Estuarine, Coastal and Shelf Science, 78(3), 563–575.

Patterson, C. C., & Settle, D. M. (1987). Review of data on eolian fluxes of industrial and natural lead to the lands and seas in remote regions on a global scale. Marine Chemistry, 22(2–4), 137–162.

Pederstad, K., Roaldset, E., & Rønningsland, T. M. (1993). Sedimentation and environmental conditions in the inner Skagerrak-outer Oslofjord. Marine Geology, 111(3–4), 245–268.

Pereira, P., & Úbeda, X. (2010). Spatial Distribution of Heavy Metals Released From Ashes After a Wildfire. Journal of Environmental Engineering and Landscape Management, 18(1), 13–22.

Persaud, M., Villamor, P., Berryman, K., Ries, W., Cousins, J., Litchfield, N., & Alloway, B. (2016). The Kerepehi Fault, Hauraki Rift, North Island, New Zealand: active fault characterisation and hazard. New Zealand Journal of Geology and Geophysics, 59(1), 117–135.

Polovodova Asteman, I., Hanslik, D., & Nordberg, K. (2015). An almost completed pollution-recovery cycle reflected by sediment geochemistry and benthic foraminiferal assemblages in a Swedish-Norwegian Skagerrak fjord. Marine Pollution Bulletin, 95(1), 126–140.

Polovodova, I., & Schönfeld, J. (2008). Foraminiferal Test Abnormalities in the Western Baltic Sea. Journal of Foraminiferal Research, 38(4), 318–336.

Pongratz, R., & Heumann, K. G. (1998). Production of methylated mercury and lead by polar macroalgae — A significant natural source for atmospheric heavy metals in clean room compartments. Chemosphere, 36(9), 1935–1946.

Price, T. D. (2000). Europe's first farmers: an introduction. In: Price, T. D. (Ed.), Europe's First Farmers (pp. 1–18). Cambridge University Press, Cambridge.

Puls, W., Heinrich, H., & Mayer, B. (1997). Suspended particulate matter budget for the German Bight. Marine Pollution Bulletin, 34(6), 398–409.

Rafter, T. A., & Fergusson, G. J. (1957). "Atom bomb effect" - Recent increase of carbon-14 content of the atmosphere and biosphere. Science, 126(3273), 557–558.

Reidinger, S., Ramsey, M. H., & Hartley, S. E. (2012). Rapid and accurate analyses of silicon and phosphorus in plants using a portable X-ray fluorescence spectrometer. New Phytologist, 195(3), 699–706.

Reimer, P. J., Bard, E., Bayliss, A., Beck, J. W., Blackwell, P. G., Ramsey, C. B., … van der Plicht, J. (2013). IntCal13 and Marine13 Radiocarbon Age Calibration Curves 0–50,000 Years cal BP. Radiocarbon, 55(4), 1869–1887.

Reineck, H. E. (1963). Sedimentgefüge im Bereich der südlichen Nordsee. Abhandlungen der Senckenbergischen Naturforschenden Gesellschaft, 505, 1–138.

Reineck, H. E., Gutmann, W. F., & Hertweck, G. (1967). Das Schlickgebiet südlich Helgoland als Beispiel rezenter Schelfablagerungen. Senckenbergiana Lethaea, 48(3/4), 219–275.

Rengel, Z. (1999). Heavy Metals as Essential Nutrients. In: Prasad, M. N. V. (Ed.), Heavy Metal Stress in Plants (pp. 231–251). Springer-Verlag, Berlin, Heidelberg.

Ridgway, J., & Shimmield, G. (2002). Estuaries as repositories of historical contamination and their impact on shelf seas. Estuarine, Coastal and Shelf Science, 55(6), 903–928.

Rodhe, J. (1987). The large-scale circulation in the Skagerrak; interpretation of some observations. Tellus A, 39(3), 245–253.

Rodhe, J. (1998). The Baltic and North Seas: a process-oriented review of the physical oceanography. In: Robinson, A.R. and Brink, K. (Eds.), The Sea (pp. 699–732). John Wiley and Sons, New York.

Rodhe, J., & Holt, N. (1996). Observations of the transport of suspended matter into the Skagerrak along the western and northern coast of Jutland. Journal of Sea Research, 35(1–3), 91–98.

Romano, E., Bergamin, L., Finoia, M. G., Carboni, M. G., Ausili, A., & Gabellini, M. (2008). Industrial pollution at Bagnoli (Naples, Italy): Benthic foraminifera as a tool in integrated programs of environmental characterisation. Marine Pollution Bulletin, 56(3), 439–457.

Rothwell, R. G., & Croudace, I. W. (2015). Micro-XRF Studies of Sediment Cores: A Perspective on Capability and Application in the Environmental Sciences. Springer, Dordrecht.

Rotstigen, A. B. (2009). Benthic foraminifera as a proxy for natural versus anthropogenic environmental change in the German Bight, North Sea: a record over the last 1000 years. Master Thesis in Geosciences. University of Oslo, Oslo.

Sale, E. V. (1978). Quest for the kauri: forest giants and where to find them. Reed, Wellington.

Salomons, W. (1985). Sediments and water quality. Environmental Technology Letters, 6(1–11), 315–326.

Samir, A. M., & El-Din, A. B. (2001). Benthic foraminiferal assemblages and morphological abnormalities as pollution proxies in two Egyptian bays. Marine Micropaleontology, 41(3–4), 193–227.

Scheurle, C., & Hebbeln, D. (2003). Stable oxygen isotopes as recorders of salinity and river discharge in the German Bight, North Sea. Geo-Marine Letters, 23(2), 130–136.

Scheurle, C., Hebbeln, D., & Jones, P. (2005). An 800-year reconstruction of Elbe River discharge and German Bight sea-surface salinity. The Holocene, 15(3), 429–434.

Schönfeld, J. (2012). History and development of methods in recent benthic foraminiferal studies. Journal of Micropalaeontology, 31(1), 53–72.

Schönfeld, J., Golikova, E., Korsun, S., & Spezzaferri, S. (2013). The Helgoland Experiment – assessing the influence of methodologies on recent benthic foraminiferal assemblage composition. Journal of Micropalaeontology, 32(2), 161-182.

Scott, D. B., Tobin, R., Williamson, M., Medioli, F. S., Latimer, J. S., Boothman, W. A., Asioli, A., & Haury, V. (2005). Pollution Monitoring in Two North American Estuaries: Historical Reconstructions Using Benthic Foraminifera. The Journal of Foraminiferal Research, 35(1), 65–82.

Serna, A., Lahajnar, N., Pätsch, J., Hebbeln, D., & Emeis, K. C. (2014). Organic matter degradation in the German Bight/SE North Sea: Implications from stable nitrogen isotopes and amino acids. Marine Chemistry, 166, 103–113.

Serna, A., Pätsch, J., Dähnke, K., Wiesner, M. G., Christian Hass, H., Zeiler, M., Hebbeln, D., & Emeis, K. C. (2010). History of anthropogenic nitrogen input to the German Bight/SE North Sea as reflected by nitrogen isotopes in surface sediments, sediment cores and hindcast models. Continental Shelf Research, 30(15), 1626–1638.

Seshan, B. R. R., Natesan, U., & Deepthi, K. (2010). Geochemical and statistical approach for evaluation of heavy metal pollution in core sediments in southeast coast of India. International Journal of Environmental Science and Technology, 7(2), 291–306.

Shackley, M. S. (2018). X-Ray Fluorescence Spectrometry (XRF). In: The Encyclopedia of Archaeological Sciences (pp. 1–5). John Wiley & Sons, Hoboken, NJ, USA.

Sharifi, A. R., Croudace, I. W., & Austin, R. L. (1991). Benthic foraminiferids as pollution indicators in Southampton Water, southern England, U.K. Journal of Micropalaeontology, 10(1), 109–113.

Sheppard, D. S., Christie, A. B., Goff, J., & Carver, R. (2009). Stream sediment geochemical survey in an area of volcanic-hosted epithermal Au-Ag-Zn-Pb-Cu deposits and porphyry Cu prospects, Thames, Coromandel Peninsula, New Zealand. Geochemistry: Exploration, Environment, Analysis, 9(3); 279–296.

Simpson, S. L., Batley, G. E., & Chariton, A. A. (2013). Revision of the ANZECC/ARMCANZ Sediment Quality Guidelines. CSIRO Land and Water Science Report 08/07, CSIRO Land and Water.

Spencer, K. L., Cundy, A. B., & Croudace, I. W. (2003). Heavy metal distribution and early-diagenesis in salt marsh sediments from the Medway Estuary, Kent, UK. Estuarine, Coastal and Shelf Science, 57(1–2), 43–54.

Steward, G. A., & Beveridge, A. E. (2010). A review of New Zealand kauri (Agathis australis (D.Don) Lindl.): its ecology, history, growth and potential for management for timber. New Zealand Journal of Forestry Science, 40, 33–59.

Stockmarr, J. (1971). Tablets with spores used in absolute pollen analysis. Pollen Spores, 13(4), 615–621.

Stuiver, M., Reimer, P. J., Bard, E., Beck, J. W., Burr, G. S., Hughen, K. A., Kromer, B., McCormac, G., van der Plicht, J., & Spurk, M. (1998b). INTCAL98 Radiocarbon Age Calibration, 24,000–0 cal BP. Radiocarbon, 40(3), 1041–1083.

Stuiver, M., Reimer, P.J., & Reimer, R.W. (2018). CALIB 7.1 [WWW program] at http://calib.org

Stuiver. M., Reimer, P. J., & Braziunas, T. F. (1998a). High-precision radiocarbon age calibration for terrestrial and marine samples. Radiocarbon, 40(3), 1127–1151.

Stuut, J. B. W. (2001). Late Quarternary southwestern African terrestrial-climate signals in the marine record of Walvis Ridge, SE Atlantic Ocean. PhD Thesis. University of Utrecht.

Suess, H. E. (1955). Radiocarbon Concentrations in Modern Wood. Science, 122, 415–417.

Svansson, A. (1975). Physical and chemical oceanography of the Skagerrak and the Kattegat, I: Open sea conditions. Fischery Board Sweden, Institute of Marine Research, Report No.1, 1-88.

Swales, A., Bentley, S. J., & Lovelock, C. E. (2015). Mangrove-forest evolution in a sediment-rich estuarine system: opportunists or agents of geomorphic change? Earth Surface Processes and Landforms, 40(12), 1672–1687.

Swales, A., Denys, P., Pickett, V. I., & Lovelock, C. E. (2016). Evaluating deep subsidence in a rapidly-accreting mangrove forest using GPS monitoring of surface-elevation benchmarks and sedimentary records. Marine Geology, 380, 205–218.

Tjallingii, R., Röhl, U., Kölling, M., & Bickert, T. (2007). Influence of the water content on X-ray fluorescence corescanning measurements in soft marine sediments. Geochemistry, Geophysics, Geosystems, 8(2), 1–12.

Traas, T. P., & van Leeuwen, C. J. (2007). Ecotoxicological Effects. In: van Leeuwen, C. J., & Vermeire, T. G. (Eds.), Risk Assessment of Chemicals – An introduction (pp. 281–356). Springer Netherlands, Dordrecht.

Turner, A., Comber, S., Rees, A. B., Gkiokas, D., & Solman, K. (2015). Metals in boat paint fragments from slipways, repair facilities and abandoned vessels: An evaluation using field portable XRF. Talanta, 131, 372–378.

Van Leeuwe, C.M. (1991). Transport of suspended sediments in the southern part of the Firth of Thames. M.Sc. Thesis, University of Waikato, New Zealand, 1-269.

Van Weering, T. C. E. (1981). Recent sediments and sediment transport in the northern North Sea: surface sediments of the Skagerrak. Special Publication of the International Association of Sedimentologists, 5, 335-359.

Van Weering, T. C. E., Berger, G. W., & Kalf, J. (1987). Recent sediment accumulation in the Skagerrak, Northeastern North Sea. Netherlands Journal of Sea Research, 21(3), 177–189.

Van Weering, T. C. E., Rumohr, J., & Liebezeit, G. (1993). Holocene sedimentation in the Skagerrak: A review. Marine Geology, 111(3–4), 379–391.

Varrica, D., Aiuppa, A., & Dongarrà, G. (2000). Volcanic and anthropogenic contribution to heavy metal content in lichens from Mt. Etna and Vulcano island (Sicily). Environmental Pollution, 108(2), 153–162.

Vidović, J., Nawrot, R., Gallmetzer, I., Haselmair, A., Tomašových, A., Stachowitsch, M., Ćosović, V., & Zuschin, M. (2016). Anthropogenically induced environmental changes in the northeastern Adriatic Sea in the last 500 years (Panzano Bay, Gulf of Trieste). Biogeosciences, 13(21), 5965–5981.

Vink, R., Behrendt, H., & Salomons, W. (1999). Development of the heavy metal pollution trends in several European rivers: An analysis of point and diffuse sources. Water Science and Technology, 39(12), 215–223.

Von Haugwitz, W., Wong, H. K., & Salge, U. (1988). The mud area southeast of Helgoland: A reflection seismic study. In: Kempe, S., Liebezeit, G., Dethlefsen, V., & Harms, U. (Eds.), Biogeochemistry and Distribution of Suspended Matter in the North Sea and Implications to Fisheries Biology. Mitteilungen aus dem Geologisch-Paläontologischen Institut der Universität Hamburg, 65, 409–422.

Wang, P. (1983). Verbreitung der Benthos-Foraminiferen im Elbe-Ästuar. Meyiana, 35, 67-83.

Wang, T., Wu, J., Hartman, R., Jia, X., & Egan, R. S. (2000). A multi-element ICP-MS survey method as an alternative to the heavy metals limit test for pharmaceutical materials. Journal of Pharmaceutical and Biomedical Analysis, 23(5), 867–890.

Webster, J. G. (1995). Chemical processes affecting trace metal transport in the Waihou River and estuary, New Zealand. New Zealand Journal of Marine and Freshwater Research, 29(4), 539–553.

Weindorf, D. C., Paulette, L., & Man, T. (2013). In-situ assessment of metal contamination via portable X-ray fluorescence spectroscopy: Zlatna, Romania. Environmental Pollution, 182, 92–100.

Williams, G. J. (1974). Economic geology of New Zealand: the TJ McKee memorial volume, 2nd Edition. Australasian Institute of Mining and Metallurgy, Parkville, Australia.

Wilmshurst, J. M. (1997). The impact of human settlement on vegetation and soil stability in Hawke's Bay, New Zealand. New Zealand Journal of Botany, 35(1), 97–111.

Wilmshurst, J. M., McGlone, M. S., Leathwick, J. R., & Newnham, R. M. (2007). A pre-deforestation pollen-climate calibration model for New Zealand and quantitative temperature reconstructions for the past 18 000 years BP. Journal of Quaternary Science, 22(5), 535–547.

Winther, N. G., & Johannessen, J. A. (2006). North Sea circulation: Atlantic inflow and its destination. Journal of Geophysical Research, 111, C12018.

Wirth, H., & Wiesner, M. G. (1988). Sedimentary Facies in the North Sea. In: Kempe, S., Liebezeit, G., Dethlefsen, V., & Harms, U. (Eds.), Biogeochemistry and Distribution of Suspended Matter in the North Sea and Implications to Fisheries Biology. Mitteilungen aus dem Geologisch-Paläontologischen Institut der Universität Hamburg, 65, 269-287.

Yanko, V., Ahmad, M., & Kaminski, M. (1998). Morphological deformities of benthic foraminiferal tests in response to pollution by heavy metals: Implications for pollution monitoring. The Journal of Foraminiferal Research, 28(3), 177–200.

Yanko, V., Arnold, A. J., & Parker, W. C. (1999). Effects of marine pollution on benthic Foraminifera. In: Sen Gupta, B. K. (Ed.), Modern Foraminifera (pp. 217–235). Kluwer Academic Publishers, Dordrecht.

Yanko, V., Kronfeld, J., & Flexer, A. (1994). Response of benthic Foraminifera to various pollution sources; implications for pollution monitoring. The Journal of Foraminiferal Research, 24(1), 1–17.

Yasuda, Y., Kitagawa, H., & Nakagawa, T. (2000). The earliest record of major anthropogenic deforestation in the Ghab Valley, northwest Syria: a palynological study. Quaternary International, 73–74, 127–136.

Yin, N.-H., Sivry, Y., Benedetti, M. F., Lens, P. N. L., & van Hullebusch, E. D. (2016). Application of Zn isotopes in environmental impact assessment of Zn–Pb metallurgical industries: A mini review. Applied Geochemistry, 64, 128–135.

Yokoyama, Y., Koizumi, M., Matsuzaki, H., Miyairi, Y., & Ohkouchi, N. (2010). Developing ultra small-scale radiocarbon sample measurement at the University of Tokyo. Radiocarbon, 52, 310–318.

Yokoyama, Y., Miyairi, Y., Matsuzaki, H., & Tsunomori, F. (2007). Relation between acid dissolution time in the vacuum test tube and time required for graphitization for AMS target preparation. Nuclear Instruments and Methods in Physics Research, Section B, 259, 330-334.

Young, K. E., Evans, C. A., Hodges, K. V., Bleacher, J. E., & Graff, T. G. (2016). A review of the handheld X-ray fluorescence spectrometer as a tool for field geologic investigations on Earth and in planetary surface exploration. Applied Geochemistry, 72, 77–87.

Supplementary Material

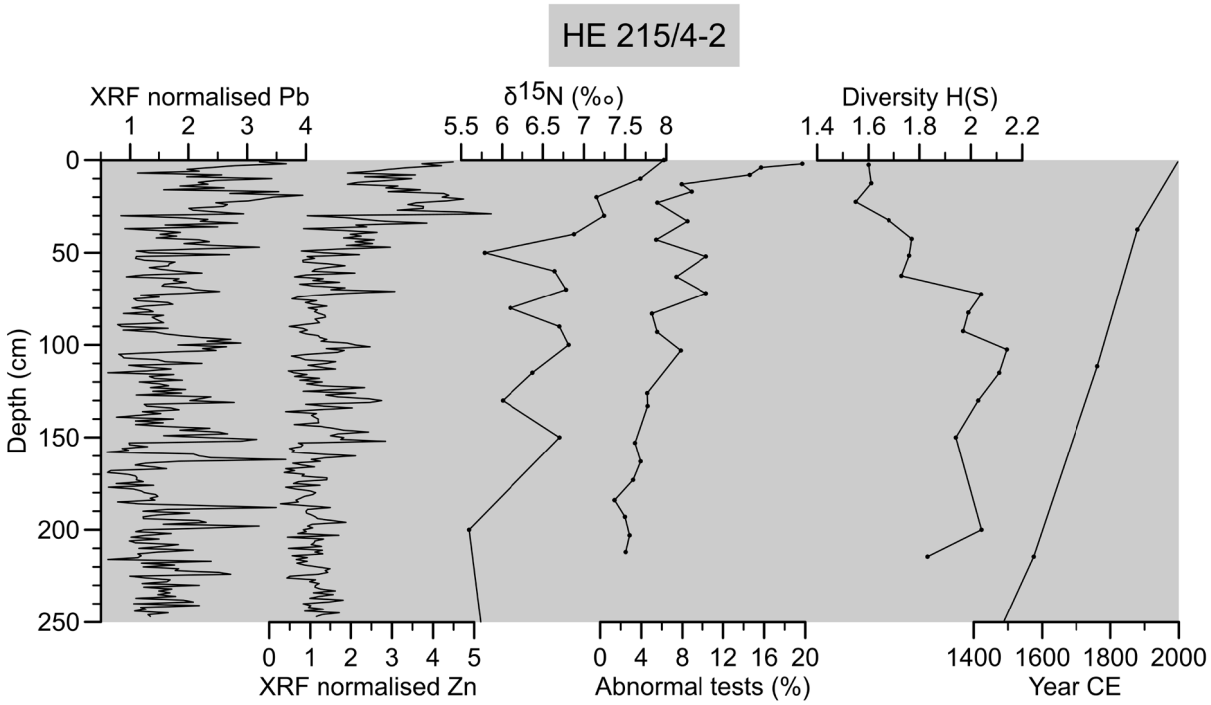

Figure S 1: Normalised XRF data (Pb and Zn), $\delta^{15}N$, proportion of abnormal tests, foraminiferal diversity and age plotted against depth for gravity core HE 215/4-2.

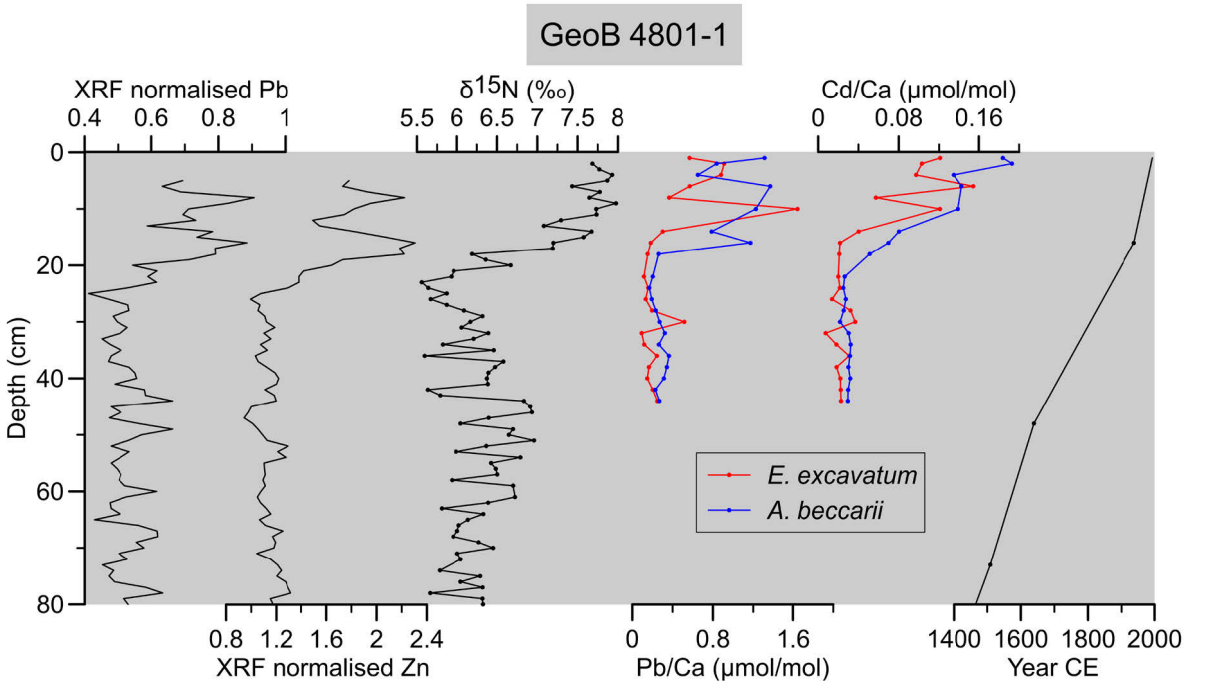

Figure S 2: Normalised XRF data (Pb and Zn), $\delta^{15}N$, Pb/Ca and Cd/Ca ratios of E. excavatum (red line) and A. beccarii (blue line) as well as age plotted against depth for gravity core GeoB 4801-1.

Versicherung an Eides Statt
/ Affirmation in lieu of an oath

gem. § 5 Abs. 5 der Promotionsordnung vom 18.06.2018 / according to § 5 (5) of the Doctoral Degree Rules and Regulations of 18 June, 2018

Ich / I, _____
(Vorname / First Name, Name / Name, Anschrift / Address, ggf. Matr.-Nr. / student ID no., if applicable)

versichere an Eides Statt durch meine Unterschrift, dass ich die vorliegende Dissertation selbständig und ohne fremde Hilfe angefertigt und alle Stellen, die ich wörtlich dem Sinne nach aus Veröffentlichungen entnommen habe, als solche kenntlich gemacht habe, mich auch keiner anderen als der angegebenen Literatur oder sonstiger Hilfsmittel bedient habe und die zu Prüfungszwecken beigelegte elektronische Version (PDF) der Dissertation mit der abgegebenen gedruckten Version identisch ist. / With my signature I affirm in lieu of an oath that I prepared the submitted dissertation independently and without illicit assistance from third parties, that I appropriately referenced any text or content from other sources, that I used only literature and resources listed in the dissertation, and that the electronic (PDF) and printed versions of the dissertation are identical.

Ich versichere an Eides Statt, dass ich die vorgenannten Angaben nach bestem Wissen und Gewissen gemacht habe und dass die Angaben der Wahrheit entsprechen und ich nichts verschwiegen habe. / I affirm in lieu of an oath that the information provided herein to the best of my knowledge is true and complete.

Die Strafbarkeit einer falschen eidesstattlichen Versicherung ist mir bekannt, namentlich die Strafandrohung gemäß § 156 StGB bis zu drei Jahren Freiheitsstrafe oder Geldstrafe bei vorsätzlicher Begehung der Tat bzw. gemäß § 161 Abs. 1 StGB bis zu einem Jahr Freiheitsstrafe oder Geldstrafe bei fahrlässiger Begehung. / I am aware that a false affidavit is a criminal offence which is punishable by law in accordance with § 156 of the German Criminal Code (StGB) with up to three years imprisonment or a fine in case of intention, or in accordance with § 161 (1) of the German Criminal Code with up to one year imprisonment or a fine in case of negligence.

_____ _____
Ort / Place, Datum / Date Unterschrift / Signature